

Indoor airborne risk assessment

in the context of SARS-CoV-2

**Description of airborne transmission mechanism and method
to develop a new standardized model for risk assessment**



World Health
Organization





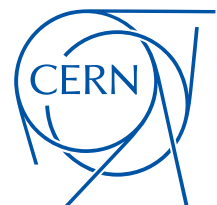
Indoor airborne risk assessment

in the context of SARS-CoV-2

**Description of airborne transmission mechanism and method
to develop a new standardized model for risk assessment**



**World Health
Organization**



Indoor airborne risk assessment in the context of SARS-CoV-2: description of airborne transmission mechanism and method to develop a new standardized model for risk assessment

ISBN 978-92-4-009057-6 (electronic version)

ISBN 978-92-4-009060-6 (print version)

© World Health Organization 2024

Some rights reserved. This work is available under the Creative Commons Attribution-NonCommercial-ShareAlike 3.0 IGO licence (CC BY-NC-SA 3.0 IGO; <https://creativecommons.org/licenses/by-nc-sa/3.0/igo>).

Under the terms of this licence, you may copy, redistribute and adapt the work for non-commercial purposes, provided the work is appropriately cited, as indicated below. In any use of this work, there should be no suggestion that WHO endorses any specific organization, products or services. The use of the WHO logo is not permitted. If you adapt the work, then you must license your work under the same or equivalent Creative Commons licence. If you create a translation of this work, you should add the following disclaimer along with the suggested citation: “This translation was not created by the World Health Organization (WHO). WHO is not responsible for the content or accuracy of this translation. The original English edition shall be the binding and authentic edition”.

Any mediation relating to disputes arising under the licence shall be conducted in accordance with the mediation rules of the World Intellectual Property Organization (<http://www.wipo.int/amc/en/mediation/rules/>).

Suggested citation. Indoor airborne risk assessment in the context of SARS-CoV-2: description of airborne transmission mechanism and method to develop a new standardized model for risk assessment. Geneva: World Health Organization; 2024. Licence: CC BY-NC-SA 3.0 IGO.

Cataloguing-in-Publication (CIP) data. CIP data are available at <https://iris.who.int/>.

Sales, rights and licensing. To purchase WHO publications, see <https://www.who.int/publications/book-orders>. To submit requests for commercial use and queries on rights and licensing, see <https://www.who.int/copyright>.

Third-party materials. If you wish to reuse material from this work that is attributed to a third party, such as tables, figures or images, it is your responsibility to determine whether permission is needed for that reuse and to obtain permission from the copyright holder. The risk of claims resulting from infringement of any third-party-owned component in the work rests solely with the user.

General disclaimers. The designations employed and the presentation of the material in this publication do not imply the expression of any opinion whatsoever on the part of WHO concerning the legal status of any country, territory, city or area or of its authorities, or concerning the delimitation of its frontiers or boundaries. Dotted and dashed lines on maps represent approximate border lines for which there may not yet be full agreement.

The mention of specific companies or of certain manufacturers' products does not imply that they are endorsed or recommended by WHO in preference to others of a similar nature that are not mentioned. Errors and omissions excepted, the names of proprietary products are distinguished by initial capital letters.

All reasonable precautions have been taken by WHO to verify the information contained in this publication. However, the published material is being distributed without warranty of any kind, either expressed or implied. The responsibility for the interpretation and use of the material lies with the reader. In no event shall WHO be liable for damages arising from its use.

Contents

Foreword	v
Acknowledgements	vii
Abbreviations	ix
Glossary	x
Executive summary	xv
Introduction	1
Mode of transmission	1
Infection risk and indoor ventilation	2
Ventilation standards for IPC	2
Ventilation standards in non-healthcare settings	3
Ventilation to lower indoor airborne infection risk	3
Scope of the document	4
Methodology	4
Model Validation	5
Inhalation transmission mechanism	6
Model description	8
Model architecture	8
Box 1: Long-range	8
Box 2: Short-range	8
Emission rate	9
Respiratory particles	9
SARS-CoV-2 viral load	10
Source control (outward)	10
Respiratory rate	10
Removal rate	11
Ventilation rate and air cleaning devices	11
Viability decay	11
Gravitational settling	11
Exposure (long-range transmission)	12
Occupancy profile	12
Room volume	12
Mass balance	12
Step-wise computation	12
Cumulative (absorbed) dose	13
Particle deposition fraction	13
Viable virus factor	14
Masks and Respirators (Inward)	14

Short-range transmission	14
Proxemics	14
Expiratory Jet	15
Exposure	15
Probability of infection	16
Dose-response	16
Variants of Concern	16
Host immunity against transmission	17
Limitations	18
Online tool	19
Examples	19
References	22
Annexes	29
Annex 1. Systematic review results	30
Annex 2. Available tools presented at ISIAQ	49
Annex 3. Model validation	50
Annex 4. Model formulas	58
Annex 5. Model values	63

Foreword

We live immersed in an ocean of air, yet we hardly ever notice its presence. However, without air we would simply not be able to survive.

In the past years, much work has been carried out on the connection between air quality and health. For instance, air pollution is a major risk factor for non-communicable diseases and the recently published WHO global air quality guidelines provide key steps to enhance a global response to reduce the burden of disease attributable to air pollution.

In 2019, a new world threat emerged with SARS-CoV-2, a virus that has affected the entire world, every country, every family. The incredibly rapid spread of this virus that transmitted efficiently between people through the air renewed the important risks related to the quality of the air we breathe. Transmission of SARS-CoV-2 has been the subject of considerable debate throughout the pandemic. For the first time on a global scale, the critical importance of settings, duration and close range exposures with infectious respiratory particles emitted by infected people into the air, forced the world to pay attention to the ventilation of our houses, our schools, and our work places, as one of the critical components to reduce SARS-CoV-2 transmission.

The science underpinning the spread of disease through the air has been studied for several decades and it has been evolving since the middle of twentieth century when the airborne transmission of tuberculosis, a major global health risk, was ultimately recognized. For decades, the scientific community, in particular epidemiologists, virologists, infection control specialists, engineers, aerobiologists, and other public health specialties, has been working tirelessly to further understand the biological and physical mechanisms driving airborne transmission of respiratory pathogens. The assiduous and determined work of numerous global scientists, before and during the COVID-19 pandemic, significantly contributed to strengthening the public health response and saving lives. The work described here reminds us, once again, of the importance and strength of a multi-disciplinary collaboration when tackling these challenges at a global scale.

This manual leverages on both longstanding and new evidence based on the expertise of scientists from a wide variety of disciplines. It provides a new, standardized, and validated model for quantifying the risk of airborne transmission of SARS-CoV-2 in indoor settings. Our aim was to provide a robust tool to inform mitigation measures for business owners, households, healthcare centres and others, to not only reduce the unacceptable and unnecessary health burden resulting from the airborne transmission of respiratory pathogens, like SARS-CoV-2, and enable a more agile and effective response.

We are immensely grateful to all the scientists, colleagues and partners around the world who have contributed their time, expertise, and resources to the development of this online tool and supplementary document. A global group of experts has derived this new model based on a robust and comprehensive review of the scientific literature, while adhering to a rigorously defined methodology. This process was overseen by a steering group hosted and coordinated by the joint effort of the WHO Environment, Climate Change and Health department, the WHO Emerging Diseases and Zoonoses Unit in the Department of Epidemic and Pandemic Prevention and Preparedness, and the Strategic Health Operations department.

Moreover, the complexity and multidisciplinary nature of this project benefited from the technical collaboration in between the World Health Organization and the European Organization for Nuclear Research (CERN). Such alliance between public health, applied science and fundamental research marks an important step in advancing the boundaries of human knowledge and lay the pathway for a more holistic approach to answer essential questions.

This manual sets an important milestone in understanding the airborne mechanism of pathogens. For the first time, the risk estimation will be directly informed by host, pathogen and environment features and their complex interactions. Addressing the possibility of SARS-CoV-2 airborne transmission through risk assessment and risk-based ventilation requirements will enable a more effective and efficient public health response. In many parts of the world, people spend most of their time indoors, ensuring healthy and safe indoor environments will contribute to mitigating the current COVID-19 pandemic, as well as inform policy decisions in hopes of protecting us from future respiratory outbreaks.

One of the learnings from this pandemic has been that we must reshape and redesign the building environment, while focusing on optimizing indoor ventilation and therefore, the air we breathe. This will be a challenging and enduring urban health and urban planning exercise, which will require sustained political commitment and engagement from many sectors and stakeholders, but it is an important step to begin awareness now so that countries can be better prepared for future outbreaks.

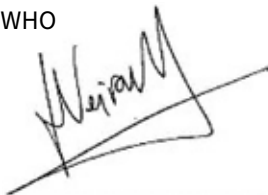
This manual comes at a time of unprecedented challenges, in the face of the ongoing COVID-19 pandemic and the existential threat of climate change. Risk-based standards, rather than absolute ventilation standards, will enable a more efficient use of our resources while the reshaping of the building environment will open the door to the adoption of new technologies and processes that can provide climate resilience, environmental sustainability and enhanced health service delivery.

The return on investment will be a healthier and safer air for us and generations to come.

Dr Maria Neira

Director, Department of Environment, Climate Change and Health

WHO



Benoît Delille

Head of the Health & Safety and Environmental Protection Unit

CERN



Dr Maria Van Kerkhove

Technical lead for COVID-19

WHO



Dr N'da Konan Michel Yao

Director, Department of Strategic Health Operations

WHO



Acknowledgements

The World Health Organization (WHO) would like to thank the collaborative efforts of all those involved to make this process efficient, trustworthy and transparent. This document was developed in consultation with the WHO Airborne Risk Indoor Assessment (ARIA) Technical Advisory Group, with the following members; and the European Organization for Nuclear Research (CERN); and reviewed by The WHO Environment and Engineering Control Expert Advisory Panel (ECAP) for COVID-19.

WHO ARIA Technical Advisory Group

Lidia Morawska (Co-Chair) (Queensland University of Technology, Australia); Nancy Hiu Lan Leung (Co-Chair) (The University of Hong Kong, Hong Kong Special Administrative Region (SAR), China); Alex Mikszewski (Queensland University of Technology, United States of America); Andre Henriques (CERN, Switzerland); Bryan E. Christensen (Centers for Disease Control and Prevention, United States of America); Daniela Wuerz (United Nations, Switzerland); Fernanda Lessa (Centers for Disease Control and Prevention, United States of America); Giorgio Buonanno (University of Cassino and Southern Lazio, Italy); Ibrahim Abubakar (University College London, United Kingdom); JIA Wei (The University of Hong Kong, Hong Kong Special Administrative Region (SAR), China); John Conly (University of Calgary, Canada); Julian W Tang (University Hospitals of Leicester NHS, United Kingdom); Kwok Wai Tham (National University of Singapore, Singapore); Luca Stabile (University of Cassino and Southern Lazio, Italy); Luis Aleixo (CERN, Switzerland); Mark Jermy (University of Canterbury, New Zealand); Michele Piero Blago (CERN, seconded to WHO, Switzerland); Mitchell Schwaber (Israel Ministry of Health, Israel); Nicolas Mounet (CERN, Switzerland); Raymond Tellier (McGill University, Canada); Shaheen Mehtar (Infection Control Africa Network, South Africa); Yuguo Li (The University of Hong Kong, Hong Kong Special Administrative Region (SAR), China);

WHO Secretariat

Abdi Rahman Mahamud; Alice Simniceanu; Anja Borojevic; Anna Silenzi; Benedetta Allegranzi; Boris Pavlin; Francis Roosevelt Mulemba; Heather Saul; Janet Diaz; Jordi Sacristan Llobet; Julia Fitzner; Kamal Ait-ikhlef; Karen Anne Grimmer; Kavita Kothari; Kevin John Carlisle; Lisa Askie; Luca Fontana; Lucy Turner; Madison Moon; Mamadou Zongo; Maria Purificacion Neira; Maria Van Kerkhove; Marta Lado; Michele Di Marco; Nathan Paul Ford; Olivier Le Polain.

CAiMIRA team (CERN)

Andre Henriques; Nicolas Mounet; Philip Elson; Gabriella Azzopardi; Luis Aleixo; James Devine; Marco Andreini; Markus Rognlien; Nicola Tarocco.

The WHO Environment and Engineering Control Expert Advisory Panel (ECAP) for COVID-19

Arnold Janssens (Indoor Environmental Quality Global Alliance, Belgium); Arsen Krikor Melikov (University of Denmark, Denmark); Baliga B Gautham (Indoor Environmental Quality Global Alliance, India); Catherine Noakes (University of Leeds, United Kingdom); Chandra Sekhar (National University of Singapore, Singapore); Donald K Milton (University of Maryland, United States of America); Frank Kelly (Imperial College London, United Kingdom); Gaetano Settimo (Istituto Superiore di Sanità, Italy); Guilherme Coelho (Technische Universität Berlin, Germany); Jarek Kurnitski (Tallinn University of Technology, Estonia); Jean-Pierre Veyrenche (School of Business and Development 3A, Lyon and Paris, France); Jim Crabb (Mazzetti, ASHRAE Advisory Committee, United States of America); Jonathan Samet (Colorado School of Public Health, United States of America); Joost Hoopman (Radboud University Medical Center Nijmegen, The Netherlands); Marcel Loomans (Eindhoven University of Technology, Netherlands); Marco Simonetti (Polytechnic University of Turin, Italy); Nastase Ilinca (Indoor Environmental Quality Global Alliance, Romania); Nino Kuenzli (Swiss Tropical and Public Health Institute, Switzerland); Nizam Damani (Southern Health and Social Care Trust, United Kingdom of Great Britain and Northern Ireland); Ollie Seppänen (Aalto University, Finland); Pawel Wargocki (University of Denmark, Denmark); Stephen Martin (Centers for Disease Control and Prevention, United States of America); Walt Vernon (Mazzetti, Vice Chair for ASHRAE 189.3, United States of America); William Bahnfleth (Indoor Environmental Quality Global Alliance, United States of America); Wing Hong Seto (University of Hong Kong, SAR, China).

Funding for this guideline was provided by the WHO COVID-19 emergency funds.

Abbreviations

ACH	Air changes per hour
CADR	Clean air delivery rate
COVID-19	Coronavirus Disease 2019
IAQ	Indoor air quality
IPC	Infection prevention and control
IRP	Infectious Respiratory Particle
MERS-CoV	Middle East respiratory syndrome coronavirus
MERV	Minimum efficiency reporting value
METS	Metabolic equivalent of work
SARS	Severe Acute Respiratory Syndrome
SARS-CoV-2	Severe Acute Respiratory Syndrome Coronavirus 2
TB	Tuberculosis
VOC	Variants of concern
VOI	Variants of interest
WHO	World Health Organization

Glossary

Aerosol: A collection of solid or liquid particles of any size suspended in a gas [1].

Airborne: Anything that is suspended or carried through the air [2].

Airborne transmission*: The process whereby aerosolized infectious respiratory particles (IRPs) are inhaled and enter the respiratory tract of a susceptible person, move through the upper and then lower parts of the respiratory tract, and can be deposited on the tissue at any point along the tract, but preferred sites of entry may be pathogen-specific. This mode of transmission can occur when IRPs have travelled either a short or a long distance (range) after emission from an infected person or after resuspension of deposited particles from surface. Can also be used interchangeably with inhalation transmission.

Air changes per hour: Ventilation airflow rate (m^3/h) divided by room volume. It is the ratio of the volume of outdoor or filtered air flowing into a given space in an hour divided by the volume of that space. [3]

Attack rate: The proportion of a specified population, or a group of individuals after a specified exposure, that experiences the outcome of interest (e.g., infection, or symptomatic illness) during a specified period of time. The numerator is new cases with the outcome during the specified period; the denominator is the population at risk at the start. Alternatively referred to as incidence proportion [4].

Clean air delivery rate (CADR): The result of the measured flow rate, delivered by an air cleaning device, at which all particles of a given size distribution are removed in a given timeframe. Usually expressed as m^3/h [5].

Close proximity: The physical distance that people are comfortable putting between themselves and others during intimate, personal and social communicative situations. While this distance can vary from person to person, four main spaces have been defined: Intimate space up to ~45 cm, personal space from 45 cm to ~120 cm, social space from 120 cm to ~365 cm, and public space from 365 cm and beyond. This document considers close proximity up to 200 cm [6] distance in between subjects. Can also be used interchangeably with conversational distance.

Contact transmission*: The process whereby infectious particles, of any size, either settle on a surface at any distance from the source following emission, or are transferred directly from (usually) the hands of an infected person (by the infected person touching their own eyes, nose or mouth); and then transferred to the mucosal membrane of a susceptible person when that person either touches the contaminated surface or the hand of the infected person followed by touching their own eyes, nose or mouth. The former (i.e., transmission via touching contaminated surface) is often referred to as indirect contact transmission and the latter (i.e., transmission via touching the hand of infected person) as direct contact transmission.

Contaminated surface: Surfaces on which there are respiratory particles or other body fluids that may be infectious (from SARS-CoV-2 or other pathogens) [7].

Cumulative dose: In the context of inhalation transmission, the total number of infectious particles inhaled and absorbed by a susceptible host during the exposure event [8].

Dilution: in the context of this document, the reduction in concentration of infectious particles by means of ventilation, equivalent ventilation and gravitational settling [9].

Equivalent ventilation: Ventilation rate expressed as CADR (m^3/h) produced by air cleaning and disinfection devices, using filter category MERV (minimum efficiency reporting value) 14 / ISO ePM1 70-80%, high efficiency particulate air (HEPA) and higher filtration efficiency filter [5], as well as UVGI technology [10].

Droplet: Liquid particle of any size [10]

Emission rate: the number of virus-laden particles exhaled by an infected person in a given time. Emission rates are commonly expressed as particles per unit time, particles per unit volume, or mass per unit volume (i.e., particles per minutes, particles per liter, or micrograms per liter) [11].

Exposure: Exposure is a product of the infectious particles concentration and the time over which a person is in contact with the infectious particles [12].

* This terminology is derived from the forthcoming WHO publication “Global technical consultation report on proposed terminology for pathogens that transmit through the air”, which will provide a comprehensive introduction and definition of these terms. This selection is made in anticipation of the standardization of this terminology, ensuring that the present document is aligned with the evolving scientific consensus.

Gravitational deposition: Sedimentation resulting from the settling of particles under the action of gravity [9].

Inhalation: The act of taking a substance into the body by breathing [14].

Inhalation transmission*: The process whereby aerosolized infectious respiratory particles (IRPs) are inhaled and enter the respiratory tract of a susceptible person, move through the upper and then lower parts of the respiratory tract, and can be deposited on the tissue at any point along the tract, but preferred sites of entry may be pathogen-specific. This mode of transmission can occur when IRPs have travelled either a short or a long distance (range) after emission from an infected person or after resuspension of deposited particles from surface. Can also be used interchangeably with airborne transmission.

Infectior: An individual who is infected and who can shed viable virus. Can also be used interchangeably with source or source of infection.

Infectious aerosol: A collection of infectious particles suspended in air, i.e., aerosolized infectious respiratory particles [15].

Infectious Respiratory Particles (IRPs)*: Particles composed of water and other constituents (including salt, proteins, mucus, etc.), containing viable pathogens exhaled in a wide range of sizes by people infected with a respiratory pathogen.

Long-range airborne transmission*: Transmission occurring via inhalation of aerosolized infectious respiratory particles by a susceptible host at a distance farther than conversational distance (2 meter) from the infected person/ source of infection [16].

Metabolic equivalent of work (METs): A dimensionless ratio of the metabolic rate (energy expenditure) of an activity to a person's resting basal metabolic rate, i.e. an energy expenditure metric used to represent activity level [17].

Direct deposition transmission*: The process whereby larger respiratory infectious particles are directly deposited onto the conjunctivae and mucous membranes of the upper respiratory tract (mouth, nasal, throat or pharynx mucosa) of a susceptible person, having followed a projectile motion after emission from the infected person. This mode of transmission only occurs at "close proximity".

Mucous membrane: The moist, inner lining of some organs and body cavities (chiefly the respiratory, digestive, and urogenital tracts. such as the nose, mouth, lungs, and stomach). Also called mucosa [18].

Filtration efficiency: the percentage of particles of a certain size that would be stopped and retained by a filter medium [19].

Oxygen consumption (VO_2): The rate at which oxygen is used by tissues, calculated by multiplying energy expenditure by volume of oxygen consumed per unit of energy. Commonly expressed as volume per time, or volume per time per unit of body weight[17].

Projectile motion: the movement of an object launched (projected) into the air. After the initial force that launches the object, it only experiences the force of gravity. The object is called a projectile, and its path is called its trajectory [20].

Removal rate: In the context of this document, the number of infectious particles removed by different means from the air in a given time [21].

Reproduction number: The reproduction number (R), also called reproductive ratio, is the average number of infected contacts per infectious individual in a population. The effective reproduction number (R_t) represents R at any time (t) during an epidemic; while the basic reproduction number (R_0) represents R at the start (time = 0) of the epidemic, i.e., the average number of infected contacts per infectious individual in a completely susceptible population. At population level, a value of R equal or larger than one implies transmission will continue among susceptible hosts if no environmental changes or external influences intervene. An R value lower than one implies transmission will decrease over time and eventually ends [22].

Respiratory tract: The respiratory tract consists of airways and lungs. The upper respiratory tract refers to the following airway structures: nasal cavities and passages (sinuses), pharynx, tonsils, and larynx (voice box). The lower respiratory tract refers to trachea (windpipe) and lungs with its substructures bronchi, bronchioles, and alveoli [23].

Short-range airborne transmission*: Transmission occurring via inhalation of aerosolized infectious Respiratory particles inhaled by a susceptible host at a distance up-to conversational distance (2 meter) from the infected person/ source of infection.

* This terminology is derived from the forthcoming WHO publication "Global technical consultation report on proposed terminology for pathogens that transmit through the air", which will provide a comprehensive introduction and definition of these terms. This selection is made in anticipation of the standardization of this terminology, ensuring that the present document is aligned with the evolving scientific consensus.

Source control (outward): The use of a face mask, personal ventilation devices and other means as a preventive strategy for covering the source of the respiratory particles (the mouth and nose) and reducing potentially infectious exhaled particles from being dispersed in the air around the infected person [9].

Susceptible host: Individuals who are likely to develop a communicable disease after exposure to the infectious agents [24]. Can also be used interchangeably with susceptible person.

Through the air transmission*: The descriptor ‘through the air’ can be used in an overarching way to characterize an infectious disease where transmission involves the pathogen travelling through or being suspended in the air.

Variants of concern (VOC): Defined by the World Health Organisation, VOC refers to a SARS-CoV-2 variant that meets the definition of a VOI (below), and also demonstrates to be associated with one or more of the following changes at a degree of global public health significance: increase in transmissibility or detrimental change in COVID-19 epidemiology; increase in virulence or change in clinical disease presentation; or decrease in effectiveness of public health and social measures or available diagnostics, vaccines, therapeutics [25].

Variants of Interest (VOI): Defined by the World Health

Organisation, VOI refers to a SARS-CoV-2 variant with genetic changes that are predicted or known to affect virus characteristics such as transmissibility, disease severity, immune escape, diagnostic or therapeutic escape; and identified to cause significant community transmission or multiple COVID-19 clusters, in multiple countries with increasing relative prevalence alongside increasing number of cases over time, or other apparent epidemiological impacts to suggest an emerging risk to global public health [25].

Ventilation (rate): Ventilation is the process of supplying outdoor air (or outdoor air plus recirculated air that has been treated) to and removing indoor air from a space, for the purpose of controlling air contaminant levels, potentially accompanied by humidity and/or temperature control, by natural or mechanical means [9]. It is usually measured as m³/hr or l/s or Air Changes per Hour (ACH).

Viral Viability: The ability of a virus to produce an infection or a replication-competent virus [26].

Viability decay: The rate of loss of infectivity [26]. Can also be used interchangeably with biological decay.

Viral concentration: The number of viral copies contained in unit quantity. Concentrations are most commonly expressed as unit per volume or mass per unit volume (i.e., viral genome copies per ml clinical sample, viral copies per liter air) [8].

Virion: an entire virus particle, consisting of an outer protein shell called a capsid and an inner core of nucleic acid [27]

* This terminology is derived from the forthcoming WHO publication “Global technical consultation report on proposed terminology for pathogens that transmit through the air”, which will provide a comprehensive introduction and definition of these terms. This selection is made in anticipation of the standardization of this terminology, ensuring that the present document is aligned with the evolving scientific consensus.

Executive summary

Context

The SARS-CoV-2 virus can spread in several ways: through zoonotic transmission, direct and indirect contact transmission, direct deposition transmission, and inhalation or airborne transmission. An increasing body of evidence [28]–[31] suggests that it is transmitted through infectious fluids released from an infected individual as particles of different sizes and quantities, such as during breathing, speaking, coughing and sneezing. While the largest particles travel downwards quite rapidly, the smaller ones remain suspended in the air for longer periods and can travel farther distances. When people are in close proximity, transmission of infectious particles can occur through direct inhalation (short-range) and deposition onto the mucous linings of the respiratory tract and ocular membranes of a susceptible host particularly in the absence of face covers and ventilation. ‘Long-range’ transmission can occur in enclosed settings when infectious particles accumulate over time in a given volume, where the concentration of virions is sufficient enough to cause infection once infectious particles are inhaled by a susceptible host.

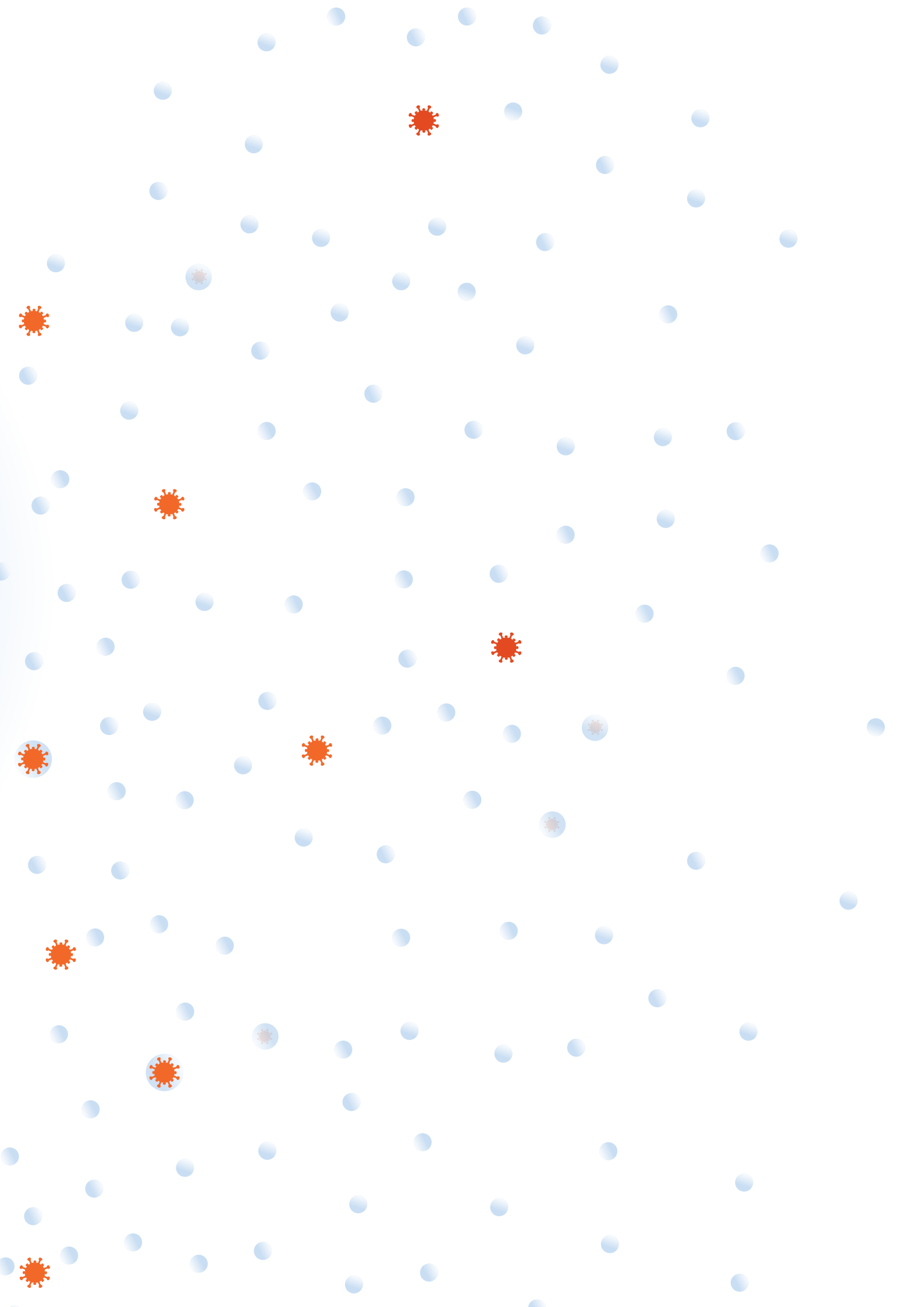
A means of quantifying the risk of SARS-CoV-2 airborne transmission in a standardized manner (using a standardized model) in residential, public and health care settings is essential to inform non-pharmaceutical risk reduction measures, such as increasing ventilation, air cleaning and disinfection, source control interventions, and controlling the occupancy, as well as to communicate the risk and enable informed decisions by the occupants.

Methods

The development process of the airborne transmission modelling included several stages: defining the mechanism of airborne transmission, identifying priority questions and outcomes, retrieving the evidence, assessing, and synthesizing the evidence, formulating, and testing the model. Key findings from the identified studies have been extracted and collated. Discrepancies in the extracted findings and recommendations were then reviewed in consultation with national and international experts. The process also required the establishment of the Airborne Risk Indoor Assessment (ARIA) Technical Advisory Group which constituted an ad-hoc advisory panel supporting WHO’s World Health Emergencies preparedness, readiness and response to COVID-19 and included, amongst others, members of the Global Infection Prevention and Control Network, members of the Environment and Engineering Control Expert Advisory Panel (ECAP) for COVID-19, representatives from the European Organization for Nuclear Research (CERN), technical experts from ministries of health and similar institutions (see Acknowledgements), and WHO staff and consultants from different departments including Environment, Climate Change and Health, Infection Prevention and Control, and Operations Support and Logistics. The external review group included WHO’s Global Infection Prevention and Control Network (GIPCN), WHO’s Environment and Engineering Control Expert Advisory Panel (ECAP) for COVID-19 and WHO’s EPI-Tag Group. Benchmarking against available literature has been undertaken to validate the model.

Outcomes

This process resulted in a new multi-box model to quantify the risk of SARS-CoV-2 airborne transmission that incorporates additional knowledge of factors related to inhalation transmission compared to the conventional Wells–Riley equation. The new model allows for uncertainty in the parameterization and description of degree of confidence in model output. Based on this model an online, user-friendly tool to assess SARS-CoV-2 airborne transmission risk in residential, public and health care settings was developed. Its application by Infection Prevention and Control specialists, building managers, health care facility managers and the general public will inform risk reduction measures and enable informed decisions by end-users.



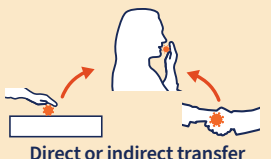
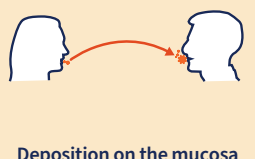
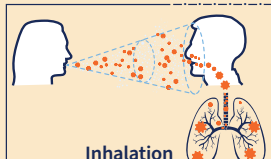


Introduction

Understanding how pathogens spread is essential for informing the development of transmission-based precautions to prevent and control infections. Since the mid-twentieth century, indoor ventilation has been intentionally used to reduce the risk of airborne transmission. However, the rationale behind ventilation standards in healthcare and residential settings may differ in purpose. This document offers an overview of the basis for these standards before introducing an innovative method to quantify the risk of SARS-CoV-2 airborne transmission in indoor settings, thereby providing an alternative approach to developing ventilation requirements that lower the risk of SARS-CoV-2 infection.

Modes of transmission

The mechanisms of infection transmission are complex, with the risk of disease determined by numerous factors that have considerable and uncertain variability, including the characteristics of the pathogen concerned, the infectiousness of the host, the media in which it passes from the source to new hosts and the immune response of the exposed host [32]–[34]. Transmission through the air complicates this further by adding other influencing factors [35] such as the dispersion and distribution of infectious respiratory particles (IRPs); the effect of temperature, relative humidity and ultraviolet radiation on the survival of the pathogen [15], [28], amongst other factors. Respiratory viruses can spread via three major modes of transmission (Table 1).

Table 1. Summary of mode of transmission terminology.

	Contact transmission	Direct deposition transmission	Airborne or inhalation transmission	
New definitions	<p>The spread of an infectious agent caused by physical contact of a susceptible host with people or objects.</p> <ul style="list-style-type: none"> Direct contact transmission involves both a direct body-surface-to-body-surface contact and physical transfer of microorganisms between an infected or colonized person and a susceptible host. Indirect contact transmission involves contact of a susceptible host with a contaminated intermediate object (e.g., contaminated hands) that carries and transfers the microorganisms. 	<p>The process whereby larger infectious respiratory particles are directly deposited onto the conjunctivae and mucous membranes of the upper respiratory tract (mouth, nasal, through or pharynx mucosa) of a susceptible person, having followed a projectile motion after emission from the infected person.</p> <p>This mode of transmission only occurs at “close proximity”.</p>	<p>The process whereby aerosolized infectious respiratory particles (IRPs) are inhaled and enter the respiratory tract of a susceptible person, move through the upper and then lower parts of the respiratory tract, and can be deposited on the tissue at any point along the tract, potentially even reaching the distal alveolar region.</p> <p>This mode of transmission can occur when IRPs have travelled either a short or a long distance (range) after emission from an infected person or after resuspension of deposited particles from surface.</p>	
			<p>Short-range</p> <p>Transmission occurring via inhalation of aerosolized infectious respiratory particles inhaled by a susceptible host at a distance up-to 2 meters from the infected person/ source of infection.</p>	<p>Long-range</p> <p>Transmission occurring via inhalation of aerosolized infectious respiratory particles by a susceptible host at a distance farther than 2 meter from the infected person/ source of infection.</p>
Distance from the source of infection & particles sizes transmission	 <p>Direct or indirect transfer</p>	 <p>Deposition on the mucosa</p>	 <p>Inhalation</p>	 <p>Inhalation</p>
				
<p>World Health Organization, Global technical consultation report on proposed terminology for pathogens that transmit through the air (In press)</p>				

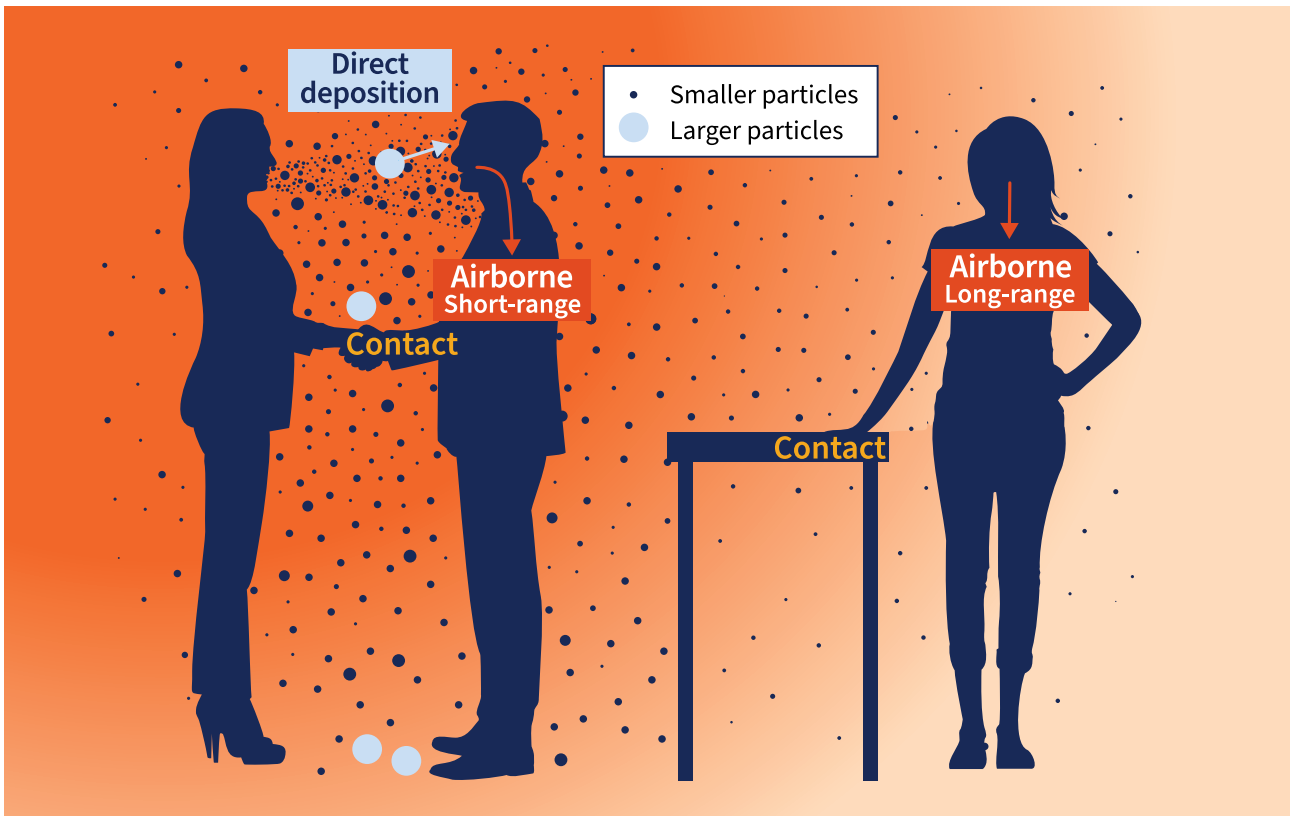


Figure 1. Mechanism of transmission through infectious respiratory particles.

Adaption with permission from: L. C. Marr and J. W. Tang, "A Paradigm Shift to Align Transmission Routes with Mechanisms," *Clin Infect Dis*, Volume 73, Issue 10, 15 November 2021, Pages 1747–1749, <https://doi.org/10.1093/cid/ciab722>

Airborne or Inhalation transmission*: The process whereby aerosolized infectious respiratory particles (IRPs) are inhaled and enter the respiratory tract of a susceptible person, move through the upper and then lower parts of the respiratory tract, and can be deposited on the tissue at any point along the tract, potentially even reaching the distal alveolar region. This mode of transmission can occur when IRPs have travelled either a short or a long distance (range) after emission from an infected person or after resuspension of deposited particles from surface. See also Figure 1.

Direct deposition transmission*: The process whereby larger infectious respiratory particles are directly deposited onto the conjunctivae and mucous membranes of the upper respiratory tract (mouth, nasal, through or pharynx mucosa) of a susceptible person, having followed a projectile motion after emission from the infected person. This mode of transmission only occurs at short range, or what can be described as at a "conversational distance" [1]. See also Figure 1.

Contact transmission*: The process whereby infectious particles, of any size, either settle on a surface at any distance from the source following emission, or are transferred directly from (usually) the hands of an infected person (by the infected person touching their own eyes, nose or mouth); and then transferred to the mucosal membrane of a susceptible person when that person either touches the contaminated surface or the hand of the infected person followed by touching their own eyes, nose or mouth. The former (i.e., transmission via touching contaminated surface) is often referred to as indirect contact transmission and the latter (i.e., transmission via touching the hand of infected person) as direct contact transmission. See also Figure 1.

The SARS-CoV-2 virus can spread in several ways: through zoonotic transmission, direct and indirect contact transmission, direct deposition transmission, and inhalation or airborne transmission. An increasing body of evidence [28]–[31] suggests that it is transmitted through infectious fluids released from an infected individual as particles of different sizes

* This terminology is derived from the forthcoming WHO publication "Global technical consultation report on proposed terminology for pathogens that transmit through the air", which will provide a comprehensive introduction and definition of these terms. This selection is made in anticipation of the standardization of this terminology, ensuring that the present document is aligned with the evolving scientific consensus.

and quantities during breathing, speaking, coughing and sneezing [36]. While the largest particles settle quite rapidly, the smaller ones remain suspended in the air for longer periods and can travel longer distances [37], [38]. When people are in close proximity, transmission of infectious particles can occur through direct inhalation (short-range) and deposition onto the mucous linings of the respiratory tract and ocular membranes of a susceptible host. The ‘long-range’ transmission can occur in indoor, enclosed settings when infectious particles accumulate over time in a given volume, at room scale, where the viral concentration is sufficient enough to cause infection once infectious particles are inhaled by a susceptible host. The concentration of infectious particles in the air can increase rapidly with poor ventilation, a small volume of air in an enclosed indoor space, overcrowding (especially with the presence of multiple infected individuals), and the amount of time spent in the space by the infected person [39].

Quantifying the probability of SARS-CoV-2 infection through the inhalation mechanism is essential to inform the development of risk reduction measures such as indoor risk-based ventilation standards.

In an attempt to fill this need, several quantitative tools have been developed by a variety of scientists and engineers to model the SARS-CoV-2 infection

risk that may be potentially associated with indoor occupancy in various settings and circumstances during the pandemic. While these tools incorporate various aspects of ventilation, air filtration and disinfection as a primary control measure, they differ in their inclusion of epidemiological aspects and variables, in how emission sources are represented, and in how risk is calculated based on a time dependent exposure to infectious aerosols. They also differ in terms of their platform, target users, and overall degree of technical complexity. For these tools to be widely used and be able to inform policy and/or induce an update in the regulatory framework, they must be applicable to a diverse building stock, apply the most up to date scientific knowledge of aerosol science and host-pathogen interaction and most importantly be validated by quality real-world epidemiological studies to reduce the bias. They must also be easy to use and understand, contribute towards a broader understanding of “airborne transmission” and improve scientific consensus surrounding its importance in public, residential and healthcare settings. For the above reasons, the World Health Organization, in collaboration with partners and external experts, decided to develop this new standardized model.

Infection risk and indoor ventilation

Prior to the COVID-19 pandemic, studies in engineering and aerosol science looked at the possible transmission routes of respiratory diseases [40] and suggested that insufficient ventilation increases the risk of transmission of these pathogens in enclosed settings [41], [42]. However, there was limited attention on the relevance of ventilation for the purpose of transmission control except for some specific diseases such as Tuberculosis. In addition, the complexity of the risk from different transmission modes during close-proximity encounters with infected people was neglected but needs to be considered.

The SARS outbreaks [43] in 2003, the MERS-CoV outbreaks in 2012 [44], and the current SARS-CoV-2 pandemic, have given a new impetus to research in this field leading to application of the existing theories and models in practice, development of new evidence, and raised awareness of the importance of ventilation strategies and indoor air quality for public health purposes – in both healthcare facilities and other public settings.

Ventilation standards for IPC

Currently, the recommended minimum ventilation rate for hospital rooms under airborne precautions is 12 air changes per hour (ACH) or 160 L/s per patient in most guidelines [45][46]. This originates from a previous requirement of 6 ACH in guidelines for preventing the transmission of *Mycobacterium tuberculosis* (TB) in isolation and treatment rooms, published in 1994 by the Center for Disease Control and Prevention (CDC) [47]. Subsequently, following the 2003 SARS outbreak, a safety factor of 2 was applied to this value for the construction of new healthcare facilities [48]. The choice of 6 ACH was based on comfort- and odour-control considerations, noting that its effectiveness in reducing transmission of airborne pathogens by reducing aerosols in the room has not been evaluated adequately. Nonetheless, ventilation rates above this threshold are likely to provide significantly greater reduction in the concentration of infectious aerosols [49]. Increasing the ventilation rate will increase the dilution effect of infectious particles in the air inside a room and thus decrease the risk of transmission of infectious aerosols to those present. However, the critical threshold for ventilation rates above which there

is no further reduction of infection risk depends on multiple factors [50], and the choice of the ventilation flow rate may be influenced by other considerations such as space allocation, type of activity performed inside the space (i.e., housing, office, gym, etc.), layout, flow directions, mixing, energy considerations, technical feasibility, carbon cost and environmental sustainability, among others [51].

The threshold of the current ventilation rate for healthcare settings is related to this rationale:

- the effect of ventilation (air-change) rate on the reduction of aerosol concentration; and
- the effect of ventilation rate on infection risk for known airborne diseases estimated by mathematical modelling using the Wells–Riley equation.

According to the Wells–Riley equation, the probability of infection through infectious aerosols is inversely proportional to the ventilation rate. The probability of infection is expressed in terms of inhaled quanta. A quantum is defined as the dose of infectious airborne particles required to infect a subject with a probability of 63% [40], [52]. The parameters used in the Wells–Riley equation include ventilation rate, quantum generation rate from the source, inhalation rate of susceptible persons, and duration of exposure [50].

$$P = \frac{D}{S} = 1 - \exp\left(-\frac{I p q t}{Q}\right)$$

Where:

P: probability of infection for susceptible persons

D: number of disease cases

S: number of susceptible persons

I: number of infectors

p: breathing rate per person (m³/s)

q: quantum generation rate by an infected person (quanta/s)

t: total exposure time (s)

Q: outdoor air supply rate (m³/s)

Based on this model, in situations of high quanta emission, assuming 5 quanta/minute and a minute volume of 6 litres/minute, in a room of around 85 cubic metres, the estimated probability of infection for a 15-minute exposure in a room with 3, 6 and 12 ACH would be 10%, 5% and 3% respectively [40].

Ventilation standards in non-healthcare settings

Many of the existing standards [53] and guidelines [40], [54], [55] that consider airborne infection risk, on top of other factors, were developed specifically for health care settings. Ventilation rate requirements in current standards for commercial, institutional and residential buildings [56]–[58] considers thermal comfort, odour control, indoor air quality (e.g. different pollutants such as dampness, moulds, combustion, and smoking), energy consumption, operating mode and occupancy. Considering the technical requirements, energy consumption and environmental sustainability, implementation of ventilation requirements which aims to reduce airborne infection risk in residential and non-residential settings should be done carefully to balance as much as possible the different requirements.

Ventilation to lower indoor airborne infection risk

Scientific expertise has evolved significantly since the mid-twentieth century, when the Wells–Riley equation was developed [59]. Important progress in molecular biology, aerobiology, aerosol physics and other disciplines expanded the understanding around airborne transmission dynamics and its mechanisms, prompting the scientific community to improve the public health guidance for a given setting and based on this, inform the development of risk-based ventilation standards and their application.

In particular, the COVID-19 pandemic has highlighted the urgent need for improved methods of conducting risk assessments to determine the risk of airborne transmission in various indoor spaces and to develop specific recommendations for indoor ventilation.

Scope of the document

This manual aims to define a new model, with a standard method to quantify the risk of SARS-CoV-2 airborne transmission in indoor settings according to the current evidence available at the time of this publication. The model aims to inform the development of risk-based ventilation recommendations to mitigate the inhalation risk, as well as to provide an agreed foundation for future guidance related to other respiratory and potentially airborne diseases. In particular, this document aims to:

1. Define a standardized model, to quantify SARS-CoV-2 airborne risk transmission in different indoor settings including residential, public and health care settings
2. Guide the development of an online, user-friendly tool to enable the general public and building managers to assess SARS-CoV-2 airborne risk transmission in residential, public and health care settings and inform risk reduction measures.

The new model will also provide a baseline from which to test the transmission capacity for SARS-CoV-2 variants of concern as well as other airborne pathogens and provide an agreed foundation for future guidance related to other respiratory and potentially airborne diseases.

IMPORTANT NOTE

While SARS-CoV-2 can spread through multiple routes of transmission, this model is only considering short- and long-range airborne transmission with short-range limited to particle inhalation and not direct deposition.

While this document provides guidance to Member States and regulatory bodies for the development of risk-based ventilation rates and inform future interventions, the online web application is meant to provide an accessible tool to estimate the infection risk probability in various indoor settings. General public and building managers can use this online, user-friendly tool to assess SARS-CoV-2 airborne risk transmission to inform risk reduction measures such as increasing ventilation, reducing occupancy, and wearing a higher filtration efficiency mask. Its application by Infection Prevention and Control specialists, building managers, health care facility managers and the general public will inform risk reduction measures as well as to enable informed decisions by the users:

<https://partnersplatform.who.int/aria>

The ARIA online tool is powered by the CAiMIRA [60] technology which was initially developed by CERN and modified over time by the ARIA Working Group, to fit the proposed model. The model on which ARIA is based, is succinctly described hereafter.

Methodology

The process of development of this manual included several stages. Firstly, it was important to define the mechanism of airborne transmission, identifying priority questions and outcomes, retrieving the evidence, assessing, and synthesizing the evidence, formulating, and testing the model, and planning for its dissemination and implementation. The process also required the establishment of the following bodies: a WHO Steering Group, a Technical Advisory Group, and an external review group, all created according to WHO's policies and procedures. The Airborne Risk Indoor Assessment (ARIA) Technical Advisory Group constituted an ad-hoc advisory panel supporting WHO's World Health Emergencies preparedness, readiness and response to COVID-19 and included, amongst others, members of the Global Infection Prevention and Control Network, members of the Environment and Engineering Control Expert Advisory Panel (ECAP) for COVID-19, representatives from the European Organization for Nuclear Research (CERN), engineers and architects from relevant professional networks, organizations and institutions specialized in health care settings, technical experts from ministries of health and similar institutions (see Acknowledgements), and WHO staff and consultants from different departments including Environment, Climate Change and Health, Infection Prevention and Control, and Operations Support and Logistics. All authors contributing to this document and members of the external and internal review panels completed and signed the declaration of interests (DOIs) forms. The technical unit collected and managed DOIs. In addition to the distribution of a DOI form, during the meeting, the WHO Secretariat described the DOI process and provided an opportunity for members to declare any interests not provided in written form. Web searches did not identify any additional interests that could be perceived to affect an individual's objectivity and independence during the development of the document. No member was judged to have a significant conflict of interest.

The external review group included the WHO's Environment and ECAP for COVID-19. Benchmarking against available literature has been undertaken to validate the model.

The development process for the model was streamlined through a framework mirroring the different components of the inhalation mechanism as defined by the Technical Advisory Group and visualized in Figure 2. The variables of each component in the model are described underneath while the interactions are articulated through the mathematical architecture of the model.

The model uses a probabilistic approach to deal with the uncertainties of the included variables. To identify the specific values for the model, different methodologies have been proposed and agreed upon by the Technical Advisory Group. Initially, experts have been invited to assess the different variables according to the model's components, including emission and removal rate, exposure, concentration, cumulative dose, and probability of infection. Subsequently, several specific research questions have been developed to inform the required systematic reviews. Search strings, eligibility criteria and data extraction are available in Annex 1. The review did not include appraisal for risk of bias as all values have been included and the probabilistic approach enables to deal with the variable's uncertainties.

Key findings from the identified studies have been extracted and collated. In addition, a review and adaptation of relevant airborne risk assessment tools published (Annex 2), reviewed and presented during the International Society of Indoor Air Quality and Climate (ISIAQ) webinar "Modelling infection risk from indoor aerosol exposure to SARS-CoV-2" [61], as well as the CERN Airborne Model for Indoor Risk Assessment (CAiMIRA), formerly known as CARA [62], and the Airborne Infection Risk Calculator (AIRC) [63], both presented during a WHO Expert Panel meeting have been considered. Discrepancies in the extracted findings and recommendations were then reviewed in consultation with national and international expert members of the Technical Advisory Group.

IMPORTANT NOTE

This manual aims to provide the rationale behind the development of the model to quantify the risk of SARS-CoV-2 airborne transmission as well as the methodology applied for value sourcing. The systematic review outcomes are presented hereafter.

Since the beginning of the SARS-CoV-2 pandemic, new pathogen-related data has been published at an unprecedented rate. In order to ensure the most up-to-date values for the model and facilitate users' accessibility and usability, an online tool has been developed and will be updated regularly.

The manual and the webapp will be disseminated through WHO channels, OpenWHO, Techne network, the Indoor Environmental Quality Alliance, CERN network and the American Society of Heating, Ventilation and Air Conditioning network. The uptake and impact assessment will be ensured by the webapp user data.

Model Validation

A series of benchmark scenarios were identified from peer-reviewed papers describing outbreaks related to long-range airborne transmission. The working group collected the data based on the scenarios reported in the rapid systematic review by Duval et al. [16] (18 outbreaks included) and the study by Miller et al [64] on the Skagit Valley Chorale event [65]. From the 19 studies/outbreak investigations, 8 were eligible to perform the corresponding model simulation. The objective was to evaluate and compare the attack rate estimated in the scientific publication against the estimation calculated by the model.

Following the analysis, it was observed that the reported attack rate in the different outbreaks was in the high percentile band of the statistical result from the model. The results fall between the 90th and 98th percentiles. In other words, the model prediction points to the fact that some random variables (i.e., viral load, IPs emission or frequency of close-range encounters) need to be significantly higher than average values to replicate the epidemiological evidence deduced in the aforementioned literature. A detailed report of the benchmark assessment is available in Annex 3.

Despite falling in the probability of infection distribution calculated by the model, these results suggest that the included papers present some specificities. For instance:

- High viral loads of the infector(s): in the model, the viral load value at 90th percentile is ~9 log RNA copies;
- The importance of possible close-proximity encounters (contribution of short-range exposure), which were neglected in both the reported studies and simulations (*Note: the model is capable of assessing the impact of close-proximity encounters*).

The high viral load percentile is comparable to the evidence observed in literature for outbreaks with (long-range) airborne transmission identified as the main mode of transmission. These clusters are often categorized as superspreading events [66] where the source was likely to be classified as an emitter shedding higher than average viral loads and emitting statistically more infectious particles, although other factors such as crowding and poor ventilation may also lead to superspreading events.

Inhalation transmission mechanism

The Technical Advisory Group agreed to describe the inhalation transmission mechanism as a sequential five steps or components process with the short- and long-range transmission terms unfolding simultaneously (Figure 2). The first component is the **emission rate** defined as the number of virus-laden particles exhaled by an infected person per unit of time. The overall volume and size distribution of respiratory particles emitted is related to the type of respiratory and expiratory activities which are affected by the physical activity performed by the infected person as well as by the voice amplitude. This complex interaction leads to the total amount of respiratory particles emitted which can be significantly reduced through the use of different types of control measures, such as masks for source control, which is dependent on their outward filtration efficiency. The number of virus-laden particles exhaled in a given time, combined with the viral RNA copies exhaled inside those same particles, produces the emission rate which concurs for the short- and long-range transmission mechanisms simultaneously.

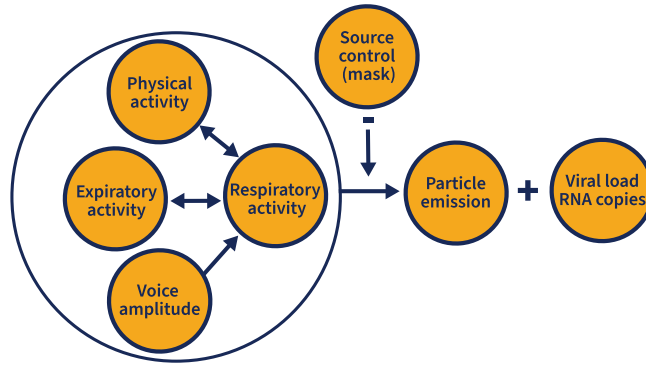
The second component affecting the inhalation transmission mechanism is the **removal rate** which can be defined as the total number of aerosolized virions removed from the air in a given time. The sum of several variables constitutes the overall removal rate including the dilution over distance from the source of emission, the dilution due to indoor ventilation or equivalent ventilation, inactivation by air cleaning or sterilization, gravitational settling, and the pathogen-specific biological decay, with the last two features affected by air distribution profiles and environmental conditions such as indoor temperature and relative humidity.

The difference between the emission rate and the removal rate leads to the third component, the **exposure**. This component can be defined as the concentration of virions in ambient air, during a given time, at which a susceptible host comes in contact with. The exposure is significantly affected by the distance from the source, for the short-range transmission, and by time (duration of event), space volume and number of infectors present in the space for the long-range transmission.

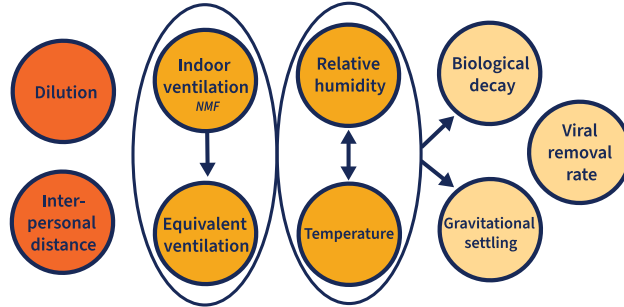
The fourth component is the **cumulative** or **absorbed dose**--meaning the total number of infectious particles inhaled and subsequently absorbed by a susceptible host during the exposure event. For short-range transmission, the cumulative dose depends mainly on the distance between infector and susceptible host, respiratory activity of the susceptible host, time spent in close proximity with the source of infection, and how often such an interaction happens. While physical activities and time spent inside the space as well as ventilation rates affect the long-range transmission, the use of a mask can reduce the overall absorbed dose for both short- and long-range transmission. Moreover, as the deposition pattern may determine their future clearance and insult to tissue, respiratory tract deposition and ratio of viable virus within the respiratory particles are important factors for the transmission mechanism.

Finally, the pathogen infectious dose, the host immunological status and the specific SARS-CoV-2 variant transmissibility, contribute to the complex dose-response model which, in combination with the cumulative absorbed dose, define the host **probability of infection** which completes the fifth and final component. Each component and its variables are described in detail hereafter.

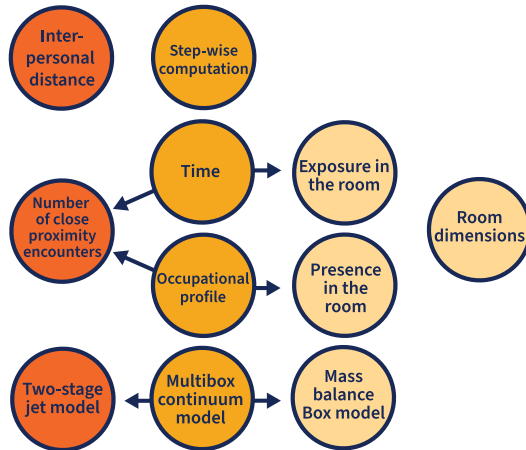
1. Emission rate



2. Removal rate



3. Exposure



4. Cumulative (absorbed) dose



5. Probability of infection (i.e. transmission/risk profile)

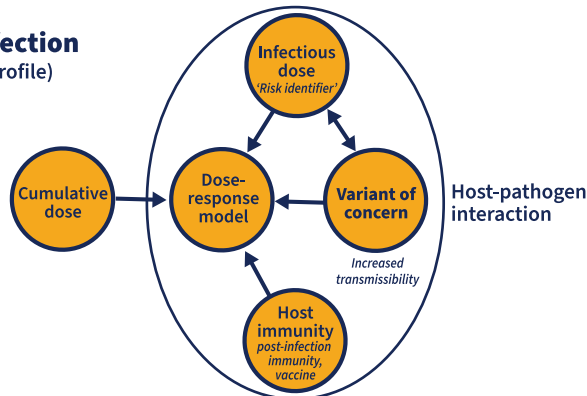
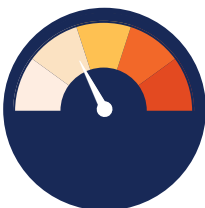


Figure 2. Inhalation transmission mechanism
Short- and long-range inhalation transmission mechanism representation.

Model description

While most existing tools rely on the concept of quanta developed by Wells and Riley, the proposed model goes beyond the pure mechanical estimation of the risk, relating physiological mechanisms of respiratory particles emission, the virological characteristics of the pathogen, immunological effects, and classical environmental features such as ventilation, temperature, and volume, among others, as described in the inhalation transmission mechanism. Each variable is described hereafter. Moreover, while airborne transmission involves a continuum of exhaled particles of different sizes [67], short- and long-range risk assessments require a divided yet complementary approach as described in the model architecture.

Model architecture

The Technical Advisory Group agreed that the proposed model should use a multi-box approach accounting separately for the short- and long-range contributions (Figure 3). Firstly, this approach is found to be the most suitable combination to include the concentration gradient between short-range (in close proximity to the infector) and long-range (room scale or farther than conversational distance) transmission, while maintaining a relatively simple algorithm from a computational and user interface point of view. Secondly, the new model incorporates multiple factors such as the biological characteristics of the pathogen, host factors, such as physiological characteristics of respiratory particle emission and immunity, and finer details of environmental features, which would allow parameterization for different settings, as well as future adaptation to new variants or other respiratory pathogens. In addition, the model follows a probabilistic approach to deal with the uncertainties tied to the concerned variables and mechanisms, such as the virological characteristics of the pathogen and the physiological characteristics of respiratory particle emission. The high-level analytical formulas used in the model are resumed in the Annex 4 while the non-setting specific values and their distributions are available in Annex 5.

Box 1: Long-range

Simplified modelling of long-range transmission relies on the well-mixed approach meaning that an immediate homogeneous viral distribution, within a given finite volume, is assumed. The infection risk results from exposure to a given concentration in the room and the inhalation of size-stabilized particles, within a given range. The long-range concentration is time-dependent, subject to different sets of measures applied (such as ventilation) and is assumed to be accumulating in an instantaneous spatially uniform way, within the concerned volume. Such concentration is determined, over time, by solving a mass-balance differential equation comparing the viral emission and removal rate as a function of different environmental and virological variables, i.e., air exchange, filtration, gravitational deposition/settling, viability decay, aerosol deposition in the respiratory tract, viral load, among others.

Box 2: Short-range

This box aims to estimate the risk when in close proximity (conversational distance) to the source of infection using the continuum and two-stage jet model developed by Jia et al. [68]. In particular, this box considers the distance within which there is an expected higher viral concentration and elevated infection risk, relative to the well-mixed room, due to the direct exposure to the expiratory jet and inhalation for potentially larger concentrations during short distance encounters, assumed to be <2 m. The short-range component of the risk assessment is then added to the long-range component for the overall risk estimation.

The probability of secondary transmission is then estimated based on the number of occupants of varying susceptibility, breathing the viral concentration in the room air over the course of time, determined by the respective inhaled doses of viable viruses (including susceptible persons entering and leaving the room at different times) plus the estimated short-range risk. In the multi-box model approach the contribution for the long-range component is added to the short-range component, i.e., the cumulative dose is a sum of both exposures.

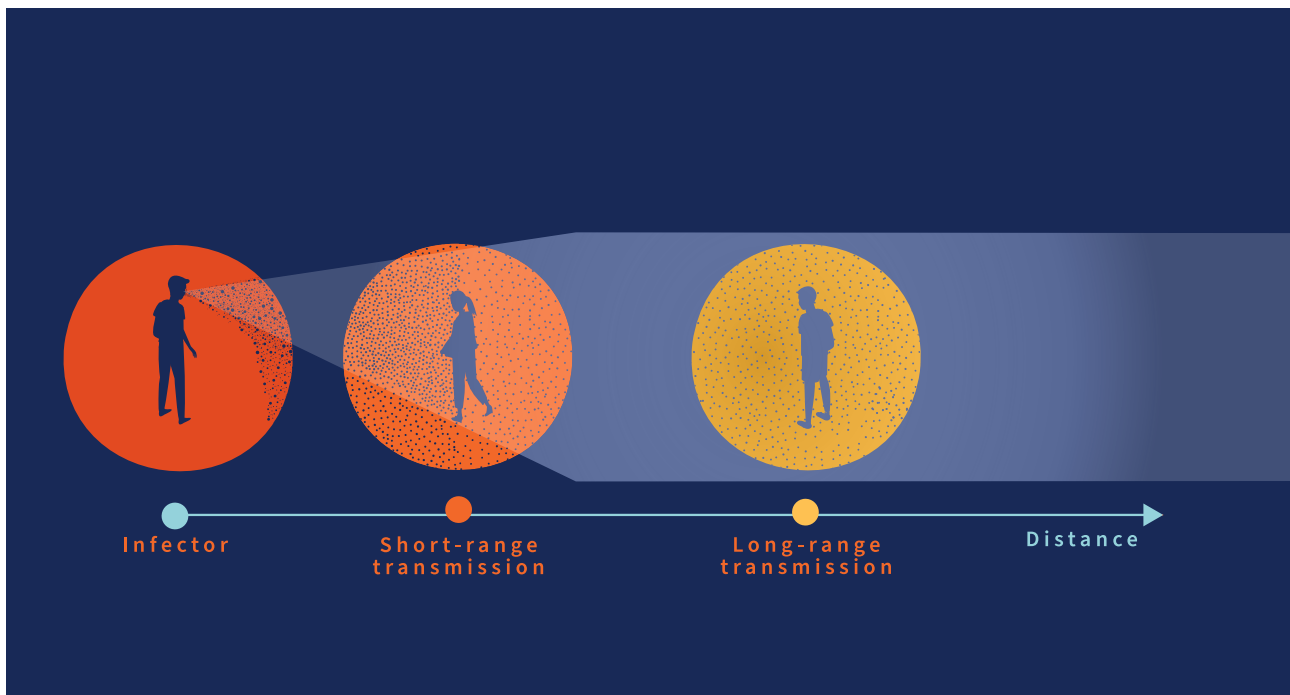


Figure 3. Multi-Box Model

Interaction of short- and long-range transmission and infection respiratory particles concentration reduction according to distance from the source of infection.

Emission rate

The emission rate of virions is a product of several variables, such as the physiological breathing mechanism, the physics of particle transport in the respiratory tract, the particle size distribution created at different locations of the respiratory tract, specific features of the pathogen and variability between host such as exhaled viral load. In particular, these variables can be further specified into the interaction of respiratory activity (including voice amplitude) and physical activity leading to respiratory particle emission, the emitted viral load (within the particles), and the possible use of source control measures (i.e., mask) which affect the overall emission rate.

Respiratory particles

Humans emit hundreds of aerosolized particles of different sizes during exhalation, and even more when speaking and singing [69]. Those aerosolized particles are water-based solutions of salts, containing mucus, proteins and may contain other material present on the surface of the respiratory tract including infectious pathogens. Thus, viruses on the surface of the respiratory tract can be released in the exhaled particles out of a person's mouth and nose [70]–[72].

Particle aerosolization mainly results from an air-stream passing sufficiently quickly over the surface of a liquid to create separation. Several physiological phenomena contribute to aerosolization of respiratory fluid [73]. When exhaling, respiratory fluid blockages

formed in the bronchioles burst and produce aerosolized particles released at the next exhalation – this is called bronchiole fluid film burst (BFFB)[74]. The vocal cord vibration during vocalization also aerosolizes the fluid by bathing the larynx, while the interactions between the tongue, teeth, palate, and lips aerosolize the saliva during speech articulation. Before being emitted, the particles undergo processes in the respiratory tract which change their size distribution. Furthermore, the respiratory tract contains relatively small-scale, curved viscous and viscoelastic films, which wrinkle during exhalation and thereby break up, leading to aerosol production. Emitted particles range in diameter from 0.01 and 1000 μm depending on the generation mechanism, respiratory and vocalization activity, age and site of origin [52], [74]–[76]. The size distribution is further affected by the quasi-instantaneous evaporation process particles have undergone after leaving the body. Particles of diameter smaller than 100 μm are likely to become airborne and remain suspended in the air from seconds to hours, because of their reduced size and settling velocity compared to larger ones [77]. The volumetric particle emission concentration can be estimated considering the specific anatomical processes originating in the aerosol, the bronchial region, the larynx, and the oral cavity. The aerosol concentration size distribution for speaking and coughing can therefore be modelled as a tri-modal lognormal distribution known as the Bronchiolar/Laryngeal/Oral (B.L.O.) tri-modal model [78].

SARS-CoV-2 viral load

SARS-CoV-2 viral load detected by RT-PCR in nasopharyngeal swabs is widely distributed, ranging from 3 to 10 log₁₀ copies/ml with a median of 6.78 log₁₀ copies per ml [79]. The limited data on viral load in exhaled breath suggests high variability between infected individuals. While not every infector has detectable virus in exhaled breath, those who present detectable virus in breath range between 2-7 log₁₀ copies for 15-60 minutes of expiratory activity [80]–[82]. Observations from SARS-CoV-2 and other coronaviruses suggest that correlations between the viral load in nasal/ throat specimens and exhaled breath may vary between specimen types [81], [83], [84]. The wide variation in viral load between individuals depends on factors such as age [85], [86], vaccination status [87], [88] and possibly exposure history, and variants of concern [89], [90]. Moreover, the highest mean viral load occurs quickly after symptom onset and at a higher magnitude in individuals with more severe COVID-19 symptoms [85], [91], [92]. The viral shedding episodes have a sharp upswing to reach the peak viral load, followed by a prolonged decay [85], [88]. The duration of viral shedding varies widely and correlates with viral load peak [93]. Although viral load and cell culture infectivity cannot be translated directly to transmission probability, it is likely that the rapid spread of certain SARS-CoV-2 VoCs is partly attributable to higher viral load [91]. Due to the large variability of the viral load [94], this model proposes a probabilistic approach considering the viral load distribution rather than a single value.

Source control (outward)

Throughout the pandemic, the use of well fitting masks to cover the mouth and nose have been widely applied as a source control measure to reduce the emission of respiratory particles and thereby reduce the potential emission of infectious particles from infected people. Studies have supported that wearing a mask to protect others from potentially infectious particles is a highly effective infection control measure to limit the spread of COVID-19 [95], [96]. Well fitting masks provide a physical barrier to the emission of both large and small respiratory particles [97]–[99], and depending on

the virus type, are also effective in reducing exhaled infectious particles [71], [84].

Both medical masks and respirators, even without fit-testing, can reduce the outward particle emission rates by 74% and 90% on average during speaking and coughing, respectively, compared to wearing no mask, corroborating their effectiveness at reducing outward emission [97]. In contrast, shedding of non-expiratory micron-scale particles from friable cellulosic fibres in homemade cotton-fabric masks may confound explicit determination of their efficacy at reducing respiratory particle emission [97].

Respiratory rate

The inhalation and exhalation processes, both for the infector and susceptible person, contributes significantly to the overall infectious particles concentration as well as to the absorbed dose [100]. It is therefore essential for the model to accurately account for the respiratory rate.

The breathing rate can vary significantly and changes with age [101] and physical activity [17]. The normal breathing rate is 12-20 respirations per minute for a resting adult while children have a higher rate [102]. The model proposes a respiratory rate categorization according to the EPA Exposure Factors Handbook [17] which is used as a reference for numeric estimates for behavioural and physiological characteristics needed to estimate exposure to environmental agents. The metabolically derived human breathing rates are based upon oxygen consumption rates by physical activity categorized by metabolic equivalent of work (METs) [17]. METs is an energy expenditure metric used by exercise physiologists and clinical nutritionists to represent activity levels. An activity's METs value represents a dimensionless ratio of its metabolic rate (energy expenditure) to a person's resting. After adjusting METs value for the oxygen consumption rate (VO₂), body weight, age and sex [17], the following categories were proposed: "sedentary", "passive", "light intensity", "moderate" and "high intensity". For each physical activity profile, there are three proposed possible combinations of respiratory activity as per Table 2.

Table 2. Physical and respiratory activity

Physical activity	Respiratory activity
Sedentary (i.e., sitting, resting)	Oral breathing Speaking Speaking loudly
Passive (i.e., standing)	
Light Intensity (i.e., walking)	
Moderate Intensity (i.e., jogging)	
High Intensity (i.e., vigorous exercising)	

Removal rate

The infectious particle removal rate is the sum of three main contributions: the ventilation rate [40] and equivalent ventilation (such as air filtration and disinfection) [103], the particle deposition via gravitational settling, and the virus inactivation or biological decay [65].

Ventilation rate and air cleaning devices

The purpose of ventilation in buildings is to provide healthy air for breathing by diluting pollutants originating in the building with clean air, and by providing an airflow rate to change this air at a given rate [40]. A well-designed, maintained, and operated ventilation system can reduce the risk of respiratory pathogens transmission, including SARS-CoV-2, in indoor spaces by diluting the concentration of potentially infectious particles through ventilation with outside air and filtration and disinfection of recirculated air. Natural ventilation can provide similar benefits. i.e., opening of windows and/or doors [9]. The removal rate due to ventilation and equivalent ventilation is obtained from the amount of air ($\text{m}^3 \text{h}^{-1}$) supplied to the space and the volume (m^3) of the room [104].

For filters that are portable and self-contained, the rate of particle removal from air passing through the filter is expressed as the clean air delivery rate (CADR), which is approximately equal to the product of airflow rate and the contaminant removal efficiency [105]. For the purpose of this document, air cleaning and disinfection devices, using filter category MERV (minimum efficiency reporting value) 14 / ISO ePM1 70-80%, high efficiency particulate air (HEPA) and higher filtration efficiency filter [9], as well as UVGI technology [106], are considered as equivalent ventilation and the Clean Air Delivery Rate (CADR) (m^3/h) is added up to the ventilation rate.

Viability decay

For inhalation transmission to occur, viruses within respiratory particles must remain infectious between emission from an infected person and inhalation by a susceptible host. Loss of infectivity during this period will decrease the likelihood of transmission [28]. The particle microenvironment is highly dynamic exposing the SARS-CoV-2 virions to extreme conditions of solute concentration, pH and evaporative cooling [107]. Several studies analysed the particle stability of SARS-CoV-2 in a controlled environment reporting similar half-life values with a median estimate of approximately 1.1 to 1.2 h [108]. However, environmental conditions, including relative humidity, UV radiation (e.g. from sunlight) and temperature, have been shown to

influence the decay rate of viruses in particles [26]. In the absence of an exhaustive database relating the SARS-CoV-2 biological decay in particle with temperature and relative humidity, an empirical regression is used, based on the experiments with simulated saliva [109]. Other possible values have been proposed for scenarios where $\text{RH} < 40\%$ and $\text{RH} > 40\%$ [104].

Gravitational settling

The residence time of virus-laden particles in air is crucial in determining their range of diffusion and concentration [28]. A primary question in the study of particle motion is the effect of turbulence on the average settling velocity of the particles. This affects the residence time of particles in the atmosphere and the growth rate of water particles falling under gravity [110]. The average settling velocity in homogeneous turbulence of a small rigid spherical particle, subject to a Stokes drag force, is shown to depend on the particle inertia and the free-fall terminal velocity in still fluid. With no inertia, the particle settles on average at the same rate as in still fluid, assuming there is no mean flow [2].

Assuming the composition of a given respiratory particle is dominated by water and/or organic solutes of similar density, the proposed mass density for ρ_p is 1000 kg m^{-3} . The process of particle diameter reduction due to evaporation is accounted by multiplying the saturated particle size with an evaporation factor, which will depend on the indoor relative humidity. If the particles are emitted from the mouth or nose of a person standing, the height at which the terminal velocity is reached is considered approximately $h = 1.5 \text{ m}$ from the floor [104]. The removal rate due to gravitational settlement is the terminal velocity (obtained from Stoke's law) and the height of 1.5 m.

Exposure (long-range transmission)

This section only refers to the long-range transmission while a detailed description of the short-range transmission mechanism and its contribution is available underneath.

For the long-range transmission, the final concentration of virions in the air is composed of the balance between the emission rate and the removal rate, including the effects of the different removal mechanisms above described, such as ventilation and gravitational settling. The exposure corresponds to the integral over time of all the different concentration profiles during the course of the event.

The exposure of the short-range box is described below (c.f. 'Short range transmission').

Occupancy profile

While the probability of infection is estimated on an individual basis, crowding is associated with increased risk of infectious diseases [111]. Knowing the number of occupants in the given space is essential to quantify the individual risk and the expected number of secondary cases. Moreover, considering reducing the overall space occupancy could be adopted as an immediate action to reduce airborne risk of infection [112].

Room volume

Room volume is a key piece of information to calculate the effect of indoor ventilation and estimate the overall virions' concentration or dilution in the given space.

Mass balance

For the long-range exposure, the concentration of virions of a given size D is derived from the following differential equation, determining the time evolution of the number of virions per unit volume per unit diameter of the particle, in a single-zone model. The solution of the mass-balance differential equation will simulate these effects.

$$\frac{\partial C}{\partial t} = \frac{vR(D) \cdot N_{inf}}{V_r} - \lambda_{vRR}(D) \cdot C(t, D)$$

Where:

vR : viral emission rate

N_{inf} : number of infected individuals in the same volume

V_r : volume of the room

λ_{vRR} : viral removal rate

Step-wise computation

The exponential form of the solution of the mass balance equation is valid when all parameters are constant in each computational step, hence, vR and λ_{vRR} must be piecewise constant functions of time in each step. A new value is assigned to each parameter every time a condition changes in the room, in particular when an infected person(s) enters or leaves the room, or when the ventilation rate changes (which leads to a modification of λ_{vRR}).

Between such transition times, e.g. t_n and t_{n+1} , all variables are constant and the differential equation is valid provided C_0 is replaced by $C(t_n, D)$, and t by $t - t_n$. $C(t_n, D)$ which in turn is computed from the knowledge of the previous regime between t_{n-1} and t_n ; in practice, all these computations are done recursively, using an efficient caching mechanism to avoid computing the same concentration twice [104]. These mathematical operations are important so that one can compute the concentration using analytical methods and avoid computationally expensive algorithms.

Cumulative (absorbed) dose

Particle deposition fraction

Because the deposition pattern of inhaled particles may determine their future clearance and insult to tissue, respiratory tract deposition is an important factor in assessing the potential risk produced by inhaled particles. Particle deposition is primarily governed by the mechanisms of inertial impaction, gravitational sedimentation, Brownian diffusion, and, to a lesser extent, by turbulence, electrostatic precipitation, and interception [13], [73]. The relative contribution of these different mechanisms is a function of the: (1) physics of particles such as size and physicochemical properties, (2) the anatomy of the respiratory tract such as airway anatomical structure and (3) the airflow patterns in the lung airways which, amongst other factors, depend on the breathing pattern (Figure 4) [28].

The forces acting on a particle and its physical and chemical properties, such as particle size or size distribution, density, shape, hygroscopic or hydrophobic character, and chemical reactions of the particle will affect the deposition. With respect to the anatomy of the respiratory tract, important parameters are the diameters, the lengths, and the branching angles of airway segments, which determine the deposition. Physiological factors include airflow and breathing patterns, which influence particle deposition [113]. The particle deposition model developed by Hind [114], an approximation of the International Commission on Radiological Protection (ICRP) model [115] is adopted here to compute the total deposition in the respiratory tract, independently of the precise location, considering the particle diameter after evaporation.

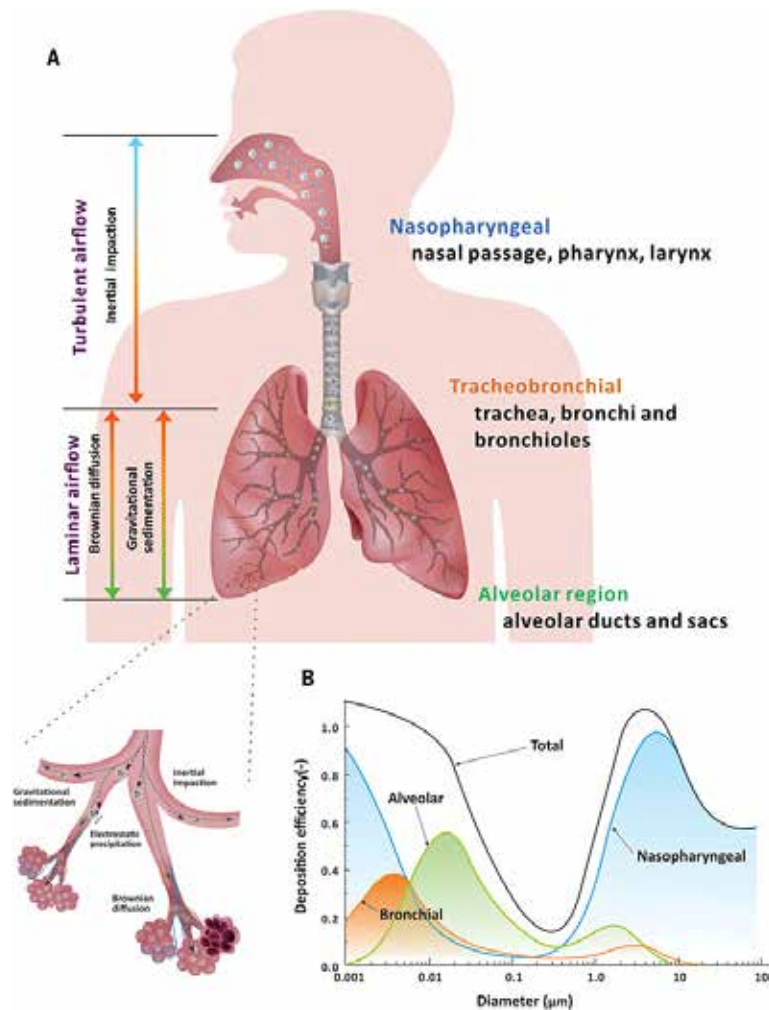


Figure 4. Size-dependent aerosol deposition mechanisms to sites in the respiratory tract.

Source : C. C. Wang et al., "Airborne transmission of respiratory viruses," Science, vol. 373, no. 6558, Aug. 2021, doi: 10.1126/SCIENCE.ABD914

Viable virus factor

Viable SARS-CoV-2 was identified in air samples from rooms occupied by COVID-19 patients in the absence of aerosol-generating health-care procedures [116] and in air samples from an infected person's car [117]. Although other studies have failed to capture viable SARS-CoV-2 in air samples, this is to be expected. Sampling of airborne virus is technically challenging for several reasons, including limited effectiveness of some sampling methods for collecting fine particles, viral dehydration during collection, viral damage due to impact forces (leading to loss of viability), aerosolization of virus during collection, and viral retention in the sampling equipment [118]. While in laboratory experiments, SARS-CoV-2 stayed infectious in the air for up to 3 hours with a half-life of 1.1 hour [119], a systematic review looking at the range of ratio of viral copies in aerosol to plaque forming units (PFU) ratio returned values in between 6 to 0.343 \log_{10} viral copies/litre of air and in between 2.15E+03 to 2.68E+04 TCID₅₀/100 μm for viral titre [116], [120] and RNA to PFU [116] respectively.

Masks and Respirators (Inward)

The use of face coverings has been promoted as a key measure to reduce the SARS-CoV-2 transmission throughout the pandemic. Specific types of face coverings including but not limited to respirators, surgical masks and cloth masks have been recommended for healthcare facilities [121], [122] and community settings [123] according to the level of risk and protection required. In the absence of mask mandates, the compliance of face coverings is an important parameter, hence the exact quantification of the risk reduction provided by the use of face coverings is highly dependent on the level of compliance. In addition, the mask composition and fit [124], [125] are also of high importance, where the standard requirements for filtration efficiency and fit are defined by NIOSH-42 CFR Part 84 [126], EN 149 [127] and ASATM F3502-21 [128]. In order to estimate the overall transmission risk, filtration efficiency values for this model have been extracted from experimental studies (Annex 1) that measured the inward and outward filtration efficiency of different types of masks for a given size of particles, with information on particles ranges, respiratory activity, particle velocity and airflow. Ultimately, however, the fit effect on the wearer's face is probably the most significant parameter.

Short-range transmission

Proxemics

In 1983, Edward Hall, a cultural anthropologist, coined the term proxemics to define studies about social distancing in everyday life [129]. Previous outbreaks of Ebola [130], influenza [131], and the ongoing COVID-19 pandemic have highlighted the importance of understanding the transmission dynamics and spread of infectious diseases, which depend fundamentally on the underlying patterns of social contact between individuals. Together, these patterns give rise to complex social networks that influence disease dynamics [132], including the capacity for emerging pathogens to become endemic [133] and the overdispersion of the offspring distribution underlying the reproduction number [22].

Social contact surveys can provide insight into the features of these networks, which are typically achieved through incorporating survey results into the mathematical models of infectious disease transmission frequently used to guide decision making in response to outbreaks [134]. Such inputs are necessary for models to have sufficient realism to evaluate relevant policy questions. However, despite the known importance of contact patterns as determinants of the infectious disease dynamics, understanding of how they vary remains far from complete [135].

Proximity distance, close interaction frequency, and duration are critical for short-range transmission of respiratory pathogens like SARS-CoV-2 since the infectious particle concentration in immediacy of the infector can be several folds higher than a few meters away [136], [137] (Figure 3). The high risk of transmission via close contact is due to direct exposure of the susceptible person to the expired jet of the infected person and the higher concentration of infectious particles.

Expiratory Jet

Besides physical distancing, indoor ventilation can significantly impact short-range airborne transmission risk [138]. This model integrates the newly developed approach to assess the infection risk via the short-range route through the two-stage jet model (Figure 5) [68]. While for long-range transmission the key parameters affecting the final virions concentration in the model are dilution by ventilation, filtration, settling and biological decay, as described above, for short-range transmission the dilution factors in the expired jet zone are governed by the buoyancy-driving flow pattern of the jet, including different mechanisms such as the exhaled flow velocity, jet-like to puff-like separation, penetration distance and indoor ventilation rate. In this regard, knowing the average initial concentration at the origin of the jet (the mouth or nose), enables the two-stage jet model to estimate the average concentration at a given distance, and an average concentration in the room zone [68]. The current two-stage jet model still presents several limitations. For instance, despite the fact that evaporation and dehydration are known to occur at close range, the current two-stage jet model has not considered particle settling and virus deactivation, although the ARIA group consider it acceptable due to the very quick travel time (seconds). Another important limitation is that the breathing profile has been simplified as a square cycle, which may lead to an underestimation of the streamwise penetration distance of the jet-like stage and an overestimation of the dilution factor at any distance in the puff-like stage. Hence, the required physical distance and ventilation rate to reduce short-range transmission may be underestimated. Furthermore, the model doesn't consider the risk of short-range transmission whenever a mask is used simply due to the absence of a forward jet.

Exposure

The exposure of virions in close proximity is therefore estimated differently from the long-range approach described above.

The concentration for the short-range is calculated based on the continuum equation from the two-stage jet model [68]. The macroscopic mass balance equations for the emitted virus-laden aerosol in the jet zone can be formulated by:

$$Q_0 C_{SR,0}(D) + (Q_{0,x} - Q_0) C_{LR}(t, D) = Q_{0,x} C_{SR,x}(t)$$

Where:

Q_0 is the initial exhaled/inhaled flow rate

$Q_{0,x}$ is the jet flow rate at a distance x from the mouth

$C_{SR,0}(D)$ is the initial viral concentration at the mouth, depending on the particle diameter D

$C_{SR,x}(t)$ is the jet viral concentration at distance x from the mouth and at time t

$C_{LR}(t, D)$ is the long-range viral concentration (calculated above)

The jet flow rate increases at a streamwise penetration distance due to entrainment of the surrounding air. Hence, the ratio between $Q_{0,x}$ and Q_0 is the average dilution factor $S(x)$ of the cross-section at a distance x from the mouth [68].

The jet infectious particles concentration becomes:

$$C_{SR,x}(t) = C_{LR}(t, D) + \frac{1}{S(x)} (C_{SR,0}(D) - C_{LR}(t, D))$$

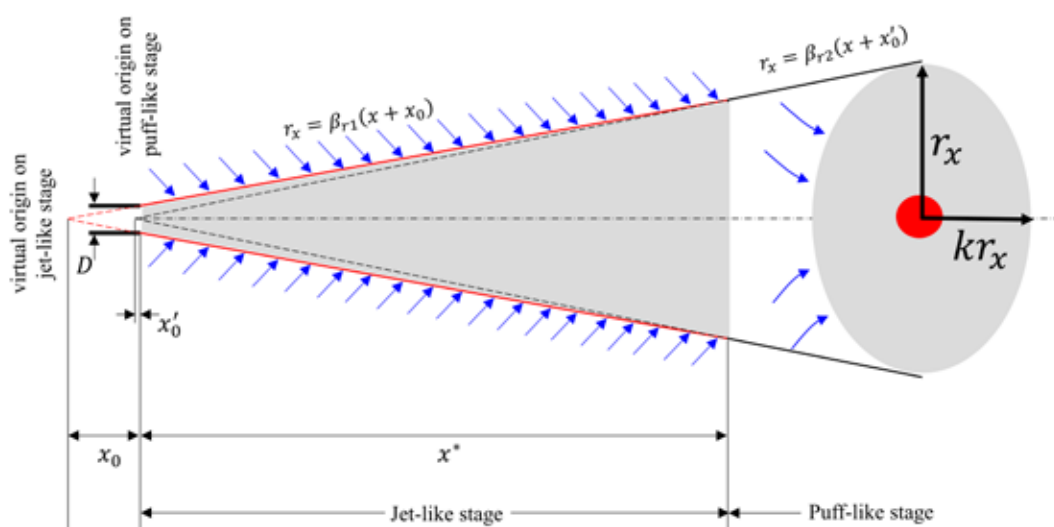


Figure 5. Schematic diagram of the expired jet using a two-stage jet model.

Source: W. Jia, J. Wei, P. Cheng, Q. Wang, and Y. Li, "Exposure and respiratory infection risk via the short-range airborne route," *Build. Environ.*, vol. 219, p. 109166, Jul. 2022, doi: 10.1016/J.BUILDENV.2022.109166.

Probability of infection

The interaction between the emission and the removal rates provides the infectious particles' concentration, which, multiplied by the exposure time, enables estimation of the cumulative absorbed dose for a given scenario. The probability of infection is then appraised considering the host-pathogen interaction which includes the dose-response model, the specific SARS-CoV-2 variant considered, the host immunity and the sum of the short- and the long-range risk.

The probability of infection is then expressed as the mean value of the probability distribution of an exposed susceptible host to get infected when exposed to a certain risk. This result can be read as the 'attack rate' in epidemiological studies. Hence, by multiplying the probability with the number of exposed hosts, it is possible to estimate the number of expected secondary cases for the assessed event.

Multiple studies evaluated the percentage of asymptomatic SARS-CoV-2 infections with results ranging from 1.4% to 78.3% [139]. For the above reason, the model aims to assess the risk of infection defined as the host probability to infection, proxy by seroconversion regardless of symptom onset.

To estimate the probability of infection, the presence of at least one infected person shedding viruses into the simulated volume is assumed. Nonetheless, it is also important to understand that the absolute risk of infection is uncertain, as it will depend on the probability that someone infected attends the event.

As mentioned above, this model deviates from the standard Wells–Riley equation to include the virological / immunological aspects while maintaining the need for a simplified physical approach using an exponential dose-response.

The probability of infection is expressed as [104]:

$$P = 1 - e^{-\left[vD \frac{\ln(2)}{ID_{50}} T_{VOC} \left(\frac{1}{(1-HI_{exp})} \right) \right]}$$

Where:

vD is the viral dose of IRPs

ID_{50} is the infectious dose

T_{VOC} is the transmissibility factor for the VOC

HI_{exp} is the Host immunity of the exposed host (i.e. susceptible)

The model, besides estimating the risk, can be used for comparing the impact and effectiveness of different mitigation measures such as ventilation, air cleaning, exposure time, physical activity, and the occupancy.

Dose-response

Since the beginning of the pandemic, several animal studies looked at the dose-response relationships for symptoms, seroconversion and viral shedding through orotracheal [140], intranasal [141] and aerosol [142] exposure. Most recently, a human challenge study enabled the identification of the Median Tissue Culture Infectious Dose (TCID₅₀) or the inoculum dose that induced infection in more than 50% of participants, corresponding to 10 TCID₅₀ or 55 Focus-forming Unit (FFU) [143].

Variants of Concern

All viruses, including SARS-CoV-2, change over time. Most changes have little to no impact on the virus' properties. However, some changes may affect the virus's properties, such as transmissibility, the associated disease severity, and vaccines effectiveness, amongst others.

During late 2020, the emergence of variants that posed an increased risk to global public health prompted the characterization of specific Variants of Interest (VOIs) and Variants of Concern (VOCs)[25]. Since then, the emergence of SARS-CoV-2 variants with novel spike protein mutations able to influence the epidemiological and clinical aspects of the COVID-19 infections have been recorded. These variants can increase the rates of virus transmission and/or increase the risk of re-infection, all the while being less resistant to the protection afforded by neutralizing monoclonal antibodies and vaccination.

This model considers the different effective reproduction numbers in between VOCs to estimate the various relative increased or reduced transmission risk. In this regard, the data are extracted from the SARS-CoV-2 sequences uploaded to the Global Initiative On Sharing All Influenza Data (GISAID) hCoV-19 database [144]. Campbell et al. analysed the increased transmissibility and global spread of SARS-CoV-2 VOCs as of June 2021. Through a multinomial logistic model of competitive growth, the effective reproduction number of each variant relative to that of the non-VOC/VOI viral population for each reporting country was estimated. Despite differences between countries, the analysis showed a statistically significant increase in the pooled mean effective reproduction number relative to non-VOC/VOI of B.1.1.7 at 29% (95% confidence interval (CI): 24–33), B.1.351 at 25% (95% CI: 20–30), P.1 at 38% (95% CI: 29–48) and B.1.617.2 at 97% (95% CI: 76–117). Of the six variants currently designated as VOI, five were considered in the analysis and among these only B.1.617.1 and B.1.525 demonstrated a statistically

significant increase in the effective reproduction number of 48% (95% CI: 28–69) and 29% (95% CI: 23–35), respectively.

Given the widespread co-circulation of VOC/VOI, the effective reproduction numbers of these variants were compared against each other in order to estimate the nature of future competitive growth between them. Notably, the pooled mean difference in the effective production number between the VOC B.1.1.7 and B.1.351 was small at 4% (95% CI: 0–8), while P.1 demonstrated an increase relative to B.1.1.7 and B.1.351 of 10% (95% CI: 3–17) and 17% (95% CI: 6–30). Given these estimates, the longer-term trends of competitive growth between these three VOC remain unclear. In contrast, the rapid observed growth of B.1.617.2 suggests a clear competitive advantage compared with B.1.1.7, B.1.351 and P.1, with estimated increases in the effective reproduction number of 55% (95% CI: 43–68), 60% (95% CI: 48–73) and 34% (95% CI: 26–43) respectively [145]. Although Omicron appears to be associated with less severe disease, transmissibility of this VOC is higher compared with all previous VOC. Omicron spread with an unprecedented speed around the world, and by February 2022, Omicron was the dominant VOC [146]. A systematic review shows that the effective reproduction number and basic reproduction number of the Omicron variant elicited 3.8- and 2.5-times higher transmissibility than the Delta variant, respectively. The Omicron variant has an average basic reproduction number of 9.5 and a range from 5.5 to 24 (median 10 and interquartile range, IQR: 7.25, 11.88). The average effective reproduction number for Omicron is 3.4, with a range from 0.88 to 9.4 (median 2.8 and IQR: 2.03, 3.85) [147].

Host immunity against transmission

The duration and effectiveness of acquired immunity from infection with and vaccination against SARS-CoV-2 are relevant to estimate the probability of infection.

Several studies looked at the vaccine association with short- and long-term protection against SARS-CoV-2 as well as at infection-acquired immunity boosted with vaccination [148]. This model uses data collected on [VIEW-Hub](#), an online, interactive, map-based platform for visualizing data on vaccine use and impact, in particular 300 studies targeting vaccines effectiveness that have been reported in preprint and published literature and reports [149].

Many systemic viral infections, such as measles, confer long-term, if not lifelong, immunity, whereas others, such as influenza, do not [150]. Although several studies on SARS-CoV-2 show that protection from reinfection is strong and persists for several months following an infection [151]–[153], it is unknown how long protective immunity truly lasts [154]. The length of current reported follow-up data prevents knowing with certainty the expected duration that previous infection will protect against COVID-19. For the above presented reasons, the proposed model only considers the protection offered by vaccine induced immunity and not elicited by natural infection.

Limitations

The aerobiology of infectious particles and the transmission dynamics to allow for a replication competent and infection competent virus to establish an invasive infection in humans is complex. The size of the particles and the distance the particles may move through the air is variable and depends on many factors, including the size distribution of the particles, the propulsive force generated by the individual or the procedure, the relative humidity, evaporation level, settling velocity, direction and velocity of air flow, the number of air changes per hour, temperature, crowding and other environmental factors. In addition, there is variability in the type of the respiratory virus in question, the dispersion, quantity, and distribution of the virus within the respiratory particles, the stability of the virus, its replication and infection competence, ability to enter the respiratory tract, ability to bind to specific host cell receptors and to establish invasive infection in a susceptible host. The process is further complicated by debate regarding how well the use of quantitative polymerase chain reaction (PCR) techniques performed on respiratory specimens can be interpreted with respect to recovery of viable virus and its titer, depending on the timing of presentation and stage of illness [155].

The proposed model relies on several assumptions from our most current understanding on the airborne transmission mechanism. Moreover, despite the systematic reviews undertaken to extract the variable values, the model presents technical limitations which can identify possible research gaps.

The first limitation of the model lies in its parameter values. Despite the systematic search and review leveraged to identify and extract the values as well as the use of a probabilistic approach instead of a deterministic one, the Technical Advisory Group acknowledges that the value identification should be a continuous exercise to ensure the most updated and accurate estimation. Moreover, scientific evidence is not always available for some variables and there are often too few data to draw reliable and valid conclusions, which hinders the decision-making process and decreases the likelihood of a precise output. Additionally, several studies are of low quality due to the weak study design therefore presenting a high risk of biases.

Another significant limitation is that the long-range transmission estimation relies on the well-mixed approach meaning that an immediate homogeneous

viral distribution, within a given finite volume, is assumed. Fluid dynamic simulation would enable a more precise analysis, but the computational capacity needed, and the technical expertise required would significantly affect the model accessibility and usability. The well-mixed assumption is partially mitigated by the introduction of the short-range exposure, where the viral concentration in close proximity with the infector is known to be higher. There are also limitations in the short-range model due to variation in posture of source and susceptible person and interaction of exhaled air flow with other air currents.

The third limitation concerns the variables related to the host-pathogen interaction as their variability is significantly affected by multiple factors including viable virus-to-RNA copies ratio, host and pathogen intrinsic features. Such variables include the emitted viral load, the infectious dose and dose-response model, the host immunity and specific variant transmissibility. The mathematical probabilistic approach and the use of the precautionary principle aim to mitigate this specific limitation while preventing underestimation of the probability of infection. By default, the results of the model are provided as the *mean* probability of infection (the full probability distribution is equally available). Illustrating the *mean* represents a more accurate estimation than the *median* as the large span of certain parameters may skew the samples avoiding an underestimation. As any probabilistic model, the uncertainties tied to the random variables and the accuracy of the results depend on the quality of the data and statistical distribution. Such variables might require regular updating, as mentioned above.

An exception amongst the host-pathogen interaction variables is the post-infection immunity which has not been included in the model due to the limited data availability and the potential issue of risk underestimation. In other words, only the contribution of vaccine immunity is considered in the model.

Another significant limitation is the number of infectors considered for the estimation. In real-life settings, the number of secondary infections arising from an identified index case might be due to overlapping exposures with variable incubation periods from multiple index cases. While the model can include more infectors simultaneously, the possible number of infected people attending the event will be a user's assumption.

Online tool

In an attempt to fill this need over the past several months, several quantitative tools have been developed by various scientists and engineers to model the SARS-CoV-2 infection risk associated with indoor occupancy during the pandemic. While these tools all incorporate ventilation as a primary control measure, they differ in their inclusion of epidemiological/virological aspects and variables, how emission sources are represented, and how the risk is assessed, based on a time-dependent exposure to infectious aerosols. They also differ in terms of their platform, target users, and overall degree of technical complexity. For these tools to be widely used and to be able to inform policy and/or induce an update in the regulatory framework, they must be applicable to a diverse building typology, be validated by real-world epidemiological studies, and apply the most up-to-date scientific knowledge of aerosol science and host-pathogen interaction. They must also be easy to use and understand, contributing towards a broader knowledge of “airborne transmission” and improved scientific consensus surrounding its importance in public, residential and health care settings.

ARIA, the online tool to estimate SARS-CoV-2 airborne transmission in indoor settings relies on the presented model and has been developed through a human-centred design approach. The interactive system developed aims to provide an interface focusing on the users, their needs, and requirements, as well as applying common application-based standards, ergonomics, and usability techniques for calculating both short- and long-range transmission. In the future, an extension of the new tool to other pathogens beyond SARS-CoV-2 could be considered.

Examples

Table 3 below resume the outputs produced by the ARIA online tool when different inputs are provided. For each example, one variable at a time was adjusted to compare the different probabilities of infection. In particular, example 1 considered poor ventilation and included short-range interactions in between the occupants. For the second example, the same scenario was analysed excluding short-range interactions. The third is exactly like the second except the ventilation has been increased from 2.5 l/s/p to 10 l/s/p. The last one mirrors the same conditions used for the third one except that the use of medical mask was considered. It's important to notice how the probability of infection reduces from example 1 to example 4.

Table 3. The outputs produced by the ARIA online tool

Input	Example 1	Example 2	Example 3	Example 4
Country			Switzerland	
City			Geneva	
Date			02-02-23	
Temperature			21 °C	
Relative Humidity			0.5	
SARS-CoV-2 Variant			Omicron	
Space dimension			135 m ³	
Duration (from - to)			8:00 to 16:00	
Break 1 (from - to)			10:00 to 10:15	
Break 2 (from - to)			12:30 to 13:30	
Occupancy			10 people	
Number of infectors			1 person	
Host immunity			No	
Setting			Office	
Physical activity			Sedentary (i.e., sitting, resting)	
Respiratory activity			67% Simple oral breathing (silence) 33% Speaking	
Use of mask	No	No	No	Medical mask
Short range interaction	Yes		No	
Short-range duration	From 9:00 to 9:15		N/A	
Short-range (activity)	Speaking		N/A	
Short-range duration	From 15:00 to 15:15		N/A	
Short-range (activity)	Speaking		N/A	
Ventilation rate	2.5 l/s/p = 90 m ³ /hour	2.5 l/s/p = 90 m ³ /hour	10 l/s/p = 360 m ³ /hour	10 l/s/p = 360 m ³ /hour
Probability of infection	15.59%	6.79%	5.06%	0.82%
Expected number of secondary cases	1.40	0.61	0.46	0.07

References

- [1] The National Institute for Occupational Safety and Health (NIOSH), "Aerosols | NIOSH | CDC," *Workplace Safety & Health Topics*, 2010. <https://www.cdc.gov/niosh/topics/aerosols/default.html> (accessed Aug. 09, 2022).
- [2] William C. Hinds, "Aerosol Technology: Properties, Behavior, and Measurement of Airborne Particles, 2nd Edition," Wiley, Ed. New York, NY: Wiley, 2021, p. 504.
- [3] J. Atkinson, Y. Chartier, C. L. Pessoa-silva, P. Jensen, and Y. Li, *Natural Ventilation for Infection Control in Health-Care Settings*. Geneva: World Health Organization, 2009.
- [4] M. Porta, *A Dictionary of Epidemiology*, 6th editio. Oxford, United States: Oxford University Press, Incorporated, 2014.
- [5] Association of Home Appliance Manufacturers, "Air Filtration Standards – AHAM Verifide," *Air filtration standards*, 2022. <https://ahamverifide.org/ahams-air-filtration-standards/> (accessed Jan. 05, 2023).
- [6] R. E. Rakel, "Establishing Rapport," *Textb. Fam. Med.*, pp. 146–159, Jan. 2012, doi: 10.1016/B978-1-4377-1160-8.10012-0.
- [7] T. L. Meister *et al.*, "Low risk of SARS-CoV-2 transmission by fomites – a clinical observational study in highly infectious COVID-19 patients," *J. Infect. Dis.*, vol. 226, no. 9, pp. 1608–1615, 2022, doi: 10.1093/infdis/jiac170.
- [8] US EPA – Environmental Protection Agency, "Exposure Assessment Tools by Routes – Inhalation," *EPA ExpoBox*, 2022. <https://www.epa.gov/expobox/exposure-assessment-tools-routes-inhalation> (accessed Aug. 16, 2022).
- [9] World Health Organization, "Roadmap to improve and ensure good indoor ventilation in the context of COVID-19," 2021. [Online]. Available: <https://www.who.int/publications/i/item/9789240021280>.
- [10] J. W. Tang *et al.*, "Dismantling myths on the airborne transmission of severe acute respiratory syndrome coronavirus-2 (SARS-CoV-2)," *J. Hosp. Infect.*, vol. 110, no. January, pp. 89–96, 2021, doi: 10.1016/j.jhin.2020.12.022.
- [11] F. K. A. Gregson *et al.*, "Comparing aerosol concentrations and particle size distributions generated by singing, speaking and breathing," *Aerosol Sci. Technol.*, vol. 55, no. 6, pp. 681–691, Jun. 2021, doi: 10.1080/02786826.2021.1883544.
- [12] World Health Organization, *WHO global air quality guidelines: particulate matter (PM_{2.5} and PM₁₀), ozone, nitrogen dioxide, sulfur dioxide and carbon monoxide*. Geneva: World Health Organization, 2021.
- [13] C. Darquenne, "Deposition Mechanisms," *J. Aerosol Med. Pulm. Drug Deliv.*, vol. 33, no. 4, pp. 181–185, Aug. 2020, doi: 10.1089/JAMP.2020.29029.CD/ASSET/IMAGES/LARGE/JAMP.2020.29029.CD_FIGURE5.JPEG.
- [14] NIH – National Institutes of Health, "Definition inhalation," *NCI Dictionaries*, 2022. <https://www.cancer.gov/publications/dictionaries/cancer-terms/def/inhalation> (accessed Aug. 16, 2022).
- [15] R. Jones and L. Brosseau, "Aerosol Transmission of Infectious Disease," *J. Occup. Environ. Med.*, vol. 57, Mar. 2015, doi: 10.1097/JOM.0000000000000448.
- [16] D. Duval *et al.*, "Long distance airborne transmission of SARS-CoV-2: rapid systematic review," *BMJ*, vol. 377, p. e068743, Jun. 2022, doi: 10.1136/BMJ-2021-068743.
- [17] U.S. Environmental Protection Agency, Washington, "U.S. EPA. Exposure Factors Handbook 2011 Edition (Final Report)," *EPA/600/R-09/052F*, 2011. <https://cfpub.epa.gov/ncea/risk/recordisplay.cfm?deid=236252> (accessed Mar. 17, 2022).
- [18] NIH – National Institutes of Health, "Definition of mucous membrane," *NCI Dictionaries*, 2022. <https://www.cancer.gov/publications/dictionaries/cancer-terms/def/mucous-membrane> (accessed Aug. 16, 2022).
- [19] R. Asmatulu and W. S. Khan, "Electrospun nanofibers for filtration applications," *Synth. Appl. Electrospun Nanofibers*, vol. 73, no. 10, pp. 135–152, Jan. 2019, doi: 10.1016/B978-0-12-813914-1.00007-9.
- [20] Rice University, "Projectile Motion – Physics," *OpenStax*, 2022. <https://openstax.org/books/physics/pages/5-3-projectile-motion> (accessed Oct. 06, 2022).
- [21] P. Kosky, R. Balmer, W. Keat, and G. Wise, "Manufacturing Engineering," *Explor. Eng.*, pp. 205–235, 2013, doi: 10.1016/B978-0-12-415891-7.00010-8.
- [22] P. L. Delamater, E. J. Street, T. F. Leslie, Y. T. Yang, and K. H. Jacobsen, "Complexity of the Basic Reproduction Number (R₀)," *Emerg. Infect. Dis.*, vol. 25, no. 1, pp. 1–4, Jan. 2019, doi: 10.3201/EID2501.171901.
- [23] C. Schönbach, "Respiratory Tract, Upper and Lower," in *Encyclopedia of Systems Biology*, W. Dubitzky, O. Wolkenhauer, K.-H. Cho, and H. Yokota, Eds. New York, NY: Springer New York, 2013, pp. 1851–1852.
- [24] OpenLearn, "Susceptible hosts and risk factors," *Communicable Diseases Module: Basic Concepts in the Transmission of Communicable Diseases*, 2022. <https://www.open.edu/openlearncreate/mod/oucontent/view.php?id=84§ion=20.4.6> (accessed Aug. 18, 2022).
- [25] World Health Organization, "Tracking SARS-CoV-2 variants," *Activities*, 2022. <https://www.who.int/activities/tracking-SARS-CoV-2-variants> (accessed Jun. 16, 2022).

- [26] M. Schuit *et al.*, “Airborne SARS-CoV-2 Is Rapidly Inactivated by Simulated Sunlight,” *J. Infect. Dis.*, vol. 222, no. 4, pp. 564–571, Jul. 2020, doi: 10.1093/INFDIS/JIAA334.
- [27] C. J. Burrell, C. R. Howard, and F. A. Murphy, “Virion Structure and Composition,” *Fenner White’s Med. Virol.*, vol. 62, no. 22, pp. 27–37, 2017, doi: 10.1016/B978-0-12-375156-0.00003-5.
- [28] C. C. Wang *et al.*, “Airborne transmission of respiratory viruses,” *Science*, vol. 373, no. 6558, Aug. 2021, doi: 10.1126/SCIENCE.ABD9149.
- [29] Y. Sheikhejad *et al.*, “Airborne and aerosol pathogen transmission modeling of respiratory events in buildings: An overview of computational fluid dynamics,” *Sustain. Cities Soc.*, vol. 79, p. 103704, Apr. 2022, doi: 10.1016/J.SCS.2022.103704.
- [30] J. Lv *et al.*, “Aerosol Transmission of Coronavirus and Influenza Virus of Animal Origin,” *Front. Vet. Sci.*, vol. 8, p. 109, Apr. 2021, doi: 10.3389/FVETS.2021.572012/BIBTEX.
- [31] J. L. Santarpia *et al.*, “Aerosol and surface contamination of SARS-CoV-2 observed in quarantine and isolation care,” *Sci. Reports 2020 101*, vol. 10, no. 1, pp. 1–8, Jul. 2020, doi: 10.1038/s41598-020-69286-3.
- [32] C. J. Noakes and P. Andrew Sleight, “Mathematical models for assessing the role of airflow on the risk of airborne infection in hospital wards,” *J. R. Soc. Interface*, vol. 6, no. SUPPL. 6, p. S791, Dec. 2009, doi: 10.1098/rsif.2009.0305.focus.
- [33] N. Leung, “Transmissibility and transmission of respiratory viruses,” *Nat. Rev. Microbiol.* 2021 198, vol. 19, no. 8, pp. 528–545, Mar. 2021, doi: 10.1038/s41579-021-00535-6.
- [34] J. S. Kutter, M. I. Spronken, P. L. Fraaij, R. A. Fouchier, and S. Herfst, “Transmission routes of respiratory viruses among humans,” *Current Opinion in Virology*, vol. 28. Elsevier B.V., pp. 142–151, Feb. 01, 2018, doi: 10.1016/j.coviro.2018.01.001.
- [35] G. N. Sze To and C. Y. H. Chao, “Review and comparison between the Wells-Riley and dose-response approaches to risk assessment of infectious respiratory diseases,” *Indoor Air*, vol. 20, no. 1, pp. 2–16, 2010, doi: 10.1111/j.1600-0668.2009.00621.x.
- [36] L. Comber *et al.*, “Airborne transmission of SARS-CoV-2 via aerosols,” *Rev. Med. Virol.*, vol. 31, no. 3, May 2021, doi: 10.1002/RMV.2184.
- [37] W. F. Wells, “On air-borne infection: Study II. Droplets and droplet nuclei,” *Am. J. Epidemiol.*, vol. 20, no. 3, pp. 611–618, Nov. 1934, doi: 10.1093/OXFORDJOURNALS.AJE.A118097/2/20-3-611.PDF.GIF.
- [38] L. Bourouiba, “Turbulent Gas Clouds and Respiratory Pathogen Emissions: Potential Implications for Reducing Transmission of COVID-19,” *JAMA*, vol. 323, no. 18, pp. 1837–1838, May 2020, doi: 10.1001/JAMA.2020.4756.
- [39] Centers for Disease Control and Prevention., “Scientific Brief: SARS-CoV-2 Transmission | CDC,” 2021. <https://www.cdc.gov/coronavirus/2019-ncov/science/science-briefs/sars-cov-2-transmission.html> (accessed Feb. 14, 2022).
- [40] J. Atkinson, Y. Chartier, C. Lúcia Pessoa-Silva, P. Jensen, Y. Li, and W.-H. Seto, *Natural Ventilation for Infection Control in Health-Care Settings*, vol. 1. Geneva: World Health Organization, 2009.
- [41] L. D. Knibbs, L. Morawska, S. C. Bell, and P. Grzybowski, “Room ventilation and the risk of airborne infection transmission in 3 health care settings within a large teaching hospital,” *Am. J. Infect. Control*, vol. 39, no. 10, pp. 866–872, 2011, doi: 10.1016/j.ajic.2011.02.014.
- [42] L. D. KNIBBS, L. MORAWSKA, and S. C. BELL, “The risk of airborne influenza transmission in passenger cars,” *Epidemiol. Infect.*, vol. 140, no. 3, pp. 474–478, 2012, doi: DOI: 10.1017/S0950268811000835.
- [43] I. T. S. Yu *et al.*, “Evidence of Airborne Transmission of the Severe Acute Respiratory Syndrome Virus,” *N. Engl. J. Med.*, vol. 350, no. 17, pp. 1731–1739, Oct. 2004, doi: 10.1056/NEJMOA032867.
- [44] S. Xiao, Y. Li, M. Sung, J. Wei, and Z. Yang, “A study of the probable transmission routes of MERS-CoV during the first hospital outbreak in the Republic of Korea,” *Indoor Air*, vol. 28, no. 1, pp. 51–63, Jan. 2018, doi: 10.1111/INA.12430.
- [45] Centers for Disease Control and Prevention (CDC), “Healthcare Infection Control Practices Advisory Committee (HICPAC): Guidelines for Environmental Infection Control in Health-Care Facilities,” in *U.S. Department of Health and Human Services Centers for Disease Control and Prevention (CDC) Atlanta, GA 30329*, no. July, MMWR. Recommendations and reports: Morbidity and mortality weekly report. Recommendations and reports / Centers for Disease Control, 2019, pp. 1–235.
- [46] World Health Organization, “Infection prevention and control of epidemic- and pandemic-prone acute respiratory infections in health care,” *WHO Guidel.*, pp. 1–156, 2014, [Online]. Available: http://apps.who.int/iris/bitstream/10665/112656/1/9789241507134_eng.pdf?ua=1.
- [47] Centers for Disease Control and Prevention, “Guidelines for preventing the transmission of Mycobacterium tuberculosis in health-care settings,” in *MMWR. Recommendations and reports: Morbidity and mortality weekly report. Recommendations and reports / Centers for Disease Control*, vol. 54, no. 17, 1994, pp. 1–141.
- [48] H. Qian and X. Zheng, “Ventilation control for airborne transmission of human exhaled bio-aerosols in buildings,” *J. Thorac. Dis.*, vol. 10, no. Suppl 19, pp. S2295–S2304, 2018, doi: 10.21037/jtd.2018.01.24.

- [49] Centers for Disease Control and Prevention., “Guidelines for Preventing the Transmission of Mycobacterium tuberculosis in Health-Care Settings,” in *MMWR. Recommendations and reports: Morbidity and mortality weekly report. Recommendations and reports / Centers for Disease Control*, MMWR. Recommendations and reports: Morbidity and mortality weekly report. Recommendations and reports / Centers for Disease Control, 2005.
- [50] J. Atkinson, Y. Chartier, C. L. Pessoa-silva, P. Jensen, and Y. Li, *Natural Ventilation for Infection Control in Health-Care Settings*. Geneva: World Health Organization, 2009. Available: <https://apps.who.int/iris/handle/10665/44167>
- [51] World Health Organization, *WHO Guidelines on Tuberculosis Infection Prevention and Control*, vol. 82, no. 11. 2019. Available: <https://apps.who.int/iris/handle/10665/311259>
- [52] K. Mahjoub Mohammed Merghani, B. Sagot, E. Gehin, G. Da, and C. Motzkus, “A review on the applied techniques of exhaled airflow and droplets characterization,” *Indoor Air*, vol. 31, no. 1, pp. 7–25, Jan. 2021, doi: 10.1111/INA.12770.
- [53] The American Society of Heating Refrigerating and Air-Conditioning Engineers (ASHRAE)., *ANSI/ASHRAE/ASHE Standard 170-2017 Ventilation of Health Care Facilities – Addendum*. ASHRAE, 2017.
- [54] A. I. A. Academy of Architecture for Health., *Guidelines for Design and Construction of Hospitals*. Facilities Guidelines Institute, 2018.
- [55] Centers for Disease Control and Prevention, *Guidelines for preventing the transmission of Mycobacterium tuberculosis in health-care settings, 2005.*, vol. 54, no. 17. 2005.
- [56] European Standard, “UNE CEN/TR 14788:2007 IN Ventilation for buildings – Design and dimensioning of residential ventilation systems,” 2007. [Online]. Available: <https://www.en-standard.eu/une-cen-tr-14788-2007-in-ventilation-for-buildings-design-and-dimensioning-of-residential-ventilation-systems/>.
- [57] The American Society of Heating Refrigerating and Air-Conditioning Engineers (ASHRAE)., “ANSI/ASHRAE Standard 62.2-2019 – Ventilation and Acceptable Indoor Air Quality in Residential Buildings,” 2019.
- [58] A. Persily, “Challenges in developing ventilation and indoor air quality standards: The story of ASHRAE Standard 62,” *Build. Environ.*, vol. 91, pp. 61–69, 2015, doi: <https://doi.org/10.1016/j.buildenv.2015.02.026>.
- [59] L. Riley, E. C. Murphy, G. Riley, R., “Airborne spread of measles in a suburban elementary school,” *Am. J. Epidemiol.*, vol. 107, no. 6, pp. 421–32, 1978.
- [60] A. Henriques *et al.*, “CAiMIRA – CERN Airborne Model for Risk Assessment,” *Zenodo*, Jan. 2023, doi: 10.5281/ZENODO.7589031.
- [61] International Society of Indoor Air Quality and Climate, “ISIAQ – Webinars,” *Webinars*, 2022. <https://www.isiaq.org/webinars.php> (accessed Jun. 17, 2022).
- [62] European Organization for Nuclear Research – CERN, “CARA | COVID Airborne Risk Assessment,” 2022. <https://cara.web.cern.ch/> (accessed Jun. 17, 2022).
- [63] G. Buonanno, L. Stabile, and L. Morawska, “Estimation of airborne viral emission: Quanta emission rate of SARS-CoV-2 for infection risk assessment,” *Environ. Int.*, vol. 141, Aug. 2020, doi: 10.1016/J.ENVINT.2020.105794.
- [64] S. L. Miller *et al.*, “Transmission of SARS-CoV-2 by inhalation of respiratory aerosol in the Skagit Valley Chorale superspreading event,” *Indoor Air*, vol. 31, no. 2, pp. 314–323, Mar. 2021, doi: 10.1111/INA.12751.
- [65] G. Buonanno, L. Morawska, and L. Stabile, “Quantitative assessment of the risk of airborne transmission of SARS-CoV-2 infection: Prospective and retrospective applications,” *Environ. Int.*, vol. 145, no. June, p. 106112, 2020, doi: 10.1016/j.envint.2020.106112.
- [66] A. Endo, S. Abbott, A. J. Kucharski, and S. Funk, “Estimating the overdispersion in COVID-19 transmission using outbreak sizes outside China [version 3; peer review: 2 approved],” *Wellcome Open Res.*, vol. 5, no. 67, 2020, doi: 10.12688/wellcomeopenres.15842.3.
- [67] K. Ram *et al.*, “Why airborne transmission hasn’t been conclusive in case of COVID-19? An atmospheric science perspective,” *Sci. Total Environ.*, vol. 773, p. 145525, Jun. 2021, doi: 10.1016/J.SCITOTENV.2021.145525.
- [68] W. Jia, J. Wei, P. Cheng, Q. Wang, and Y. Li, “Exposure and respiratory infection risk via the short-range airborne route,” *Build. Environ.*, vol. 219, p. 109166, Jul. 2022, doi: 10.1016/J.BUILDENV.2022.109166.
- [69] M. Alsvéd *et al.*, “Exhaled respiratory particles during singing and talking,” *Aerosol Sci. Technol.*, vol. 54, no. 11, pp. 1245–1248, 2020, doi: 10.1080/02786826.2020.1812502.
- [70] L. Morawska and G. Buonanno, “The physics of particle formation and deposition during breathing,” *Nat. Rev. Phys.* 2021 35, vol. 3, no. 5, pp. 300–301, Mar. 2021, doi: 10.1038/s42254-021-00307-4.
- [71] O. O. Adenaiye *et al.*, “Infectious Severe Acute Respiratory Syndrome Coronavirus 2 (SARS-CoV-2) in Exhaled Aerosols and Efficacy of Masks During Early Mild Infection,” *Clin. Infect. Dis.*, Sep. 2021, doi: 10.1093/CID/CIAB797.
- [72] J. L. Santarpia *et al.*, “The size and culturability of patient-generated SARS-CoV-2 aerosol,” *J. Expo. Sci. Environ. Epidemiol.* 2021, pp. 1–6, Aug. 2021, doi: 10.1038/s41370-021-00376-8.
- [73] L. Morawska, G. Buonanno, A. Mikszewski, and L. Stabile, “The physics of respiratory particle generation, fate in the air, and inhalation,” *Nat. Rev. Phys.*, 2022, doi: 10.1038/s42254-022-00506-7.
- [74] G. R. Johnson and L. Morawska, “The mechanism of breath aerosol formation,” *J. Aerosol Med. Pulm. Drug Deliv.*, vol. 22, no. 3, pp. 229–237, 2009, doi: 10.1089/jamp.2008.0720.

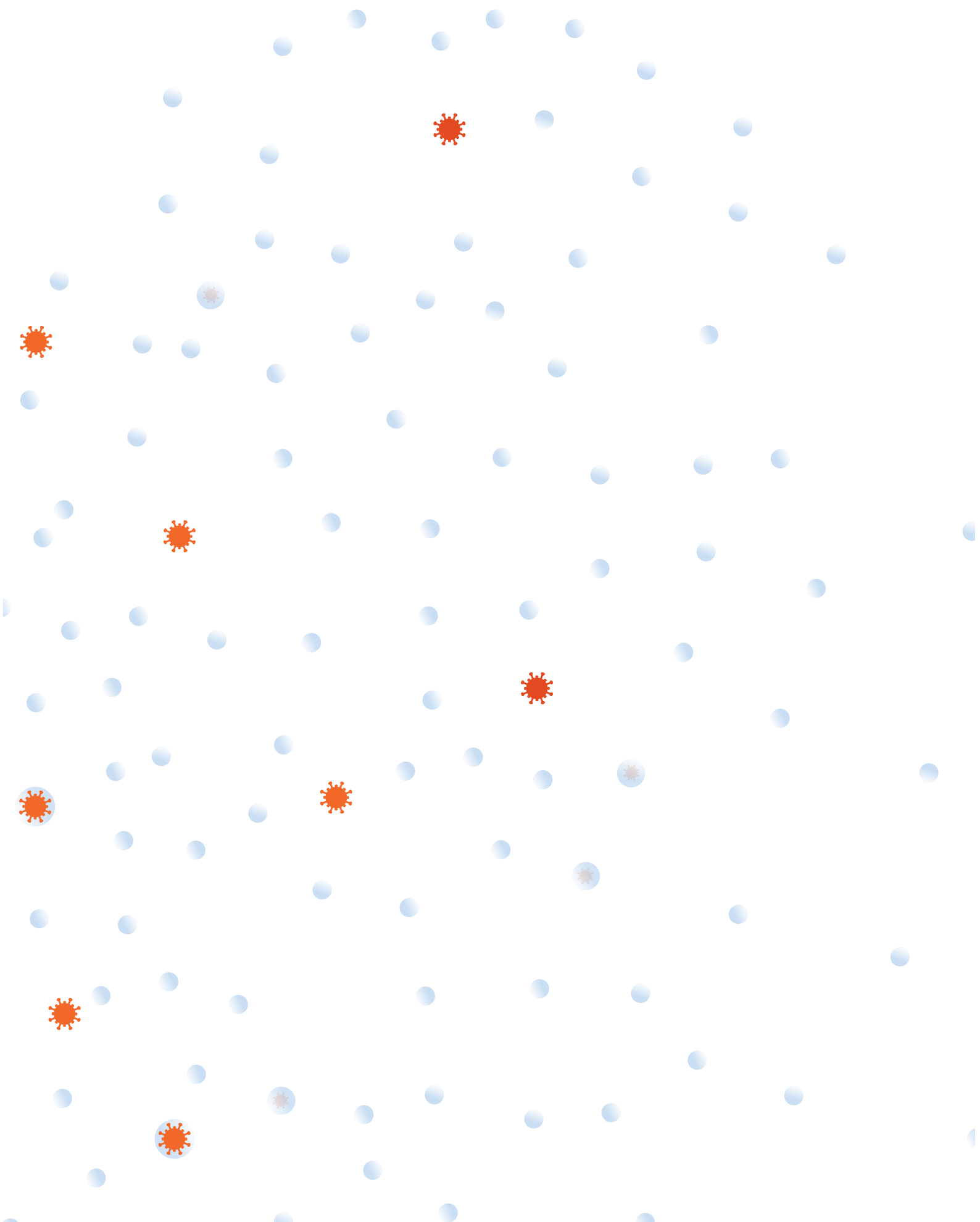
- [75] B. Bake, P. Larsson, G. Ljungkvist, E. Ljungström, and A. C. Olin, "Exhaled particles and small airways," *Respir. Res.*, vol. 20, no. 1, pp. 1–14, 2019, doi: 10.1186/s12931-019-0970-9.
- [76] D. A. Edwards *et al.*, "Exhaled aerosol increases with COVID-19 infection, age, and obesity," *Proc. Natl. Acad. Sci. U. S. A.*, vol. 118, no. 8, Feb. 2021, doi: 10.1073/PNAS.2021830118/SUPPL_FILE/PNAS.2021830118.SAPP.PDF.
- [77] M. G. Da Silva, "An analysis of the transmission modes of COVID-19 in light of the concepts of Indoor Air Quality," *REHVA Eur. HVAC J.*, vol. 57, no. 3, pp. 46–54, 2020, [Online]. Available: <https://www.rehva.eu/rehva-journal/chapter/an-analysis-of-the-transmission-modes-of-covid-19-in-light-of-the-concepts-of-indoor-air-quality>.
- [78] G. R. Johnson *et al.*, "Modality of human expired aerosol size distributions," *J. Aerosol Sci.*, vol. 42, no. 12, pp. 839–851, Dec. 2011, doi: 10.1016/J.JAEROSCI.2011.07.009.
- [79] D. Jacot, G. Greub, K. Jatton, and O. Opota, "Viral load of SARS-CoV-2 across patients and compared to other respiratory viruses," *Microbes Infect.*, vol. 22, no. 10, pp. 617–621, Nov. 2020, doi: 10.1016/J.MICINF.2020.08.004.
- [80] K. K. Coleman *et al.*, "Viral Load of SARS-CoV-2 in Respiratory Aerosols Emitted by COVID-19 Patients while Breathing, Talking, and Singing," *Clin. Infect. Dis.*, Aug. 2021, doi: 10.1093/CID/CIAB691.
- [81] M. Malik, A. C. Kunze, T. Bahmer, S. Herget-Rosenthal, and T. Kunze, "SARS-CoV-2: Viral Loads of Exhaled Breath and Oronasopharyngeal Specimens in Hospitalized Patients with COVID-19," *Int. J. Infect. Dis.*, vol. 110, pp. 105–110, Sep. 2021, doi: 10.1016/J.IJID.2021.07.012.
- [82] J. Ma *et al.*, "Coronavirus Disease 2019 Patients in Earlier Stages Exhaled Millions of Severe Acute Respiratory Syndrome Coronavirus 2 Per Hour," *Clin. Infect. Dis.*, vol. 72, no. 10, pp. e652–e654, May 2021, doi: 10.1093/CID/CIAA1283.
- [83] X. Li *et al.*, "Detecting SARS-CoV-2 in the Breath of COVID-19 Patients," *Front. Med.*, vol. 8, p. 604392, Mar. 2021, doi: 10.3389/FMED.2021.604392/FULL.
- [84] N. H. L. Leung *et al.*, "Respiratory virus shedding in exhaled breath and efficacy of face masks," *Nat. Med.* 2020, vol. 26, no. 5, pp. 676–680, Apr. 2020, doi: 10.1038/s41591-020-0843-2.
- [85] N. Néant *et al.*, "Modeling SARS-CoV-2 viral kinetics and association with mortality in hospitalized patients from the French COVID cohort," *Proc. Natl. Acad. Sci. U. S. A.*, vol. 118, no. 8, Feb. 2021, doi: 10.1073/PNAS.2017962118/SUPPL_FILE/PNAS.2017962118.SD01.CSV.
- [86] S. Euser *et al.*, "SARS-CoV-2 viral-load distribution reveals that viral loads increase with age: a retrospective cross-sectional cohort study," *Int. J. Epidemiol.*, vol. 50, no. 6, pp. 1795–1803, Jan. 2022, doi: 10.1093/IJE/DYAB145.
- [87] M. Levine-Tiefenbrun *et al.*, "Initial report of decreased SARS-CoV-2 viral load after inoculation with the BNT162b2 vaccine," *Nat. Med.* 2021 275, vol. 27, no. 5, pp. 790–792, Mar. 2021, doi: 10.1038/s41591-021-01316-7.
- [88] A. Singanayagam *et al.*, "Community transmission and viral load kinetics of the SARS-CoV-2 delta (B.1.617.2) variant in vaccinated and unvaccinated individuals in the UK: a prospective, longitudinal, cohort study," *Lancet Infect. Dis.*, vol. 22, no. 2, pp. 183–195, Feb. 2022, doi: doi.org/10.1016/S1473-3099(21)00648-4.
- [89] Public Health England, "SARS-CoV-2 variants of concern and variants under investigation in England," *Sage*, no. April, pp. 1–50, 2021.
- [90] Y. Wang *et al.*, "Transmission, viral kinetics and clinical characteristics of the emergent SARS-CoV-2 Delta VOC in Guangzhou, China," *EclinicalMedicine*, vol. 40, p. 101129, Oct. 2021, doi: 10.1016/J.ECLINM.2021.101129.
- [91] T. C. Jones *et al.*, "Estimating infectiousness throughout SARS-CoV-2 infection course," *Science (80-)*, vol. 373, no. 6551, Jul. 2021, doi: 10.1126/SCIENCE.ABI5273/SUPPL_FILE/ABI5273_REPRODUCIBILITY-CHECKLIST.PDF.
- [92] M. D *et al.*, "Dynamics of SARS-CoV-2 shedding in the respiratory tract depends on the severity of disease in COVID-19 patients," *Eur. Respir. J.*, vol. 58, no. 1, p. 743, Oct. 2021, doi: 10.1183/13993003.02724-2020.
- [93] H. C. Stankiewicz Karita *et al.*, "Trajectory of Viral RNA Load Among Persons With Incident SARS-CoV-2 G614 Infection (Wuhan Strain) in Association With COVID-19 Symptom Onset and Severity," *JAMA Netw. Open*, vol. 5, no. 1, pp. e2142796–e2142796, Jan. 2022, doi: 10.1001/JAMANETWORKOPEN.2021.42796.
- [94] R. Verma, E. Kim, N. Degner, K. S. Walter, U. Singh, and J. R. Andrews, "Variation in Severe Acute Respiratory Syndrome Coronavirus 2 Bioaerosol Production in Exhaled Breath," *Open Forum Infect. Dis.*, vol. 9, no. 1, Jan. 2022, doi: 10.1093/OFID/OFAB600.
- [95] H. Joo *et al.*, "Decline in COVID-19 Hospitalization Growth Rates Associated with Statewide Mask Mandates — 10 States, March–October 2020," *MMWR. Morb. Mortal. Wkly. Rep.*, vol. 70, no. 6, pp. 212–216, Feb. 2021, doi: 10.15585/MMWR.MM7006E2.
- [96] N. Ford *et al.*, "Mask use in community settings in the context of COVID-19: A systematic review of ecological data," *eClinicalMedicine*, vol. 38, p. 101024, Aug. 2021, doi: 10.1016/J.ECLINM.2021.101024/ATTACHMENT/F3EFE7A1-2EF3-4AAE-8BA2-7DA2B9431876/MMC1.PDF.
- [97] S. Asadi, C. D. Cappa, S. Barreda, A. S. Wexler, N. M. Bouvier, and W. D. Ristenpart, "Efficacy of masks and face coverings in controlling outward aerosol particle emission from expiratory activities," *Nat. - Sci. Reports*, vol. 10, no. 1, pp. 1–13, Sep. 2020, doi: 10.1038/s41598-020-72798-7.
- [98] A. Weber *et al.*, "Aerosol penetration and leakage characteristics of masks used in the health care industry," *Am. J. Infect. Control*, vol. 21, no. 4, pp. 167–173, 1993, doi: 10.1016/0196-6553(93)90027-2.

- [99] C. C. Chen and K. Willeke, "Aerosol penetration through surgical masks," *Am. J. Infect. Control*, vol. 20, no. 4, pp. 177–184, 1992, doi: 10.1016/S0196-6553(05)80143-9.
- [100] R. Greenwald *et al.*, "Estimating minute ventilation and air pollution inhaled dose using heart rate, breath frequency, age, sex and forced vital capacity: A pooled-data analysis," *PLoS One*, vol. 14, no. 7, p. e0218673, Jul. 2019, doi: 10.1371/JOURNAL.PONE.0218673.
- [101] G. Sharma and J. Goodwin, "Effect of aging on respiratory system physiology and immunology," *Clin. Interv. Aging*, vol. 1, no. 3, p. 253, 2006, doi: 10.2147/CIIA.2006.1.3.253.
- [102] C. Chourpiliadis and A. Bhardwaj, "Physiology, Respiratory Rate," *StatPearls*, Sep. 2021, Accessed: Mar. 17, 2022. [Online]. Available: <https://www.ncbi.nlm.nih.gov/books/NBK537306/>.
- [103] D. T. Liu, K. M. Philips, M. M. Speth, G. Besser, C. A. Mueller, and A. R. Sedaghat, "Portable HEPA Purifiers to Eliminate Airborne SARS-CoV-2: A Systematic Review," *Otolaryngol. – Head Neck Surg. (United States)*, Jun. 2021, doi: 10.1177/01945998211022636.
- [104] A. Henriques *et al.*, "Modelling airborne transmission of SARS-CoV-2 using CARA: risk assessment for enclosed spaces," *Interface Focus*, vol. 12, no. 2, Apr. 2022, doi: 10.1098/RSFS.2021.0076.
- [105] The American Society of Heating Refrigerating and Air-Conditioning Engineers (ASHRAE), "ASHRAE Position Document on Unvented Combustion Devices Approved by ASHRAE Board of Directors," *Ashrae Stand.*, 2020.
- [106] M. Biasin *et al.*, "UV-C irradiation is highly effective in inactivating SARS-CoV-2 replication," *Sci. Reports 2021 111*, vol. 11, no. 1, pp. 1–7, Mar. 2021, doi: 10.1038/s41598-021-85425-w.
- [107] H. P. Oswin *et al.*, "The Dynamics of SARS-CoV-2 Infectivity with Changes in Aerosol Microenvironment," *medRxiv*, pp. 1–42, 2022.
- [108] L. Patients, D. Taylor, A. C. Lindsay, and J. P. Halcox, "Aerosol and Surface Stability of SARS-CoV-2 as Compared with SARS-CoV-1," *new engl J. Med.*, pp. 0–2, 2020.
- [109] P. Dabisch *et al.*, "The influence of temperature, humidity, and simulated sunlight on the infectivity of SARS-CoV-2 in aerosols," *Aerosol Sci. Technol.*, vol. 55, no. 2, pp. 142–153, 2020, doi: 10.1080/02786826.2020.1829536.
- [110] M. R. Maxey, "The gravitational settling of aerosol particles in homogeneous turbulence and random flow fields," *J. Fluid Mech.*, vol. 174, pp. 441–465, 1987, doi: 10.1017/S0022112087000193.
- [111] R. W. Aldridge *et al.*, "Household overcrowding and risk of SARS-CoV-2: analysis of the Virus Watch prospective community cohort study in England and Wales," *Wellcome Open Res. 2021 6347*, vol. 6, p. 347, Dec. 2021, doi: 10.12688/wellcomeopenres.17308.1.
- [112] H. C. Burrige, S. Fan, R. L. Jones, C. J. Noakes, and P. F. Linden, "Predictive and retrospective modelling of airborne infection risk using monitored carbon dioxide," Sep. 2021, doi: 10.1177/1420326X211043564.
- [113] H. C. Yeh, R. F. Phalen, and O. G. Raabe, "Factors influencing the deposition of inhaled particles.," *Environ. Health Perspect.*, vol. 15, p. 147, 1976, doi: 10.1289/EHP.7615147.
- [114] W. C. Hinds, *Aerosol Technology: Properties*. 1999.
- [115] ICRP, "Human Respiratory Tract Model for Radiological Protection," ICRP Publi., ICRP Publication 66. Ann, Ed. ICRP Publication 66. Ann, 1994.
- [116] J. A. Lednicky *et al.*, "Viable SARS-CoV-2 in the air of a hospital room with COVID-19 patients," *Int. J. Infect. Dis.*, vol. 100, pp. 476–482, Nov. 2020, doi: 10.1016/j.ijid.2020.09.025.
- [117] J. A. Lednicky *et al.*, "Isolation of SARS-CoV-2 from the air in a car driven by a COVID patient with mild illness," *Int. J. Infect. Dis.*, vol. 108, pp. 212–216, Jul. 2021, doi: 10.1016/J.IJID.2021.04.063.
- [118] T. Greenhalgh, J. L. Jimenez, K. A. Prather, Z. Tufekci, D. Fisman, and R. Schooley, "Ten scientific reasons in support of airborne transmission of SARS-CoV-2.," *Lancet (London, England)*, vol. 0, no. 0, Apr. 2021, doi: 10.1016/S0140-6736(21)00869-2.
- [119] N. van Doremalen *et al.*, "Aerosol and Surface Stability of SARS-CoV-2 as Compared with SARS-CoV-1," *N. Engl. J. Med.*, vol. 382, no. 16, pp. 1564–1567, Apr. 2020, doi: 10.1056/NEJMC2004973/SUPPL_FILE/NEJMC2004973_DISCLOSURES.PDF.
- [120] O. Puhach *et al.*, "Infectious viral load in unvaccinated and vaccinated individuals infected with ancestral, Delta or Omicron SARS-CoV-2," *Nat. Med.* 2022, pp. 1–1, Apr. 2022, doi: 10.1038/s41591-022-01816-0.
- [121] Centers for Disease Control and Prevention, "Masks and Respirators," *COVID-19*, 2022. <https://www.cdc.gov/coronavirus/2019-ncov/prevent-getting-sick/types-of-masks.html> (accessed Jun. 16, 2022).
- [122] World Health Organization, "Infection prevention and control in the context of coronavirus disease (COVID-19): A living guideline I," no. March, pp. 1–74, 2022. Available: <https://apps.who.int/iris/handle/10665/352339>
- [123] World Health Organization, "COVID-19 infection prevention and control living guideline: mask use in community settings," no. December, 2021, doi: 10.1201/b16551.
- [124] T. Jefferson *et al.*, "Physical interventions to interrupt or reduce the spread of respiratory viruses: systematic review," *BMJ*, vol. 336, no. 7635, pp. 77–80, Jan. 2008, doi: 10.1136/BMJ.39393.510347.BE.
- [125] J. Xiao *et al.*, "Nonpharmaceutical Measures for Pandemic Influenza in Nonhealthcare Settings—Personal Protective and Environmental Measures—Volume 26, Number 5—May 2020—Emerging Infectious Diseases journal—CDC," *Emerg. Infect. Dis.*, vol. 26, no. 5, pp. 967–975, May 2020, doi: 10.3201/EID2605.190994.

- [126] NIOSH, “42 CFR Part 84 Respiratory Protective Devices,” *Centers Dis. Control Prev.*, vol. 60, no. 110, p. Chapter I, Subchapter G., 1995, [Online]. Available: <https://www.cdc.gov/niosh/npptl/topics/respirators/pt84abs2.html>.
- [127] European Committee for Standardization, “EN 149:2001+A1:2009 – Respiratory protective devices – Filtering half masks to protect against particles – Requirements, testing, marking,” 2009. Accessed: Jun. 16, 2022. [Online]. Available: <https://standards.iteh.ai/catalog/standards/cen/f440f60a-91c1-497b-815e-4e9d46436256/en-149-2001a1-2009>.
- [128] ASTM INTERNATIONAL, “Standard Specification for Barrier Face Coverings,” *Standards Products*, 2021. <https://www.astm.org/f3502-21.html> (accessed Jun. 16, 2022).
- [129] H. A. Chang, “Social Distancing,” *Acad. Psychiatry*, vol. 44, no. 6, p. 681, 2020, doi: 10.1007/s40596-020-01283-0.
- [130] P. Mbala-Kingebeni *et al.*, “Medical countermeasures during the 2018 Ebola virus disease outbreak in the North Kivu and Ituri Provinces of the Democratic Republic of the Congo: a rapid genomic assessment,” *Lancet. Infect. Dis.*, vol. 19, no. 6, pp. 648–657, Jun. 2019, doi: 10.1016/S1473-3099(19)30118-5.
- [131] K. Khan *et al.*, “Spread of a Novel Influenza A (H1N1) Virus via Global Airline Transportation,” *N. Engl. J. Med.*, vol. 361, no. 2, pp. 212–214, Dec. 2009, doi: 10.1056/NEJMC0904559.
- [132] J. Zhang *et al.*, “Changes in contact patterns shape the dynamics of the COVID-19 outbreak in China,” *Science (80-.)*, vol. 368, no. 6498, pp. 1481–1486, Jun. 2020, doi: 10.1126/SCIENCE.ABB8001/SUPPL_FILE/PAPV2.PDF.
- [133] J. A. Jacquez, C. P. Simon, J. Koopman, L. Sattenspiel, and T. Perry, “Modeling and analyzing HIV transmission: the effect of contact patterns,” *Math. Biosci.*, vol. 92, no. 2, pp. 119–199, Dec. 1988, doi: 10.1016/0025-5564(88)90031-4.
- [134] N. G. Davies *et al.*, “Effects of non-pharmaceutical interventions on COVID-19 cases, deaths, and demand for hospital services in the UK: a modelling study,” *Lancet. Public Heal.*, vol. 5, no. 7, pp. e375–e385, Jul. 2020, doi: 10.1016/S2468-2667(20)30133-X.
- [135] A. Mousa *et al.*, “Social contact patterns and implications for infectious disease transmission: A systematic review and meta-analysis of contact surveys,” *Elife*, vol. 10, 2021, doi: 10.7554/eLife.70294.
- [136] C. T. Semelka *et al.*, “Detection of Environmental Spread of SARS-CoV-2 and Associated Patient Characteristics,” *Open Forum Infect. Dis.*, vol. 8, no. 6, Jun. 2021, doi: 10.1093/OFID/OFAB107.
- [137] W. E. Bischoff, K. Swett, I. Leng, and T. R. Peters, “Exposure to influenza virus aerosols during routine patient care,” *J. Infect. Dis.*, vol. 207, no. 7, pp. 1037–1046, Apr. 2013, doi: 10.1093/INFDIS/JIS773.
- [138] Y. Li, P. Cheng, and W. Jia, “Poor ventilation worsens short-range airborne transmission of respiratory infection,” *Indoor Air*, vol. 32, no. 1, Jan. 2022, doi: 10.1111/INA.12946.
- [139] M. Alene *et al.*, “Magnitude of asymptomatic COVID-19 cases throughout the course of infection: A systematic review and meta-analysis,” *PLoS One*, vol. 16, no. 3, p. e0249090, Mar. 2021, doi: 10.1371/JOURNAL.PONE.0249090.
- [140] C. Blaurock *et al.*, “Compellingly high SARS-CoV-2 susceptibility of Golden Syrian hamsters suggests multiple zoonotic infections of pet hamsters during the COVID-19 pandemic,” *bioRxiv*, p. 2022.04.19.488826, Apr. 2022, doi: 10.1101/2022.04.19.488826.
- [141] M. Martins, M. H. V. Fernandes, L. R. Joshi, and D. G. Diel, “Age-Related Susceptibility of Ferrets to SARS-CoV-2 Infection,” *J. Virol.*, vol. 96, no. 3, Feb. 2022, doi: 10.1128/JVI.01455-21/ASSET/958FA7D8-97DD-4FBD-84A6-39F61FBEA500/ASSETS/IMAGES/LARGE/JVI.01455-21-F009.JPG.
- [142] P. A. Dabisch *et al.*, “Seroconversion and fever are dose-dependent in a nonhuman primate model of inhalational COVID-19,” *PLOS Pathog.*, vol. 17, no. 8, p. e1009865, Aug. 2021, doi: 10.1371/JOURNAL.PPAT.1009865.
- [143] B. Killingley *et al.*, “Safety, tolerability and viral kinetics during SARS-CoV-2 human challenge in young adults,” *Nat. Med.* 2022, pp. 1–11, Mar. 2022, doi: 10.1038/s41591-022-01780-9.
- [144] GISAID, “GISAID – Initiative,” *Global Initiative On Sharing All Influenza Data (GISAID) hCoV-19 database*, 2022. <https://www.gisaid.org/> (accessed Jun. 17, 2022).
- [145] F. Campbell *et al.*, “Increased transmissibility and global spread of SARSCoV- 2 variants of concern as at June 2021,” *Eurosurveillance*, vol. 26, no. 24, pp. 1–6, Jun. 2021, doi: 10.2807/1560-7917.ES.2021.26.24.2100509/CITE/PLAINTEXT.
- [146] K. Ito, C. Piantham, and H. Nishiura, “Estimating relative generation times and relative reproduction numbers of Omicron BA.1 and BA.2 with respect to Delta in Denmark,” *medRxiv*, p. 2022.03.02.22271767, Mar. 2022, doi: 10.1101/2022.03.02.22271767.
- [147] Y. Liu and J. Rocklöv, “The effective reproductive number of the Omicron variant of SARS-CoV-2 is several times relative to Delta,” *J. Travel Med.*, vol. 29, no. 3, pp. 1–4, May 2022, doi: 10.1093/JTM/TAAC037.
- [148] V. Hall *et al.*, “Protection against SARS-CoV-2 after Covid-19 Vaccination and Previous Infection,” *N. Engl. J. Med.*, vol. 386, no. 13, pp. 1207–1220, Mar. 2022, doi: 10.1056/NEJMOA2118691/SUPPL_FILE/NEJMOA2118691_DISCLOSURES.PDF.
- [149] VIEW-Hub, “Effectiveness Studies | ViewHub,” *Effectiveness Studies*, 2022. https://view-hub.org/covid-19/effectiveness-studies?target=variant&field=covid_studies_variant_tabl=9872&&planned=false (accessed Jun. 17, 2022).

- [150] S. Pilz *et al.*, “SARS-CoV-2 re-infection risk in Austria.” *Eur. J. Clin. Invest.*, vol. 51, no. 4, p. e13520, Apr. 2021, doi: 10.1111/eci.13520.
- [151] J. M. Dan *et al.*, “Immunological memory to SARS-CoV-2 assessed for up to 8 months after infection.” *Science*, vol. 371, no. 6529, Feb. 2021, doi: 10.1126/science.abf4063.
- [152] N. K. Shrestha, P. C. Burke, A. S. Nowacki, P. Terpeluk, and S. M. Gordon, “Necessity of Coronavirus Disease 2019 (COVID-19) Vaccination in Persons Who Have Already Had COVID-19,” *Clin. Infect. Dis.*, p. ciac022, Jan. 2022, doi: 10.1093/cid/ciac022.
- [153] V. J. Hall *et al.*, “SARS-CoV-2 infection rates of antibody-positive compared with antibody-negative health-care workers in England: a large, multicentre, prospective cohort study (SIREN).” *Lancet (London, England)*, vol. 397, no. 10283, pp. 1459–1469, Apr. 2021, doi: 10.1016/S0140-6736(21)00675-9.
- [154] N. Kojima and J. D. Klausner, “Protective immunity after recovery from SARS-CoV-2 infection,” *Lancet Infect. Dis.*, vol. 22, no. 1, pp. 12–14, Jan. 2022, doi: 10.1016/S1473-3099(21)00676-9.
- [155] J. Conly *et al.*, “Use of medical face masks versus particulate respirators as a component of personal protective equipment for health care workers in the context of the COVID-19 pandemic,” *Antimicrob. Resist. Infect. Control*, vol. 9, no. 1, p. 126, Aug. 2020, doi: 10.1186/s13756-020-00779-6.
- [156] P. Z. Chen, N. Bobrovitz, Z. Premji, M. Koopmans, D. N. Fisman, and F. X. Gu, “Heterogeneity in transmissibility and shedding SARS-CoV-2 via droplets and aerosols,” *Elife*, vol. 10, Apr. 2021, doi: 10.7554/ELIFE.65774.
- [157] N. Zhang, B. Su, P.-T. Chan, T. Miao, P. Wang, and Y. Li, “Infection Spread and High-Resolution Detection of Close Contact Behaviors.” *Int. J. Environ. Res. Public Health*, vol. 17, no. 4, Feb. 2020, doi: 10.3390/ijerph17041445.

Annexes



Annex 1. Systematic review results

On the 26/04/2022, we searched the WHO COVID-19 database <https://search.bvsalud.org/global-literature-on-novel-coronavirus-2019-ncov/>. The search strategy was developed by a WHO librarian (please see Annex 1) and included studies published before the 26/04/2022.

Q 1: Respiratory activities-specific exhaled particle emission

Search strings

(droplet* OR particle* OR *aerosol*) AND (size diameter OR volume* OR CM OR centimetre OR centimeter) AND (“expiratory activity” OR “Respiratory Activity” OR “Respiratory Activities” OR breath* OR speak* OR talk* OR shout* OR sing* OR cough* OR sneez*)

Eligibility criteria for study selection

Experimental studies that measured the 1) particle number size distribution (μm) per second (number of particles per second/particles size); 2) total particle mass concentration with an aerodynamic diameter within a given size ranges (number of particles cm^{-3}) 3) Total particle volume concentration per unit diameter (in $\text{mL m}^{-3} \mu\text{m}^{-1}$)

Main outcome measures

1. Particles size distribution
2. volumetric particle emission concentration
3. Mass

Results

Experts independently screened the titles and abstracts and excluded studies that did not match the inclusion criteria. Discrepancies were resolved in discussion with the other experts. The same experts retrieved full text articles and determined whether to include or exclude studies on the basis of predetermined selection criteria. A total of 1125 studies were initially screened, of which 1088 were considered irrelevant. After exclusions, 26 studies were eligible for full text review and 15 met the inclusion criteria.

Data extraction

Reference	Study design	Range size	Respiratory activity		
			Breathing	Talking	Singing
Alsved et al. ¹	Experimental study	0.5 – 10 μm	Median mas: 135 particle/s (85-691)	Talking: Median mas: 270 (120-1380) Loud talking: Median mas 570 (180-1760)	Singing: Median mas: 980 (390-2870) Loud singing: Median mas 1480 (500-2820)
Bagheri et al. ²	Experimental study				
Chao et al. ³	Experimental study	mean diameter 16.0 μm		Total number 112–6720 Concentration 0.004–0.223 cm^{-3}	

Reference	Study design	Range size	Respiratory activity				
			Breathing	Talking	Singing		
Ding et al. ⁴	Experimental study	0.3–10 µm		315 particles/s	413 particles/s		
Good et al. ⁵	Experimental study	0.25 – 33 µm	239 particles/s (<56 – 909) 1915 particles/L ⁻¹ (<450 – 7269)		411 particles/s (<56 -1194) 3289 particles/L ⁻¹ (<450 – 9551)		
Kappelt et al. ⁶	Experimental study	< 10 µm	6210 ± 5630 min ⁻¹	14,600 ± 16,800 min ⁻¹			
Murbe et al. ⁷	Experimental study	0.3–10 µm	5 particles/sec (0 – 28)	66 particles/sec (14 – 391)	1537 particles/sec (753 – 6093)		
			>99 % of all detected particles were ≤5 µm (>80% of all particles ≤1 µm)				
Murbe et al. ⁸	Experimental study	>0.3 µm–25.0 µm		16 – 267 particles/s	141 – 1240 particles/s		
Mimura et al. ⁹	Experimental study	PM 2.5	23.1 ± 9.9 µg/m ³	32.3 ± 14.7 µg/m ³			
		PM 10	40.4 ± 17.8 µg/m ³	1.4 ± 17.8 µg/m ³			
J. Duguid ¹⁰	Experimental study	> 20 µm	0 particle	0 – 650 particles			
Papineni et al. ¹¹	Experimental study	< 1 µm	12.5 (83.2) particles L ⁻¹				
		> 1 µm	1.9 (13.4) particles L ⁻¹				
Morawska et al. ¹²	Experimental study	0.5-20 µm	98 particles L ⁻¹	672 particles L ⁻¹	1088 particles L ⁻¹		
Asadi et al. ¹³	Experimental study	<5 µm	1 – 50 particles/s				
Stadnytskyi et al. ¹⁴	Experimental study	0.5 – 5 µm		2600 particles/s			
Morawska et al. ¹² Johnson et al. ¹⁵		Mode	C _{n,i} (cm ⁻³)	µ _{Di} (µm)	GM (µm)	σ _{Di} (µm)	GSD (µm)
		B (bronchial)	0.06	0.99	2.69	0.26	1.30
		L (larynx)	0.2	1.39	4.01	0.51	1.67
		O (oral)	0.001	4.98	145.5	0.59	1.80

BLO model details ^{12,15}			
	Breathing	Talking	Singing
Total volumetric particle emission concentration (ml m ⁻³)	8.4 E -7	2.2 E -5	1.1 E -4
Total particle emission concentration (particles L-1)	60	260	1060
Size range (long range) (µm)	0.1 – 30		
Size range (Short-range) (µm)	0.1 – 100		

Q 2: Viral load Search strings

("viral load"~3 OR "viral loads"~3 OR "virus load"~3 OR "virus loads"~3 OR "virus burden"~3 OR "viral burden"~3 OR "virus titre" OR "viral titre"~3 OR "virus titer" OR "viral titer"~3 OR "virus titres" OR "viral titres"~3 OR "virus titers" OR "viral titers"~3 OR "viral level"~3 OR "Viral levels"~3 OR "virus level"~3 OR "Virus levels"~3 OR "RNA load"~3 OR "RNA loads"~3) AND (metaanaly* OR metanaly* OR "meta analysis" OR "meta analyses" OR meta-analysis OR meta-analyses OR "research overview" OR "research overviews" OR "collaborative review" OR "collaborative overview" OR "systematic review"~3 OR "systematic reviews" OR "systematic overviews" OR "systematic overview" OR "systematized review" OR "systematized reviews" OR "rapid review" OR "rapid reviews" OR "narrative review" OR "literature review" OR "literature reviews" OR "living guidelines" OR "living guideline" OR "living review" OR "living reviews" OR "scoping review" OR "scoping reviews" OR "umbrella reviews" OR "umbrella review" OR "evidence mapping" OR "evidence map" OR "evidence maps" OR "mapping review" OR "mapping reviews" OR "critical review" OR "critical reviews" OR "mixed studies review" OR "mixed methods review" OR "mixed studies reviews" OR "mixed methods reviews" OR "evidence synthesis" OR "evidence syntheses" OR "health technology assessment" OR "biomedical technology assessment" OR "bio-medical technology assessment" OR "technology overview" OR "technology assessment" OR "technology assessments" OR "technology overviews" OR HTA OR HTAs OR "methodological overview" OR "methodological overviews" OR "methodologic overview" OR "methodological overviews" OR "methodological review" OR "methodological reviews" OR "quantitative review" OR "quantitative reviews" OR "quantitative overview" OR "quantitative overviews" OR "quantitative syntheses" OR "quantitative synthesis" OR "systematic search" OR "systematic searching" OR "systematic searches" OR "pooled analysis" OR "pooled analyses" OR pubmed OR medline OR embase OR ti:Cochrane OR ab:Cochrane OR ti:Campbell OR ab:Campell OR "grey literature" OR handsearch* OR "hand searching" OR "hand searched" OR "citation searching" OR "reference searching" OR "pearl growing" OR "data mining" OR "citation mining" OR snowballing OR "meta regression" OR metaregression* OR "data synthesis" OR "data synthesis" OR "data extraction" OR "data abstraction" OR "data abstractions" OR "mantel haenszel" OR ab:peto OR der-simonian OR dersimonian OR "der simonion")

Eligibility criteria for study selection

Studies that measured the distribution of Viral Load through NP across multiple patients (>15.000), systematic reviews, or meta-analysis

Main outcome measures

1. Viral load distribution
2. Range of log₁₀ RNA copies per mL

Results

Experts independently screened the titles and abstracts and excluded studies that did not match the inclusion criteria. Discrepancies were resolved in discussion with the other experts. The same experts retrieved full text articles and determined whether to include or exclude studies on the basis of predetermined selection criteria. A total of 201 studies were initially screened, of which 187 were considered irrelevant. After exclusions, 14 studies were eligible for full text review and 3 met the inclusion criteria.

Data extraction

Reference	Study design	Viral load			
		Min copies/mL	Max copies/mL	Median copies/mL	Mean (SD) log ₁₀ RNA copies per ml
Gilad et al. ¹⁶	Systematic review	1.2 x10 ³		8.14 x10 ⁶	
Chen et al. ¹⁷	Systematic review				8.63 (95% CI: 8.04–9.26) and 6.01 (95% CI: 4.65–7.78) log ₁₀ copies/ml for severe and non severe disease, respectively
Jacot et al. ¹⁸	Retrospective case serie				6.6 log ₁₀ copies/ml
Chen et al. ¹⁹	Systematic review and meta-analysis			8.91 (95% CI: 8.83–9.00) log ₁₀	2.04 log ₁₀

Q 3: Biological decay in air

Search strings

(air OR particl* OR *aerosol*) AND (“biological decay” OR inactivat* OR decay OR stability)

Eligibility criteria for study selection

Studies that measured the SARS-CoV-2 biological decay in aerosol.

Main outcome measures

1. Range of estimated biological decay constant k (min-1 or h-1)

Results

Experts independently screened the titles and abstracts and excluded studies that did not match the inclusion criteria. Discrepancies were resolved in discussion with the other experts. The same experts retrieved full text articles and determined whether to include or exclude studies on the basis of predetermined selection criteria. A total of 941 studies were initially screened, of which 632 were considered irrelevant. After exclusions, 72 studies were eligible for full text review and 7 met the inclusion criteria.

Data extraction

Reference	Study design	Conditions						Decay				
		Temp. (°C)	HR (%)	Time (m)	Light	Measure	Lineage	Start concentration	End concentration	K _{Infectivity}	Minutes for 50% decay	Decay Rate
Van Doremalen et al. ²⁰	Experimental	23	65	180	NR	TCID ₅₀	NR	10 ^{3.5}	10 ^{2.7}	1.1 h ⁻¹		
Robey et al. ²¹	Modeling	22	40	240	NR	TCID ₅₀	NR			0.108 h ⁻¹		
		22	65	240	NR	TCID ₅₀	NR			0.288 h ⁻¹		
Schuit et al. ²²	Experimental	20.1 ± 0.3	70	60	No light	K _{Infectivity} min ⁻¹	hCoV-19/USA/WA-1/2020			0.008 ± 0.011 min ⁻¹		0.8 ± 1.1 %/min
		20.1 ± 0.3	70	60	Simulated sunlight mild intensity	Decay Rate, %/min				0.121 ± 0.017 min ⁻¹		11.4 ± 1.5 %/min
		20.1 ± 0.3	70	60	Simulated sunlight high intensity					0.306 ± 0.097 min ⁻¹		26.1 ± 7.1 %/min

Reference	Study design	Conditions						Decay				
		Temp. (°C)	HR (%)	Time (m)	Light	Measure	Lineage	Start concentration	End concentration	K _{Infectivity}	Minutes for 50% decay	Decay Rate
Schuit et al. ²³	Experimental	40	20	60	Simulated sunlight		hCoV-19/USA/WA-1/2020			0.216 ± 0.056 min ⁻¹		
		40	20	60			hCoV-19/USA/CA_CDC_5574/2020			0.209 ± 0.063 min ⁻¹		
		40	20	60			hCoV-19/USA/NY-PV08449/2020			0.299 ± 0.047 min ⁻¹		
		40	20	60			hCoV-19/France/IDF0372/2020			0.312 ± 0.051 min ⁻¹		
		20	20	60	Darkness		0.000 ± 0.011 min ⁻¹					
		40	20	60	Darkness	All above lineages	0.012 ± 0.008 min ⁻¹					
Oswin et al. ²⁴	Experimental	18-21	40-70	5	Simulated sunlight	Decay rate	REMRQ0001				10	
Chatterjee et al. ²⁵	Modeling	21	65	180	NR	TCID ₅₀	NR	10 ^{3.5}	10 ^{2.7}	1.1 h ⁻¹		
Smither et al. ²⁶	Experimental	19-22	40-60	300	Darkness	TCID ₅₀	SARS-CoV-2 England-2	10 ⁶		0.75 h ⁻¹		0.91 – 2.27 % min ⁻¹
		19-22	68-88	300	Darkness	TCID ₅₀	SARS-CoV-2 England-2			0.80 h ⁻¹		0.40 – 1.59 % min ⁻¹
Dabisch et al. ²⁷	Experimental / Regression	10 – 30	20 – 70	20 – 60	Simulated sunlight and darkness	TCID ₅₀	SARS-CoV-2 (Passage 4; BetaCoV/USA/WA1/2020)			Max values: 0.066±0.028 min ⁻¹ (Darkness) 0.488±0.146 min ⁻¹ (Sunlight) Empirical regression in Eq 1.		Max values: 6.3±2.6 % min ⁻¹ (Darkness) 38.1±8.9 % min ⁻¹ (Sunlight)

Q 4: Host immune response

Range of vaccine effectiveness against SARS-CoV-2 infection stratified by vaccine formulation, time, age and VoC

A search of the grey, preprint, and published literature for COVID-19 Vaccine Effectiveness and Impact studies is conducted daily.

Details here https://view-hub.org/covid-19/effectiveness-studies?target=variant&field_covid_studies_variant_tabl=9872

The model uses data published on the: “Results of COVID-19 Vaccine Effectiveness Studies: An Ongoing Systematic Review”, Weekly Summary Tables, Updated 8th September 2022. https://view-hub.org/sites/default/files/2022-09/COVID19_Vaccine_Effectiveness_Transmission_Studies_Summary_Tables_20220908.pdf

Q 5: Particle to PFU ratio (PFU> TCID50%)

Search strings

("viral load"~3 OR "viral loads"~3 OR "virus load"~3 OR "virus loads"~3 OR "virus burden"~3 OR "viral burden"~3 OR "virus titre" OR "viral titre"~3 OR "virus titer" OR "viral titer"~3 OR "virus titres" OR "viral titres"~3 OR "virus titers" OR "viral titers"~3 OR "viral level"~3 OR "viral levels"~3 OR "virus level"~3 OR "Virus levels"~3 OR "RNA load"~3 OR "RNA loads"~3) AND ("viable RNA"~3 OR culturable OR "live virus" OR "viral culture" OR "viable virus" OR PFU OR "plaque forming unit" OR "live sars-cov-2" OR "positive culture" OR "positive cultures" OR infectious OR infective OR "virus isolation"~2 OR ratio* OR "culture positivity" OR "positive culture" OR "positive cultures") AND (Exhal* OR expirat* OR *aerosol* OR breath* OR air)

Eligibility criteria for study selection

Studies relating SARS-CoV-2 Viral Loads and viable virus in exhaled breath (EB) and air expressed as CPE (PFU), TCID50% or multiplicity of infection (moi). VoCs VS wild virus

Main outcome measures

1. Range of ratio of viral copies in aerosol to plaque forming units (PFU) ratio for SARS-CoV-2 (log10) OR TCID50% or moi

Results

Experts independently screened the titles and abstracts and excluded studies that did not match the inclusion criteria. Discrepancies were resolved in discussion with the other experts. The same experts retrieved full text articles and determined whether to include or exclude studies on the basis of predetermined selection criteria. A total of 259 studies were initially screened, of which 195 were considered irrelevant. After exclusions, 61 studies were eligible for full text review and 5 met the inclusion criteria.

Data extraction

Full vaccination (defined as >2weeks after reception of 2nd dose during primary vaccination series)

FFA: focus forming assay

Reference	Study design	Conditions								Viable-to-RNA virus ratio				
		Cohort	Sampling method	DPOS	Clinical manifestation	Vaccination status	Lineage	qRT-PCR	CT threshold for culturability assay	culturability assay	Successful viral cell culture	Viral titre	RNA to PFU	
Puhach et al. ²⁸	Experimental	565	NPS	5	Mild	NA	Wild	0.4744 log ₁₀	<27	FFA	91.9%	0.343 log ₁₀		
						No	Delta	0.44 log ₁₀			91.7%			
						Fully	Delta				83.8%			
						No	Omicron				95%			
						Fully	Omicron				85.7%			
Heitzman-Breen et al. ²⁹	Modeling from animal studies	NA	NA	NA	NA	NA	Wild						10 ³ :1 to 10 ⁶ :1	
Hawks et al. ³⁰	Animal study	NA	EB	2	NA	NA	USA-WA1/2020	1.4·log ₁₀ PFU/hour		Vero cell plaque assay				10 ² :1
Basile et al.	Experimental	195	URT/LRT	4.5	Mix				<32		24% (CPE)			
Lednicky et al. ³¹	Experimental	2	Air sample	2-4	NA	No	Wild	94 Viral genome equ/L air	NA	TCID ₅₀ tests	74 virus/L air		2.68E+04 TCID ₅₀ /100 μm	
								30 Viral genome equ/L air			18 virus/L air		6.31E+03 TCID ₅₀ /100 μm	
								44 Viral genome equ/L air			27 virus/L air		1.00E+04 TCID ₅₀ /100 μm	
								16 Viral genome equ/L air			6 virus/L air		2.15E+03 TCID ₅₀ /100 μm	

Q 6: VoC increased transmissibility

Increased transmissibility and global spread of SARS-CoV-2 variants of concern as at June 2021³²

Analysis

1,722,652 SARS-CoV-2 sequences uploaded to the Global Initiative On Sharing All Influenza Data (GISAID) hCoV-19 database, considering only VOC or VOI reported at least 25 times in at least three countries (see Supplementary Tables S1 and S2 for sequence numbers per variant per country). GISAID sequences used for this work are acknowledged in Supplement 2. Multinomial logistic model of competitive growth was used to estimate the effective reproduction number of each variant relative to that of the non-VOC/VOI viral population for each reporting country. It is assumed that the generation time of VOC/VOI remained unchanged compared with previously circulating variants.

Results

Despite differences between countries, our analysis showed a statistically significant increase in the pooled mean effective reproduction number relative to non-VOC/VOI of B.1.1.7 at 29% (95% confidence interval (CI): 24–33), B.1.351 at 25% (95% CI: 20–30), P.1 at 38% (95% CI: 29–48) and B.1.617.2 at 97% (95% CI: 76–117) (Figure 1). Of the six variants currently designated as VOI, five were considered in our analysis and among these, only B.1.617.1 and B.1.525 demonstrated a statistically significant increase in the effective reproduction number of 48% (95% CI: 28–69) and 29% (95% CI: 23–35), respectively. In line with these estimates, our results showed rapid replacement of previously circulating variants by VOC/VOI in nearly all countries; of the 64 countries considered in this analysis, we estimate VOC/VOI to be the most frequently circulating lineage on the last day of available data in 52 countries, the most common variants being B.1.1.7 (40 countries) and B.1.617.2 (India, Singapore, United Kingdom and Australia).

Given the widespread co-circulation of VOC/VOI, we also compared the effective reproduction numbers of these variants against each in order to estimate the nature of future competitive growth between them (Figure 3, excluding P.2 and B.1.427/B.1.429). Notably, the pooled mean difference in the effective production number between the VOC B.1.1.7 and B.1.351 was small at 4% (95% CI: 0–8), while P.1 demonstrated an increase relative to B.1.1.7 and B.1.351 of 10% (95% CI: 3–17) and 17% (95% CI: 6–30). Given these estimates, the longer-term trends of competitive growth between these three VOC remain unclear. In contrast, the rapid observed growth of B.1.617.2 suggests a clear competitive advantage compared with B.1.1.7, B.1.351 and P.1, with estimated increases in the effective reproduction number of 55% (95% CI: 43–68), 60% (95% CI: 48–73) and 34% (95% CI: 26–43) respectively.

A systematic review results show that the effective reproduction number and basic reproduction number of the Omicron variant elicited 3.8- and 2.5-times higher transmissibility than the Delta variant, respectively. The Omicron variant has an average basic reproduction number of 9.5 and a range from 5.5 to 24 (median 10 and interquartile range, IQR: 7.25, 11.88). The average effective reproduction number for Omicron is 3.4 with a range from 0.88 to 9.4 (median 2.8 and IQR: 2.03, 3.85)³³.

Q 7: Dose-response model

Search strings

("Infectious Dose" OR "infective dose" OR "ID50" OR "TCID50" OR PFU OR "plaque forming unit" OR ("dose response" AND model*) OR "infectious particle"~5) AND (Seroconver* OR seropositive* OR "sero epidemiological" OR infection* OR infected OR "antibody positivity" OR "antibody positive"~3)

Eligibility criteria for study selection

Published studies estimating the SARS-CoV-2 and other coronaviruses infectious dose for airborne transmission

Main outcome measures

- Number of infectious viral particles needed to cause an infection OR Range of ID⁵⁰ for airborne transmission OR PFU range inhalation for TCID50%

Results

Experts independently screened the titles and abstracts and excluded studies that did not match the inclusion criteria. Discrepancies were resolved in discussion with the other experts. The same experts retrieved full text articles and determined whether to include or exclude studies on the basis of predetermined selection criteria. A total of 656 studies were initially screened, of which 585 were considered irrelevant. After exclusions, 71 studies were eligible for full text review and 11 met the inclusion criteria.

Data extraction

FFU: 1. Focus-forming unit

Reference	Study design	Virus / Lineage	Exposure	Sample	Cell line	Control	Infectious dose	
							ID ₅₀	TCID ₅₀
Blaurock et al. ³⁴	Animal study	SARS-CoV-2 2019_nCoV Muc-1MB-1	oro-tracheal	Golden Syrian hamsters	Vero E6 cells and Vero E6 in DMEM with 2% FCS	Symptoms, Histopathology		(MID) 10x10 ⁻³ TCID ₅₀
Killingley et al. ³⁵	Human challenge	SARS-CoV-2/ human/ GBR/484861/2020	Intranasal drops	36 naïve volunteers 18-36 y	cGMP Vero cell	Symptoms, Seroconversion, virus shedding	55 FFU	10 TCID ₅₀
Martins et al. ³⁶	Animal study	NY167-20 (B.1 lineage)	Intranasal drops	Ferret	Vero E6 (ATCC CRL-1586) and Vero E6/TMPRSS2	Symptoms, Seroconversion, virus shedding	31.6 PFU (aged animals) 100.1 PFU (young animals)	
Totura et al. ³⁷	Animal study	MERS-CoV EMC/2012, #NR-44260	aerosol	African green monkey	Vero E6 cells and Vero (CCL-81)	Symptoms, Seroconversion, histopathology	103-105 PFU	
Watanabe et al. ³⁸	Modeling, pooled data	HCoV-229E SARS-CoV-1	NA NA	mice	NA	NA	9 PFU 280 PFU	13 TCID ₅₀ 400 TCID ₅₀
Hayden et al. ³⁹	Human challenge	H1N1 influenza A/ Texas/91	Intranasal drops	166 adult volunteers	Madin-Darby canine kidney (MDCK) cells	Symptoms, Seroconversion	700 PFU	1.0x10 ³ TCID ₅₀
Alford et al. ⁴⁰	Human challenge	H2N2	aerosol	Adult volunteers			0.42 – 2.1 PFU	0.6 – 3 TCID ₅₀
Treanor et al. ⁴¹	Human challenge	H3N2	Intranasal drops	130 Adult volunteers	Rhesus Monkey Kidney (RhMK) cells	Symptoms, Seroconversion	7 000 000 PFU	1.0x10 ⁷ TCID ₅₀
Riediker et al. ⁴²	Modeling	WT Delta Omicron	aerosol aerosol aerosol	NA NA NA	NA	NA NA NA	500 PFU 300 PFU 100 PFU	
Dabish et al. ⁴³	Animal study	SARS-CoV-2 hCoV-19/USA/WA-1/2020	aerosol	16 young adult cynomolgus macaques	Vero cells (ATCC CCL-81) and Vero E6 cells (ATCC CRL-1586)	Seroconversion Fever	36.4 PFU 179.2 PFU	52 (23 – 363) TCID ₅₀ 256 (102 – 603) TCID ₅₀
Prentiss et al. ⁴⁴	Modeling from case studies	NA	NA	NA	NA	NA	250 – 1400 PFU	

Q 8: Mask filtration efficiency

Search strings

((mask* OR facemask* OR facepiece* OR n95 OR masking OR N100 OR FFP* OR FFP2 OR FFP3 OR FFR OR “neck gaiters” OR “face shield”~3 OR “face piece”~3 OR “facial piece”~3 OR “facial shield”~3 OR “face covering”~3 OR “facial covering”~3 OR “face cover”~3 OR “facial cover”~3 OR (“personal protection” OR PPE) AND (face OR facial))) AND (filtration OR effectiveness)) AND (metaanaly* OR metanaly* OR “meta analysis” OR “meta analyses” OR meta-analysis OR meta-analyses OR “research overview” OR “research overviews” OR “collaborative review” OR “collaborative overview” OR “systematic review”~3 OR “systematic reviews” OR “systematic overviews” OR “systematic overview” OR “systematized review” OR “systematized reviews” OR “rapid review” OR “rapid reviews” OR “narrative review” OR “literature review” OR “literature reviews” OR “living guidelines” OR “living guideline” OR “living review” OR “living reviews” OR “scoping review” OR “scoping reviews” OR “umbrella reviews” OR “umbrella review” OR “evidence mapping” OR “evidence map” OR “evidence maps” OR “mapping review” OR “mapping reviews” OR “critical review” OR “critical reviews” OR “mixed studies review” OR “mixed methods review” OR “mixed studies reviews” OR “mixed methods reviews” OR “evidence synthesis” OR “evidence syntheses” OR “health technology assessment” OR “biomedical technology assessment” OR “bio-medical technology assessment” OR “technology overview” OR “technology assessment” OR “technology assessments” OR “technology overviews” OR HTA OR HTAs OR “methodological overview” OR “methodological overviews” OR “methodologic overview” OR “methodological overviews” OR “methodological review” OR “methodological reviews” OR “quantitative review” OR “quantitative reviews” OR “quantitative overview” OR “quantitative overviews” OR “quantitative syntheses” OR “quantitative synthesis” OR “systematic search” OR “systematic searching” OR “systematic searches” OR “pooled analysis” OR “pooled analyses” OR pubmed OR medline OR embase OR ti:Cochrane OR ab:Cochrane OR ti:Campbell OR ab:Campbell OR “grey literature” OR handsearch* OR “hand searching” OR “hand searched” OR “citation searching” OR “reference searching” OR “pearl growing” OR “data mining” OR “citation mining” OR snowballing OR “meta regression” OR metaregression* OR “data synthesis” OR “data synthesis” OR “data extraction” OR “data abstraction” OR “data abstractions” OR “mantel haenszel” OR ab:peto OR der-simonian OR dersimonian OR “der simonion”)

Eligibility criteria for study selection

Studies that measured the inward and outward filtration efficiency of different type of masks for a given size of particles with information on particles ranges and/or respiratory activity/particle velocity/airflow.

Main outcome measures

1. Inward and outward filtration efficiency per type of mask or respiratory activity or particle range

Results

Experts independently screened the titles and abstracts and excluded studies that did not match the inclusion criteria. Discrepancies were resolved in discussion with the other experts. The same experts retrieved full text articles and determined whether to include or exclude studies on the basis of predetermined selection criteria. A total of 230 studies were initially screened, of which 147 were considered irrelevant. After exclusions, 83 studies were eligible for full text review and 14 met the inclusion criteria.

Data extraction

CM: Cloth mask

C: cotton

L: layer

ML: multiple layer

NR: not reported Y: yes

N: not

PES: polyester

PP: polypropylene

Reference	Study design	Type of mask	Fit test (Y/N/NR)	Particles ranges	Respiratory activity/flow rate/velocity	Filtration efficiency		
						inward	outward	not specified
Asadi et al. ⁴⁵	Experimental	Surgical Unvented KN95	n	0.3 – 20 µm	breathing, talking, and coughing		90% 74%	
Sousa et al. ⁴⁶	Literature review	CM 100% C 1L CM 100% C 2L CM Linen 1L Surgical	NR	20 – 1000 nm 20 – 1000 nm	Aerosol dispersion speed 16.5 cm/s	69% 70% 60% 96%		
Konda et al. ⁴⁷	Experimental	N95 Surgical	NR	>300 nm <300 nm >300 nm <300 nm	3.2 CFM or ~90 L/min	99% 85% 99% 76%		
Maher et al. ⁴⁸	Experimental	CM 1,2,3L	NR	1 µm	300 L/min			74.4–95.2%
Xiao et al. ⁴⁹	Experimental	CM 6L	NR	0.75 µm 8.2 µm	4440 cm/s			53.2–93.8% 36.7–90.4%
O’Kelly et al. ⁵⁰	Experimental	CM ML	NR	0.02–0.1 µm	1650 cm/s			10–62%
Park and Jayaraman ⁵¹	Experimental	CM PES/PP	N	0.3 µm	8.7 cm/			9 – 88%
Lindsley et al. ⁵²	Experimental	CM C 3L	N	<0.6 µm	28.3 L/min			30%
Liu et al. ⁵³	Experimental	CM reusable	N	0.075 µm	85 L/min			20%
Li et al. ⁵⁴	Experimental	CM 100% C	N	0.01–1 µm	20.5 L/min		77%	
Davies et al. ⁵⁵	Experimental	CM 100% C Surgical	N N	0.023 µm	30 L/min	50.85% 89.52%		
Neupane et al. ⁵⁶	Experimental	CM Surgical	Yes (Sealed)	<10 µm	2.7 m/s	63-84% 94%		

Reference	Study design	Type of mask	Fit test (Y/N/NR)	Particles ranges	Respiratory activity/flow rate/velocity	Filtration efficiency		
						inward	outward	not specified
Shakya et al. ⁵⁷	Experimental	N95	N	<1 µm	8 L/min	65 – 97%		
		CM	N	<1 µm	8 L/min	50 – 90%		
		Surgical	N	<1 µm	8 L/min	86 – 93%		
		CM	N	<1 µm	19 L/min	10 – 82%		
		Surgical	N	<1 µm	19 L/min	60 – 65%		
		N95	N	<1 µm	19 L/min	75 – 90%		
Ma et al. ⁵⁸	Experimental	CM 4L	N	Median 3.9 µm	2.2 m/s to 9.9 m/s	99.98%		
		Surgical	N			97.14%		
		N95	N			95.15%		
Pan et al. ⁵⁹	Experimental	Surgical mask	N	Outward experiment	Outward experiment	80%	50 – 75%	
		Thin cotton	N	0.04 – 1 µm	5.3 L/m	50%	30 – 50%	
		Thin acrylic	N	Inward experiment	3.2 to 3.4 m/s	5 – 40%	75% (2µm)	
		CDC non-sewn	N		5 – 40%			
		CDC sewn	N	Inward experiment	Inward experiment	5 – 40%	50% (2µm)	
		Microfiber	N	0.5 – 2 µm	15 L/m		<25% (2µm)	
Huang et al. ⁶⁰	Experimental (<i>in vivo</i> bacterial filtration efficiency)	N95	Yes	bacterial pneumonia patients			99.95%	
		Surgical mask	Yes				99.91%	
Gawn et al. ⁶¹	Experimental	Surgical (tie)	Yes	< 1 µm to > 200 µm	Mean values of the reduction factor for ambient particles and simulated sneeze	2 – 4		
		Surgical (strap)	Yes	Distribution		2 – 9		
		FFP2	Yes	~50% <20 µm		52 – 258		
		FFP3	Yes	10% >100 µm		145 – 766		
Milton et al. ⁶²	Experimental	Surgical	No	> 5 µm	Breathing	2.8 (95%CI 1.5 – 5.2)		
		Surgical	No	< 5 µm	Fold reduction of exhaled particles	25 (95%CI 3.5 – 150)		

Q 9: close encounter interactions

Social contact patterns and implications for infectious disease transmission: A systematic review and meta-analysis of contact surveys⁶³

Methods

Systematic review and individual-participant meta-analysis of surveys carried out in low- and middle-income countries and compare patterns of contact in these settings to surveys previously carried out in high-income countries. Using individual-level data from 28,503 participants and 413,069 contacts across 27 surveys, we explored how contact characteristics (number, location, duration, and whether physical) vary across income settings). A negative binomial regression model was used to explore the association between the total number of daily contacts and the participant's age, sex, employment/student status, and household size, as well as methodology and survey day. Incidence rate ratios from these regressions are referred to as 'contact rate ratios' (CRRs

Results

The median number of contacts made per day across all the studies was 9 (IQR = 5–17), and was similar across income strata (LIC/LMIC = 10[5–17], UMIC = 8[5–16], HIC = 9[5–17]). Contact rates declined with age in high- and upper-middle-income settings, but not in low-income settings, where adults aged 65+ made similar numbers of contacts as younger individuals and mixed with all age groups. Across all settings, increasing household size was a key determinant of contact frequency and characteristics, with low-income settings characterised by the largest, most intergenerational households. A higher proportion of contacts were made at home in low-income settings, and work/school contacts were more frequent in high-income strata. We also observed contrasting effects of gender across income strata on the frequency, duration, and type of contacts individuals made.

Data extraction

The total number of observations, as well as the mean, median, and interquartile range (p25 and p75) of total daily contacts shown by participant and study characteristics.

Group	Categorization	Observation (N)	Mean	P25	Median	P75
Overall		28,503	14.5	5	9	17
Gender	Male	13,218	15.3	5	9	18
	Female	14,598	13.7	5	9	16
Age	<15	8,561	14.6	6	10	19
	15 – 65	8,330	14.9	5	9	17
	>65	10,267	10.4	3	6	12
Income status	LIC/LMIC	9,906	15.4	5	10	17
	UMIC	8,330	14.4	5	8	16
	HIC	10,267	13.7	5	9	17
Day type	Weekend	4,308	14.7	5	9	16
	Weekday	21,579	14.1	5	9	17
Employment (in those aged >18)	Yes	8,879	15.4	5	9	17
	No	6,158	9.8	4	7	12
Student (in those aged 5 – 18)	Yes	4,438	18.4	8	14	24
	No	600	10.4	5	8	14
Household size	1	1,479	10.4	3	6	12
	2	3,220	11.8	4	7	14
	3	4,130	12.0	4	7	14
	4	5,240	13.4	5	8	17
	5	3,109	12.5	4	8	14
	6+	8,873	17.7	7	11	20

Data on the duration of contact (<1 or ≥1 hr) were available for 22,822 participants. The percentage of contacts lasting at least 1 hr was 63.2% and was highest for UMICs (76.0%) and lowest for LICs/LMICs (53.1%). Across both UMICs and HICs, duration of contacts was lower in individuals aged over 15 years compared to those aged 0–15, with the extent of this disparity most stark for HICs (for ages 65+ compared to <15 years: adjCRR [95%CrI]: LIC/LMIC = 0.61[0.57–0.64], UMIC = 0.61[0.58–0.65], HIC = 0.35[0.33–0.37]).

Annex 1 – References

1. Alsved, M. *et al.* Exhaled respiratory particles during singing and talking. *Aerosol Sci. Technol.* **54**, 1245–1248 (2020).
2. Bagheri, G. *et al.* Exhaled particles from nanometre to millimetre and their origin in the human respiratory tract. *medRxiv* 2021.10.01.21264333 (2021) doi:10.1101/2021.10.01.21264333.
3. Chao, C. Y. H. *et al.* Characterization of expiration air jets and droplet size distributions immediately at the mouth opening. *J. Aerosol Sci.* **40**, 122 (2009).
4. Ding, S., Teo, Z. W., Wan, M. P. & Ng, B. F. Aerosols from speaking can linger in the air for up to nine hours. *Build. Environ.* **205**, 108239 (2021).
5. Good, N. *et al.* Respiratory Aerosol Emissions from Vocalization: Age and Sex Differences Are Explained by Volume and Exhaled CO₂. *Environ. Sci. Technol. Lett.* **8**, 1071–1076 (2021).
6. Kappelt, N., Russell, H. S., Kwiatkowski, S., Afshari, A. & Johnson, M. S. Correlation of Respiratory Aerosols and Metabolic Carbon Dioxide. *Sustain.* 2021, Vol. 13, Page 12203 **13**, 12203 (2021).
7. Mürbe, D., Kriegel, M., Lange, J., Rotheudt, H. & Fleischer, M. Aerosol emission in professional singing of classical music. *Sci. Reports* 2021 111 **11**, 1–11 (2021).
8. Murbe, D. *et al.* Aerosol emission of adolescents voices during speaking, singing and shouting. *PLoS One* **16**, e0246819 (2021).
9. Mimura, T. *et al.* Concentration of Droplets from Patients during Normal Breathing and Speech and Their Importance in Protection from Coronavirus SARS-CoV-2 (COVID-19) Infection. *Open Ophthalmol. J.* **15**, 103–107 (2021).
10. DUGUID, J. P. The Numbers and the Sites of Origin of the Droplets Expelled during Expiratory Activities. *Edinb. Med. J.* **52**, 385 (1945).
11. Papineni, R. S. & Rosenthal, F. S. The Size Distribution of Droplets in the Exhaled Breath of Healthy Human Subjects. <http://www.liebertpub.com/jam> **10**, 105–116 (2009).
12. Morawska, L. *et al.* Size distribution and sites of origin of droplets expelled from the human respiratory tract during expiratory activities. *J. Aerosol Sci.* **40**, 256–269 (2009).
13. Asadi, S. *et al.* Aerosol emission and superemission during human speech increase with voice loudness. *Sci. Reports* 2019 91 **9**, 1–10 (2019).
14. Stadnytskyi, V., Bax, C. E., Bax, A. & Anfinrud, P. Brief Report: The airborne lifetime of small speech droplets and their potential importance in SARS-CoV-2 transmission. *Proc. Natl. Acad. Sci. U. S. A.* **117**, 11875 (2020).
15. Johnson, G. R. *et al.* Modality of human expired aerosol size distributions. *J. Aerosol Sci.* **42**, 839–851 (2011).
16. Gilad, R. *et al.* Evaluation of the relationship between quantitative PCR results and cell culturing of SARS2-CoV with respect to symptoms onset and Viral load – a systematic review. *medRxiv* 2021.08.23.21262162 (2021) doi:10.1101/2021.08.23.21262162.
17. Chen, P. Z. *et al.* SARS-COV-2 shedding dynamics across the respiratory tract, sex, and disease severity for adult and pediatric COVID-19. *Elife* **10**, (2021).
18. Jacot, D., Greub, G., Jatou, K. & Opota, O. Viral load of SARS-CoV-2 across patients and compared to other respiratory viruses. *Microbes Infect.* **22**, 617–621 (2020).
19. Chen, P. Z. *et al.* Heterogeneity in transmissibility and shedding SARS-CoV-2 via droplets and aerosols. *Elife* **10**, (2021).
20. van Doremalen, N. *et al.* Aerosol and Surface Stability of SARS-CoV-2 as Compared with SARS-CoV-1. *N. Engl. J. Med.* **382**, 1564–1567 (2020).
21. Robey, A. J. & Fierce, L. Sensitivity of airborne transmission of enveloped viruses to seasonal variation in indoor relative humidity. *Int. Commun. Heat Mass Transf.* **130**, 105747 (2022).
22. Schuit, M. *et al.* Airborne SARS-CoV-2 Is Rapidly Inactivated by Simulated Sunlight. *J. Infect. Dis.* **222**, 564–571 (2020).
23. Schuit, M. *et al.* The Stability of an Isolate of the SARS-CoV-2 B.1.1.7 Lineage in Aerosols Is Similar to 3 Earlier Isolates. *J. Infect. Dis.* **224**, 1641–1648 (2021).
24. Oswin, H. P. *et al.* The Dynamics of SARS-CoV-2 Infectivity with Changes in Aerosol Microenvironment. *medRxiv* 2022.01.08.22268944 (2022) doi:10.1101/2022.01.08.22268944.
25. Chatterjee, S., Murallidharan, J. S., Agrawal, A. & Bhardwaj, R. How coronavirus survives for hours in aerosols. *Phys. Fluids* **33**, 081708 (2021).
26. Smither, S. J., Eastaugh, L. S., Findlay, J. S. & Lever, M. S. Experimental aerosol survival of SARS-CoV-2 in artificial saliva and tissue culture media at medium and high humidity. *Emerg. Microbes Infect.* **9**, 1415 (2020).
27. Dabisch, P. *et al.* The influence of temperature, humidity, and simulated sunlight on the infectivity of SARS-CoV-2 in aerosols. *Aerosol Sci. Technol.* **55**, 142–153 (2020).
28. Puhach, O. *et al.* Infectious viral load in unvaccinated and vaccinated individuals infected with ancestral, Delta or Omicron SARS-CoV-2. *Nat. Med.* 2022 1–1 (2022) doi:10.1038/s41591-022-01816-0.
29. Heitzman-Breen, N. & Ciupe, S. M. Modeling within-host and aerosol dynamics of SARS-CoV-2: the relationship with infectiousness. *bioRxiv* 2022.03.08.483569 (2022) doi:10.1101/2022.03.08.483569.
30. Hawks, S. A. *et al.* Infectious SARS-CoV-2 Is Emitted in Aerosol Particles. *MBio* **12**, (2021).
31. Lednicky, J. A. *et al.* Viable SARS-CoV-2 in the air of a hospital room with COVID-19 patients. *Int. J. Infect. Dis.* **100**, 476–482 (2020).

32. Campbell, F. *et al.* Increased transmissibility and global spread of SARS-CoV-2 variants of concern as at June 2021. *Eurosurveillance* **26**, 1–6 (2021).
33. Liu, Y. & Rocklöv, J. The effective reproductive number of the Omicron variant of SARS-CoV-2 is several times relative to Delta. *J. Travel Med.* **29**, 1–4 (2022).
34. Blaurock, C. *et al.* Compellingly high SARS-CoV-2 susceptibility of Golden Syrian hamsters suggests multiple zoonotic infections of pet hamsters during the COVID-19 pandemic. *bioRxiv* 2022.04.19.488826 (2022) doi:10.1101/2022.04.19.488826.
35. Killingley, B. *et al.* Safety, tolerability and viral kinetics during SARS-CoV-2 human challenge in young adults. *Nat. Med.* 2022 1–11 (2022) doi:10.1038/s41591-022-01780-9.
36. Martins, M., Fernandes, M. H. V., Joshi, L. R. & Diel, D. G. Age-Related Susceptibility of Ferrets to SARS-CoV-2 Infection. *J. Virol.* **96**, (2022).
37. Totura, A. *et al.* Small particle aerosol exposure of african green monkeys to MERS-CoV as a model for highly pathogenic coronavirus infection. *Emerg. Infect. Dis.* **26**, 2835–2843 (2020).
38. Watanabe, T., Bartrand, T. A., Weir, M. H., Omura, T. & Haas, C. N. Development of a dose-response model for SARS coronavirus. *Risk Anal.* **30**, 1129–1138 (2010).
39. Hayden, F. G. *et al.* Safety and Efficacy of the Neuraminidase Inhibitor GG167 in Experimental Human Influenza. *JAMA* **275**, 295–299 (1996).
40. Alford, R. H., Kasel, J. A., Gerone, P. J. & Knight, V. Human Influenza Resulting from Aerosol Inhalation. *Proc. Soc. Exp. Biol. Med.* **122**, 800–804 (1966).
41. Treanor, J. J. *et al.* Evaluation of trivalent, live, cold-adapted (CAIV-T) and inactivated (TIV) influenza vaccines in prevention of virus infection and illness following challenge of adults with wild-type influenza A (H1N1), A (H3N2), and B viruses. *Vaccine* **18**, 899–906 (1999).
42. Riediker, M. *et al.* Higher viral load and infectivity increase risk of aerosol transmission for Delta and Omicron variants of SARS-CoV-2. *Swiss Med. Wkly.* **152**, w30133 (2022).
43. Dabisch, P. A. *et al.* Seroconversion and fever are dose-dependent in a nonhuman primate model of inhalational COVID-19. *PLoS Pathog.* **17**, e1009865 (2021).
44. Prentiss, M., Chu, A. & Berggren, K. K. Superspreading Events Without Superspreaders: Using High Attack Rate Events to Estimate N. *medRxiv* (2020).
45. Asadi, S. *et al.* Efficacy of masks and face coverings in controlling outward aerosol particle emission from expiratory activities. *Nat. – Sci. Reports* **10**, 1–13 (2020).
46. Sousa, I. T. C. de, Pestana, A. M., Pavanello, L., Franz-Montan, M. & Cogo-Müller, K. Máscaras caseiras na pandemia de COVID-19: recomendações, características físicas, desinfecção e eficácia de uso. *Epidemiol. e Serviços Saúde* **30**, (2021).
47. Konda, A. *et al.* Aerosol Filtration Efficiency of Common Fabrics Used in Respiratory Cloth Masks. *ACS Nano* **14**, 6339–6347 (2020).
48. Maher, B., Chavez, R., Tomaz, G. C. Q., Nguyen, T. & Hassan, Y. A fluid mechanics explanation of the effectiveness of common materials for respiratory masks. *Int. J. Infect. Dis.* **99**, 505–513 (2020).
49. Xiao, L., Sakagami, H. & Miwa, N. A New Method for Testing Filtration Efficiency of Mask Materials Under Sneeze-like Pressure. *In Vivo* **34**, 1637–1644 (2020).
50. O’Kelly, E., Pirog, S., Ward, J. & Clarkson, P. J. Ability of fabric face mask materials to filter ultrafine particles at coughing velocity. *BMJ Open* **10**, e039424 (2020).
51. Park, S. & Jayaraman, S. From containment to harm reduction from SARS-CoV-2: a fabric mask for enhanced effectiveness, comfort, and compliance. <https://doi.org/10.1080/00405000.2020.1805971> **112**, 1144–1158 (2020).
52. Lindsley, W. G., Blachere, F. M., Law, B. F., Beezhold, D. H. & Noti, J. D. Efficacy of face masks, neck gaiters and face shields for reducing the expulsion of simulated cough-generated aerosols. *medRxiv* 2020.10.05.20207241 (2020) doi:10.1101/2020.10.05.20207241.
53. Liu, Z. *et al.* Understanding the factors involved in determining the bioburdens of surgical masks. *Ann. Transl. Med.* **7**, 754–754 (2019).
54. Li, L., Niu, M. & Zhu, Y. Assessing the effectiveness of using various face coverings to mitigate the transport of airborne particles produced by coughing indoors. *Aerosol Sci. Technol.* **55**, 332–339 (2020).
55. Davies, A. *et al.* Testing the Efficacy of Homemade Masks: Would They Protect in an Influenza Pandemic? *Disaster Med. Public Health Prep.* **7**, 413 (2013).
56. Neupane, B. B., Mainali, S., Sharma, A. & Giri, B. Optical microscopic study of surface morphology and filtering efficiency of face masks. *PeerJ* **2019**, e7142 (2019).
57. Shakya, K. M., Noyes, A., Kallin, R. & Peltier, R. E. Evaluating the efficacy of cloth facemasks in reducing particulate matter exposure. *J. Expo. Sci. Environ. Epidemiol.* 2017 273 **27**, 352–357 (2016).
58. Ma, Q. X. *et al.* Potential utilities of mask-wearing and instant hand hygiene for fighting SARS-CoV-2. *J. Med. Virol.* **92**, 1567–1571 (2020).
59. Pan, J., Harb, C., Leng, W. & Marr, L. C. Inward and outward effectiveness of cloth masks, a surgical mask, and a face shield. <https://doi.org/10.1080/02786826.2021.1890687> **55**, 718–733 (2021).
60. Huang, J. T. & Huang, V. J. Evaluation of the efficiency of medical masks and the creation of new medical masks. *J. Int. Med. Res.* **35**, 213–223 (2007).
61. Gawn, J., Clayton, M., Makison, C., Crook, B. & Hill, H. Evaluating the protection afforded by surgical masks against influenza bioaerosols. *Heal. Saf. Exec.* (2008).
62. Milton, D. K., Fabian, M. P., Cowling, B. J., Grantham, M. L. & McDevitt, J. J. Influenza Virus Aerosols in Human Exhaled Breath: Particle Size, Culturability, and Effect of Surgical Masks. *PLoS Pathog.* **9**, (2013).
63. Mousa, A. *et al.* Social contact patterns and implications for infectious disease transmission: A systematic review and meta-analysis of contact surveys. *Elife* **10**, (2021).

Annex 2. Reviewed available tool at ISIAQ

Tool name	Link
Personal Relative COVID Risk Modelling Tool. Matti J. Jantunen, University Kuopio, Finland	https://worldaccordingtomatti.blog/2020/12/05/personal-covid-infection-and-death-risk-models/
COVID-19 Multi-rooms Calculator Livio Mazzarella, Polytechnic of Milan, Italy	https://www.rehva.eu/activities/covid-19-guidance/covid-19-multi-room-calculator
Airborne.cam Royal Society's RAMP guide, UK Aerosol Society COVID-19	https://airborne.cam/
REHVA COVID-19 Ventilation Calculator Federation of European Heating, Ventilation and Air Conditioning Associations	https://www.rehva.eu/covid19-ventilation-calculator
Aerosol transmission of COVID-19 and infection risk in indoor environments Jos Lelieveld, Max Planck Institute, Germany	https://www.mpic.de/4747361/risk-calculator?en
RESET Index: Real-time Aerosol Infection Estimator RESET Standards	https://reset.build/resources/indexes
Indoor Scenario Simulator Michael Riediker ¹ ; Dai-Hua Tsai ² 1: Swiss Centre for Occupational and Environmental Health, Switzerland. 2: University Hospital of Psychiatry, University of Zurich, Switzerland	https://doi.org/10.4209/aaqr.2020.08.0531 https://jamanetwork.com/journals/jamanetworkopen/fullarticle/2768712
COVID-19 Aerosol Transmission Estimator & Monte Carlo Version Prof. Jose L Jimenez & Dr. Zhe Peng, Dept. of Chem. & CIRES, Univ. Colorado-Boulder	http://tinyurl.com/covid-estimator
Harvard-University of Colorado Boulder Portable Air Cleaner Calculator for Schools Joseph Allen ¹ , Jose Cedeno-Laurent ¹ , Shelly Miller ² , 1: Healthy Buildings Program, Harvard T.H. Chan School of Public Health. 2: Mechanical Engineering, College of Engineering and Applied Science, University of Colorado Boulder	https://tinyurl.com/portableaircleanertool
Airborne Infection Risk Calculator Alex Mikszewski ¹ , Giorgio Buonanno ² , Luca Stabile ² , Antonio Pacitto ² , Lidia Morawska ³ 1: The City University of New York, New York, USA. 2: University of Cassino and Southern Lazio, Cassino, Frosinone, Italy. 3: Queensland University of Technology, Brisbane, Queensland, Australia	https://research.qut.edu.au/ilagh/wp-content/uploads/sites/174/2021/04/AIRC-v3.0-Beta-Draft-Manual.pdf
The SAFEAIRSPACES COVID-19 Aerosol Relative Risk Estimator Richard Corsi ¹ , Kevin Van Den Wymelenberg ² , Hooman Parhizkar ³ , Isaac Martinotti ⁴ , 1: Dean of the Maseeh College of Engineering and Computer Science, 2: Dean and Professor of Architecture at the University of Nebraska-Lincoln, 3: Postdoctoral Scholar at Rutgers University, 4: Researcher at the Institute for Health in the Built Environment.	https://safeairspaces.com/
COVID-19 Risk Calculator Harvard T.H. Chan, School of Public Health	https://covid-19.forhealth.org/covid-19-transmission-calculator/
COVID-19 Indoor Safety Guideline Massachusetts Institute of Technology	https://indoor-covid-safety.herokuapp.com/
Fate and Transport of Indoor Microbiological Aerosols (FaTIMA) William Stuart Dols, Brian Polidoro	https://www.nist.gov/services-resources/software/fatima https://doi.org/10.6028/NIST.TN.2095
COVID Airborne Risk Assessment (CARA) European Organization for Nuclear Research - CERN	https://gitlab.cern.ch/cara/cara

Annex 3. Model validation

The objective of this report is to:

- Extract all the required model input from each of the outbreaks described in the included papers.
- For the eligible outbreaks, identify the “attack rate”.
- Perform a model simulation (long-range only) for each outbreak and see how close the result is to the “attack rate” from the paper and references therein.

The benchmark scenarios only cover the long-range component of airborne transmission due to the unavailability of data for the short-range component.

Note that there may be several factors that influence the differences between the attack rates extracted from each study, and the respective probability of infection from the model simulations. Some possible reasons:

- The infected person has higher/lower viral load than the considered.
- Close contacts and fomite transmission that were not considered.
- Exposed and Infected presence time differences.
- Inaccurate data to estimate the room dimensions.
- Inaccurate data to estimate ventilation values.

For each simulation, if the “secondary” key word from the “attack rate” is missing is because either there was no single primary case identified, or because the study from the source paper considered it only as “attack rate”.

For some of the studies, beside the mean, 5th and 95th percentile from the probability of infection, other percentiles have been calculated.

Source paper: [Long distance airborne transmission of SARS-CoV-2: rapid systematic review](#)

In total, the paper describes studies/outbreak investigations in indoor settings such as restaurants, public transport, workplaces, or choir venues. Long distance airborne transmission was likely to have occurred for some or all transmission events in 16 studies and was unclear in two studies (GRADE: very low certainty). (Methodological quality was high in three, medium in five, and low in 10. Each included study is here described individually.

The studies describing transmission events happened in apartment blocks (as defined categorized by the authors) are not presented in this report because the transmissions took place in different settings.

[Eichler et al](#) (**high** methodological quality) – **not** eligible. Quarantine hotel, New Zealand, August-September 2020. **9** confirmed cases, with one secondary case considered for long-distance transmission.

Attack rate: Unknown total number of people

Limitation: In this study the transmission event spans over more than two weeks and includes a variety of settings.

Model simulation: not performed.

[Fox-Lewis et al](#) (**high** methodological quality) – **not** eligible. Quarantine hotel, New Zealand, July 2021.

5 confirmed cases in two rooms.

Attack rate: (5/6) 0.83

Limitation: Possible transmission through close contact within the group that shared one of the rooms.

Model simulation: not performed due to lack of required inputs (dimensions) and possible transmission in different settings.

[Li et al](#) (**medium** methodological quality) – **not** eligible. Restaurant, China, 2020. **10** confirmed cases from 3 tables.

Attack rate: Reported potential secondary and tertiary cases from the tables

Limitation: Transmission through different tables, with different presence times.

Model simulation: not performed

[Kwon et al](#) (**high** methodological quality) – **not** eligible. Restaurant, South Korea, June 2020. **3** confirmed cases.

Secondary attack rate: (2/13) 0.15

Limitation: Transmission through different tables, with different presence times.

Model simulation: not performed.

[Shen et al](#) (**medium** methodological quality) – eligible. Buses, China, January 2020. **24** confirmed cases.

Secondary attack rate: (23/67) 0.34

Model simulation		Probability of infection				
Total exposed	67	P(I)_mean	P(I)_05	P(I)_95	P(I)_96	P(I)_97
Duration	100 min (1.67)	$3.67 * 10^{-2}$	$1.77 * 10^{-7}$	0.23	0.29	0.39
Activity	Seated, Talking	Reproduction number				
Ventilation	1.25 ACH	N_mean	N_95		N_96	N_97
Volume	45m ³	2.46	15.32		19.35	26.20

Analysis: The secondary attack rate is between the 96th and 97th percentile of the probability of infection from model.

Data source: Y. Shen *et al.*, “Community Outbreak Investigation of SARS-CoV-2 Transmission Among Bus Riders in Eastern China Multimedia Supplemental content,” *JAMA Intern Med*, vol. 180, no. 12, pp. 1665–1671, 2020, doi: 10.1001/jamainternmed.2020.5225.

[Luo et al](#) (**low** methodological quality) – eligible. Buses, China, January 2020. **9** confirmed cases.

1st ride – tour coach bus:

Attack rate: (7/48) 0.15

Model simulation		Probability of infection				
Total exposed	48	P(I)_mean	P(I)_05	P(I)_90	P(I)_91	P(I)_95
Duration	200 min (2.5)	3.59×10^{-2}	1.76×10^{-7}	0.13	0.17	0.22
Activity	Seated, Talking	Reproduction number				
Ventilation	6.12 m ³ /h	N_mean	N_90	N_91	N_95	
Volume	56.5m ³	0.43	1.60	2.03	2.64	

Analysis: The secondary attack rate is between the 90th and 91st percentile of the probability of infection from model.

Data source: K. Luo *et al.*, “Transmission of SARS-CoV-2 in Public Transportation Vehicles: A Case Study in Hunan Province, China,” *Open Forum Infect. Dis.*, vol. 7, no. 10, p. ofaa430, Oct. 2020, doi: 10.1093/ofid/ofaa430.

[Luo et al](#) (**low** methodological quality) – eligible. Buses, China, January 2020. **9** confirmed cases.

2nd ride – minibus:

Attack rate: (2/12) 0.17

Model simulation		Probability of infection				
Total exposed	12	P(I)_mean	P(I)_05	P(I)_93	P(I)_94	P(I)_95
Duration	60 min (1.0)	3.59×10^{-2}	1.76×10^{-7}	0.13	0.17	0.22
Activity	Seated, Talking	Reproduction number				
Ventilation	11.52 m ³ /h	N_mean	N_93	N_94	N_95	
Volume	27.5m ³	0.43	1.60	2.03	2.64	

Analysis: The secondary attack rate is between the 93rd and 94th percentile of the probability of infection from the model.

Data source: K. Luo *et al.*, “Transmission of SARS-CoV-2 in Public Transportation Vehicles: A Case Study in Hunan Province, China,” *Open Forum Infect. Dis.*, vol. 7, no. 10, p. ofaa430, Oct. 2020, doi: 10.1093/ofid/ofaa430.

[Gunther et al](#) (**medium** methodological quality) – **not** eligible. Beef and pork processing complex, Rheda-Wiedenbruck, Germany. More than **1400** tested positive.

Model simulation: due to the number of infected/exposed participants, lack of data regarding the dimensions of the workspace, as well as the close contact and fomite transmission, this study was discarded.

[Groves et al](#) (**low** methodological quality) – **not** eligible. Fitness facilities, Hawaii, US.

Secondary attack rate: ?

Limitation: Transmission through different fitness classes, with different presence times. There is no data regarding the dimensions of the room.

Model simulation: not performed.

[Vernez et al](#) (**low** methodological quality) – eligible. Courtroom, Switzerland, September 2020. **5** COVID-19 confirmed cases.

Secondary attack rate: (3/9) 0.33

Limitation: No information regarding what happened during the breaks.

Model simulation		Probability of infection		
Total exposed	9	P(I)_mean	P(I)_05	P(I)_95
Duration	180 min (3.0)	2.96×10^{-2}	1.33×10^{-7}	0.17
Activity	Seated, Talking	Reproduction number		
Breaks	7', 15', 24'	N_mean	N_95	
Ventilation	1.23 ACH 0.23 ACH (no breaks)	0.27	1.53	
Volume	150m ³			

Analysis: The difference between the secondary attack rate value and respective model output can be related to close contact events, inaccurate room dimensions or differences in the infected viral load.

Data source: D. Vernez, S. Schwarz, J.-J. Sauvain, C. Petignat, and G. Suarez, “Probable aerosol transmission of SARS-CoV-2 in a poorly ventilated courtroom,” *Indoor Air*, vol. 31, no. 6, pp. 1776–1785, Nov. 2021, doi: <https://doi.org/10.1111/ina.12866>.

[Sarti et al](#) (**low** methodological quality) – eligible. Workspace, Italy. **5** COVID-19 cases.

Secondary attack rate: (4/5) 0.8

Limitation: This study encompasses a continuous exposition of five consecutive days.

Model simulation		Probability of infection		
Total exposed	5	P(I)_mean	P(I)_05	P(I)_95
Duration	8.0	2.03×10^{-2}	7.99×10^{-8}	0.11
Activity	Breathing (67%), Talking (33%)	Reproduction number		
Breaks	1.0 (lunch)	N_mean	N_95	
Ventilation	0.25ACH	0.10	0.53	
Volume	312m ³			

Analysis: The difference between the secondary attack rate value and respective model output can be related the long (5 days) continuous exposure, as well as the fact that the dimensions of the workspace include the working area, the archive, the meeting room, the photocopier area, and toilet, and not only the enclosed office where the transmission occurred.

Data source: D. Sarti, T. Campanelli, T. Rondina, and B. Gasperini, “COVID-19 in Workplaces: Secondary Transmission,” *Ann. Work Expo. Heal.*, vol. 65, no. 9, pp. 1145–1151, Nov. 2021, doi: 10.1093/annweh/wxab023.

[Jiang et al](#) (**low** methodological quality) – **not** eligible. Baodi department store in Tianjin,

China. **24** confirmed COVID-19 cases.

Secondary attack rate: ?

Limitations: This study is not eligible because there is not enough information about the total number of exposed people, as well as the dimensions of the described store.

Model simulation: not performed.

Singing events

For each of the singing events, in case of absence of activity type, we considered “**seated**”.

[Katelaris et al](#) (**high** methodological quality) – **not** eligible. Church singing in Sydney, Australia. **12** secondary cases.

Secondary attack rate: ?

Limitations: This study is not eligible because we don’t have enough information about the exact number of people that were presented in the church, as well as the correct dimensions of the church. The transmission may have occurred during different periods.

Model simulation: not performed.

[Shah et al](#) (**medium** methodological quality) – eligible. Five singing events, Netherlands. **48** confirmed cases.

Attack rates from paper.

Event **1**:

Attack rate: (14/19) 0.74

Model simulation		Probability of infection		
Total exposed	19	P(I)_mean	P(I)_05	P(I)_95
Duration	90 min (1.5)	$1.32 \cdot 10^{-2}$	$4.67 \cdot 10^{-8}$	$6.36 \cdot 10^{-2}$
Activity	Singing	Reproduction number		
Ventilation	3ACH	N_mean	N_95	
Volume	510m ³	0.24	1.15	

Analysis: The low probability of infection from the CAiMIRA simulation may be related to the inaccurate data from the scenario description.

Data source: A. Shah *et al.*, “High SARS-CoV-2 attack rates following exposure during singing events in the Netherlands, September-October 2020,” *medRxiv*, p. 2021.03.30.21253126, Jan. 2021, doi: 10.1101/2021.03.30.21253126.

[Shah et al](#) (**medium** methodological quality) – eligible. Five singing events, Netherlands. **48** confirmed cases.

Attack rates from paper.

Event **2**:

Attack rate: (14/21) 0.67

Model simulation		Probability of infection				
Total exposed	20	P(I)_mean	P(I)_05	P(I)_95	P(I)_98	P(I)_99
Duration	120 min (2.0)	$4.24 \cdot 10^{-2}$	$2.28 \cdot 10^{-7}$	0.27	0.63	0.82
Activity	Singing (67%), Speaking (33%)	Reproduction number				
Ventilation	0.25ACH	N_mean	N_95	N_98	N_99	
Volume	212.8m ³	0.85	5.49	12.53	16.41	

Analysis: The prediction of the church’s volume may be wrong. We only have information about the floor area and ceiling height, but not about the church’s shape. The attack rate is close the 98th percentile from the model simulation.

Data source: A. Shah *et al.*, “High SARS-CoV-2 attack rates following exposure during singing events in the Netherlands, September-October 2020,” *medRxiv*, p. 2021.03.30.21253126, Jan. 2021, doi: 10.1101/2021.03.30.21253126.

[Shah et al](#) (**medium** methodological quality) – eligible. Five singing events, Netherlands. **48** confirmed cases. Attack rates from paper.

Event **3**:

Attack rate: (4/16) 0.25

Limitations: This event was not studied because we don't have enough data to perform the simulation, namely the room dimensions.

[Shah et al](#) (**medium** methodological quality) – eligible. Five singing events, Netherlands. **48** confirmed cases. Attack rates from paper.

Event **4**:

Attack rate: (8/15) 0.53

Model simulation		Probability of infection				
Total exposed	14	P(I)_mean	P(I)_05	P(I)_95	P(I)_98	P(I)_99
Duration	150 min (2.5)	2.93×10^{-2}	1.31×10^{-7}	0.17	0.43	0.63
Activity	Singing (80%), Speaking (20%)	Reproduction number				
Ventilation	0.25ACH	N_mean	N_95		N_98	N_99
Volume	561m ³	0.41	2.36		6.05	8.79

Analysis: The attack rate is between the 98th and 99th percentile from the model simulation.

Data source: A. Shah *et al.*, “High SARS-CoV-2 attack rates following exposure during singing events in the Netherlands, September-October 2020,” *medRxiv*, p. 2021.03.30.21253126, Jan. 2021, doi: 10.1101/2021.03.30.21253126.

[Shah et al](#) (**medium** methodological quality) – eligible. Five singing events, Netherlands. **48** confirmed cases. Attack rates from paper.

Event **5**:

Attack rate: (8/14) 0.57

Model simulation		Probability of infection		
Total exposed	13	P(I)_mean	P(I)_05	P(I)_95
Duration	120 min (2.0)	2.09×10^{-2}	8.26×10^{-8}	0.11
Activity	Singing (75%), Speaking (25%)	Reproduction number		
Ventilation	3ACH	N_mean	N_95	
Volume	320m ³	0.27	1.43	

Analysis: The differences between the attack rate may be related to the dimensions of the scenario.

The **6th** event as not considered due to the dimensions of the venue (around 3000 m³).

Data source: A. Shah *et al.*, “High SARS-CoV-2 attack rates following exposure during singing events in the Netherlands, September-October 2020,” *medRxiv*, p. 2021.03.30.21253126, Jan. 2021, doi: 10.1101/2021.03.30.21253126.

[Charlotte et al](#) (**low** methodological quality) – eligible. Indoor choir rehearsal, France. **19** confirmed cases.

Secondary attack rate: (19/27) 0.70

Model simulation		Probability of infection				
Total exposed	26	P(I)_mean	P(I)_05	P(I)_95	P(I)_96	P(I)_97
Duration	120 min (2.0)	6.59×10^{-2}	4.87×10^{-7}	0.50	0.61	0.75
Activity	Singing	Reproduction number				
Ventilation	0.25ACH	N_mean	N_95		N_96	N_97
Volume	135 m ³	1.71	12.90		15.85	19.39

Analysis: The secondary attack rate is between the 96th and 97th percentile of the probability of infection from the model.

Data source: N. Charlotte, “High Rate of SARS-CoV-2 Transmission Due to Choir Practice in France at the Beginning of the COVID-19 Pandemic,” *J. Voice*, vol. 37, no. 2, pp. 292.e9-292.e14, 2023, doi: <https://doi.org/10.1016/j.jvoice.2020.11.029>.

[Hamner et al](#) – (**low** methodological quality) – eligible. Choir practice in Washington, US. **32** confirmed cases.

Secondary attack rate: (32/60) 0.53 – confirmed cases; (52/60) 0.87 – suspect cases.

Model simulation		Probability of infection		
Total exposed	60	P(I)_mean	P(I)_05	P(I)_95
Duration	150 min (2.5)	9.82×10^{-2}	1.09×10^{-6}	0.79
Activity	Moderate activity, singing	Reproduction number		
Ventilation	0.7ACH	N_mean	N_95	
Volume	810m ³	5.89	47.25	

Analysis: The secondary attack rate for the confirmed cases is between the mean and the 95th percentile of the probability of infection from the model.

Data source: L. Hamner *et al.*, “High SARS-CoV-2 Attack Rate Following Exposure at a Choir Practice — Skagit County, Washington, March 2020,” *MMWR. Morb. Mortal. Wkly. Rep.*, vol. 69, no. 19, pp. 606–610, May 2022, doi: 10.15585/MMWR.MM6919E6.

An outbreak occurred following attendance of a symptomatic index case at a weekly rehearsal on 10 March of the Skagit Valley Chorale (SVC). After that rehearsal, 53 members of the SVC among 61 in attendance were confirmed or strongly suspected to have contracted COVID-19 and two died. Due to the detailed information about the environmental conditions (during the outbreak), we consider this study to have medium methodological quality.

Secondary attack rate: 0.53 to 0.87

Model simulation		Probability of infection				
Total exposed	60	P(I)_mean	P(I)_05	P(I)_95	P(I)_97	P(I)_98
Duration	2h 30 min	7.01×10^{-2}	5.59×10^{-7}	0.54	0.79	0.91
Activity	Light activity, Singing	Reproduction number				
Ventilation	0.7 ACH	N_mean	N_95		N_97	N_98
Volume	810 m ³	4.24	32.61		47.49	54.62

Analysis: The secondary attack rate is between the 95th and 98th percentile of the probability of infection from Model.

Conclusion

From the **18** studies/outbreak investigations, **7** are eligible to perform a model simulation. From these, **5** were considered as **low**, **2** as **medium** and **none** as with **high** methodological quality.

Since most of the eligible studies have **low** methodological quality, it is reasonable that the (secondary) attack rate and the model probability of infection have some differences. Besides, the data extracted from these studies that are needed to perform a model simulation may have significant differences from the reality, as the case of the activity profile, or expiratory type.

Most of the comparison relates to the high percentile band of the statistical result from the model. The results fall in between the 90th and 98th percentile. This could be due to the following situations:

- 1) High viral loads of the infectors: the viral load at 90th percentile is ~9 log RNA copies
- 2) The absence of the contribution of short-range interactions in the studies

This is comparable to the evidence observed in literature, where several outbreaks with (long-range) airborne identified as the main mode of transmission, is related to superspreading events where the infector was likely to be classified as a super-emitter shedding higher than average viral loads and emitting more Infectious Particles.

Annex 4. Model formulas

This annex describes the high-level analytical formulas used in the model. More information are available at [1] and [2]. The complete code is available on the ARIA online tool at <https://partnersplatform.who.int/aria>

Emission Rate (vR)

The viral emission rate (RNA copies h⁻¹) can be calculated using the following formulation:

$$vR(D)_j = vI_{in} \cdot E_{c,j}(D, f_{amp}, \eta_{out}(D)) \cdot BR_k \quad (1)$$

where vI_{in} is the viral load inside the infected host's respiratory tract (in RNA copies per mL); $E_{c,j}$ represents the volumetric particle emission concentration per unit diameter (in mL m⁻³ μm⁻¹), for a given expiratory activity j and as a function of the vocalization amplification factor f_{amp} and the outward mask efficiency $\eta_{out}(D)$ (which also depends on the particle size); BR_k (in m³ h⁻¹) is the breathing flow rate for a given physical activity k .

The total emission rate, vR^{total} in RNA copies h⁻¹, can be obtained by integrating the emission rate over the specific particle size range of diameter D .

Expiratory particle emissions (E_{c,j})

The volumetric particle emission concentration ($E_{c,j}$) is modeled using a tri-modal log-normal distribution model (BLO model [3]).

$$E_{c,j}(D) = N_p(D) \cdot V_p(D) \cdot (1 - \eta_{out}(D)) \quad (2)$$

where $N_p(D)$ is the number of particles of this size, $V_p(D)$ is their individual volume.

$$N_p(D) = \frac{1}{D} \sum_{i \in I(j)} \left[\frac{c_{n,i} \cdot f_{amp,j,i}}{\sqrt{2\pi} \cdot \sigma_{D_i}} \exp\left(-\frac{(\ln D - \mu_{D_i})^2}{2(\sigma_{D_i})^2}\right) \right], \quad (3)$$

where $I(j)$ is a subset of {B, L, O} determined by the expiratory activity j : for breathing $I(b) = \{B\}$, for speaking or shouting $I(sp) = I(sh) = \{B, L, O\}$; μ_L and σ_{D_i} are the mean and standard deviation of the natural logarithm of the diameter for each mode (in ln μm); $c_{n,i}$ is the total particle emission concentration for each mode. The amplification factor $f_{amp,j}(i)$ follows [4]:

$$f_{amp,j,i} = \begin{cases} 1, & \text{if } i = B \\ 1, & \text{Breathing and Speaking} \\ 5, & \text{Shouting} \end{cases} \text{ if } i \in \{L, O\}$$

Viral removal rate (vRR)

The viral removal rate per hour is described by means of the following summation [5]:

$$\lambda_{vRR} = \lambda_{ACH} + \lambda_{dep} + \lambda_{bio} + \lambda_{CADR} \quad (4)$$

where λ_{ACH} , λ_{dep} , λ_{bio} and λ_{CADR} (all in h⁻¹) are the removal rates related to ventilation, gravitational settlement, biological decay and particulate filtration, respectively.

Effect of ventilation

The removal rate due to ventilation (λ_{ACH}) via mechanical or natural means, is obtained from the amount of fresh air supplied to the space and the volume of the room:

$$\lambda_{ACH} = \frac{Q_{ACH}}{V_r} \quad (5)$$

in which Q_{ACH} represents the volumetric flow rate of fresh air supplied to the room (in m³ h⁻¹) and V_r its volume (in m³). Q_{ACH} will depend on the type of ventilation used.

The fresh air flow Q_{ACH} for single-sided natural ventilation is derived from a combination of Bernoulli's equation and the ideal gas law [6]:

$$Q_{ACH} = \frac{C_d \cdot A}{3} \sqrt{\frac{g \cdot h \cdot \Delta T}{T_{avg}}} \quad (6)$$

where C_d is the discharge coefficient; A is the area of the opening (in m^2); g is the gravitational acceleration (in $m \cdot s^{-2}$); h is the height of the opening (in m); ΔT is the indoor/outdoor temperature difference and T_{avg} is the average indoor/outdoor air temperature (in K). Equation (6) is valid when

ΔT is positive and not too large (≤ 20 K).

For top- or bottom- hung windows, C_d is estimated at 0.6 [6], [7]. For top- or bottom-hung windows, C_d depends on the opening angle ϕ (in deg) and the ration $\frac{w}{h}$ (with w the width of the window), according to the following rule [7]:

$$C_d = C_{d,max} [1 - \exp(-M \cdot \phi)] \quad (7)$$

where M and $C_{d,max}$ are given for different values of $\frac{w}{h}$. The opening angle ϕ can be obtained via:

$\sin\left(\frac{\phi}{2}\right) = \frac{L}{2h}$, with L the size of the opening (i.e., such that $A=h \cdot L$). In the absence of natural and mechanical ventilation, the removal rate λ_{ACH} will be governed by the air infiltration of typical buildings. In this model we assume a constant average value of 0.25 h^{-1} [8].

Biological decay

The viral removal rate due to biological decay (λ_{bio}) in min^{-1} is obtained from the following equation[9]:

$$\lambda_{bio} = 0.16030 + 0.04018 \cdot \frac{(T-20.615)}{10.585} + 0.02176 \cdot \frac{RH-45.235}{28.665} - 0.14369 - 0.02636 \cdot \frac{T-20.615}{10.585} \quad (8)$$

where T is the temperature, in $^{\circ}C$, and RH the relative humidity, in percentage. The final decay constant is divided by 60 to convert from infectivity decay per minute (min^{-1}) to infectivity decay per hour (h^{-1}).

Gravitational settlement

Using Stokes law, the settling velocity is:

$$v(D) = \frac{(\rho_p - \rho_{air})(D_{evap} \cdot 10^{-6})^2 \cdot g}{18 \mu_{air}} \quad (9)$$

where, ρ_p and ρ_{air} (in kg m^{-3}) are the mass densities of the particle and air, respectively; g is the gravitational acceleration (in m s^{-2}); D_{evap} is the diameter (in μm) of the desiccated particle, following evaporation ($D_{evap} = D \cdot f_{evap}$, with $f_{evap} = 0.3$), and $\mu_{air} \approx 1.8 \cdot 10^{-5} \text{ kg m}^{-1} \text{ s}^{-1}$ is the dynamic viscosity of air (at room temperature and atmospheric pressure).

The proposed mass density for ρ_p is 1000 kg m^{-3} [3]. The mass density of air (ρ_{air}) is taken at 1.2 kg m^{-3} . Assuming that the droplets are falling from the mouth or nose of a person standing, the height at which the terminal velocity (obtained from Eq. (9)) is reached, is considered at approximately $h = 1.5 \text{ m}$ from the floor, which yields $\lambda_{dep} = v / h$.

Air filtration or equivalent ventilation

The effect of increasing the air exchange rate of air cleaning devices can be determined by:

$$\lambda_i \lambda_{CADR} = \frac{Q_{CADR}}{V_r} \quad (10)$$

in which Q_{CADR} (in $\text{m}^3 \text{h}^{-1}$) is the Clean Air Delivery Rate of the device and V_r is the room volume.

Viral Concentration

Long-range Box

The concentration of viruses in aerosols of a given size D , is derived from the following differential equation:

$$\frac{\partial C}{\partial t} = \frac{vR(D) \cdot N_{inf}}{V_r} - \lambda_{vRR}(D) \cdot C(t, D) \quad (11)$$

where v_r and λ_{vRR} both depend on the particle diameter D ; V_r (in m^3) is the room volume; N_{inf} is the number of infected hosts emitting the viruses at the same time and in equal quantities.

Solving the differential equation, we get (in RNA copies m^{-3}):

$$C(t, D) = \frac{vR(D) \cdot N_{inf}}{\lambda_{vRR}(D) \cdot V_r} - \left(\frac{vR(D) \cdot N_{inf}}{\lambda_{vRR}(D) \cdot V_r} - C_0(D) \right) e^{-\lambda_{vRR}(D)t} \quad (12)$$

where $C_0(D) \equiv C(t = 0, D)$, and the quantity $C_{equilibrium} \equiv \frac{vR \cdot N_{inf}}{\lambda_{vRR} \cdot V_r}$ represents the equilibrium value that is reached in the steady-state regime.

Short-range box

The short-range concentration of viruses in the expiratory jet at close distance of a given size D , is given from the following Equation [2]:

$$C_{SR}(t, D) = C(t, D) + \frac{1}{S(x)} \cdot (C_{0,SR}(D) - C(t, D)) \quad (13)$$

where $C(t, D)$ is the long-range concentration of viruses, the dilution factor $S(x)$ is described in the following Section, and $C_{0,SR}(D)$ is the initial concentration of viruses at mouth/nose defined by:

$$C_{0,SR}(D)_j = E_{c,j}(D, f_{amp}, \eta_{out} = 0) \cdot v l_{in} \cdot 10^{-6}, \quad (14)$$

Where 10^{-6} is to convert from $\mu m^3 cm^{-3}$ to $mL m^{-3}$.

Dilution factor ($S(x)$)

The dilution factor is calculated in a two-stage interrupted jet. The dilution factor, in a given distance x , is given by [2]:

$$S(x) = \begin{cases} \frac{2\beta_{r1}(x+x_0)}{D_m} & 0 < x < x^* \\ S(x^*) \left(1 + \frac{\beta_{r2}(x-x^*)}{\beta_{r1}(x+x_0)} \right)^3 & x \geq x^* \end{cases} \quad (15)$$

Dose

For a simulation event in which the susceptible hosts are exposed to multiple independent exposure scenarios, the dose, which can be either the short- or long-range concentration, is given by:

$$vD(D) = \sum_{i=1}^n \int_{t_i}^{t_{i+1}} C(t, D) dt \cdot f_{inf} \cdot BR_k \cdot f_{dep}(D) \cdot (1 - \eta_{in}) \quad (16)$$

where t_i and t_{i+1} are the start and end times (in h) of each sub-exposure, respectively; n is the total amount of independent exposures in the same event; f_{inf} is the fraction of infectious virus which is determined by the viable-to-RNA virus ratio; $f_{dep}(D)$ is the (diameter-dependent) deposition fraction in the respiratory tract; and η_{in} is the inward efficiency of the face mask.

The total dose (in infectious virions) then results from the sum of all the doses accumulated for each particle size; it is given by an integral of the form

$$vD^{total} = \int_0^{D^{max}} vD(D) dD \quad (17)$$

In this model, f_{dep} depends on the aerosol particle diameter (after evaporation) and uses the ICRP deposition model [10]:

$$f_{dep}(D) = I_{frac}(D) \left(0.0587 + \frac{0.911}{1 + e^{4.77 + 1.185 \cdot \ln D_{evap}}} + \frac{0.943}{1 + e^{0.508 - 2.58 \cdot \ln D_{evap}}} \right)$$

With

$$I_{frac}(D) = 1 - 0.5 \left(1 - \frac{1}{1 + 0.00076 \cdot D_{evap}^{2.8}} \right) \quad (18)$$

Estimation of the probability of airborne transmission

The probability of a COVID-19 infection is represented by

$$P(I|vD^{total}, ID_{50}) = 1 - e^{-\frac{vD^{total}}{\ln 2} \cdot T_{voc} \cdot \left(\frac{1}{1 - HI_{exp}} \right)} \quad (19)$$

where $P(I|vD^{total}, ID_{50})$ denotes the conditional probability of event I (infection) for given values of the total absorbed and infection doses vD^{total} and ID_{50} , respectively. T_{voc} is the reported increase of transmissibility of a VOC, given by the ratio of basic reproductions numbers (R_0) between non-VOC strains and the VOC itself. HI_{exp} is the host immunity of the exposed occupants, given by the report vaccine efficiencies.

Annex 4 – References

- [1] A. Henriques *et al.*, “Modelling airborne transmission of SARS-CoV-2 using CARA: risk assessment for enclosed spaces,” *Interface Focus*, vol. 12, no. 2, Apr. 2022, doi: 10.1098/RSFS.2021.0076.
- [2] W. Jia, J. Wei, P. Cheng, Q. Wang, and Y. Li, “Exposure and respiratory infection risk via the short-range airborne route,” *Build. Environ.*, vol. 219, p. 109166, Jul. 2022, doi: 10.1016/J.BUILDENV.2022.109166.
- [3] G. R. Johnson *et al.*, “Modality of human expired aerosol size distributions,” *J. Aerosol Sci.*, vol. 42, no. 12, pp. 839–851, Dec. 2011, doi: 10.1016/J.JAEROSCI.2011.07.009.
- [4] S. Asadi, A. S. Wexler, C. D. Cappa, S. Barreda, N. M. Bouvier, and W. D. Ristenpart, “Aerosol emission and superemission during human speech increase with voice loudness,” *Sci. Reports 2019 91*, vol. 9, no. 1, pp. 1–10, Feb. 2019, doi: 10.1038/s41598-019-38808-z.
- [5] W. Yang and L. C. Marr, “Dynamics of Airborne Influenza A Viruses Indoors and Dependence on Humidity,” *PLoS One*, vol. 6, no. 6, p. e21481, Jun. 2011, [Online]. Available: <https://doi.org/10.1371/journal.pone.0021481>.
- [6] C. Allocca, Q. Chen, and L. R. Glicksman, “Design analysis of single-sided natural ventilation,” *Energy Build.*, vol. 35, no. 8, pp. 785–795, 2003, doi: [https://doi.org/10.1016/S0378-7788\(02\)00239-6](https://doi.org/10.1016/S0378-7788(02)00239-6).
- [7] R. Daniels, “BB 101: Ventilation, thermal comfort and indoor air quality 2018,” London, 2018. Accessed: Feb. 07, 2023. [Online]. Available: <https://www.gov.uk/government/publications/building-bulletin-101-ventilation-for-school-buildings>.
- [8] W. Bobenhausen, *Simplified Design of HVAC Systems*, John Wiley. John Wiley & Sons, Ltd, 1994.
- [9] P. Dabisch *et al.*, “The influence of temperature, humidity, and simulated sunlight on the infectivity of SARS-CoV-2 in aerosols,” *Aerosol Sci. Technol.*, vol. 55, no. 2, pp. 142–153, 2020, doi: 10.1080/02786826.2020.1829536.
- [10] William C. Hinds, *Aerosol Technology: Properties, Behavior, and Measurement of Airborne Particles, 2nd Edition*, 2nd Editio. New Publisher, 2021.

Annex 5. Model values

Variable	symbol	mean or [range]	SD	unit	Fitting distribution model
Breathing flowrate	BR_k				
seated	BR_{se}	0.51	0.053	$m^3 h^{-1}$	Lognormal (c.f. fig 1)
standing	BR_{st}	0.57	0.053		
light activity	BR_l	1.24	0.12		
moderate activity	BR_m	1.77	0.34		
heavy activity	BR_h	3.28	0.72		
Viral load	vl_{in}	6.2	1.8	\log_{10} RNA copies ml^{-1}	Weibull Kernel Density Estimation from dataset [156] ¹ (c.f. fig 2)
Mask efficiency:					
Surgical	$\eta_{in,surgical}$	[0.25–0.80]			uniform
Respirator	$\eta_{in,PPE}$	[0.83–0.91]	—	—	
Cloth	$\eta_{in,cloth}$	[0.05–0.40]			
viable-to-RNA virus ratio	r_{inf}	[0.01–0.60]	—	—	uniform
infectious dose	ID_{50}	[10–100]	—	PFU ²	Uniform
Conversational distance	X	0.99	0.34	m	Gaussian Kernel Density Estimation from dataset [157] ³ (c.f. fig 3)

1 Values truncated at $vl_{in} = 2$ and $vl_{in} = 10$

2 The dose can simply be expressed as infectious viruses or viable viruses.

3 Values truncated at $x = 0.5$ and $x = 2$

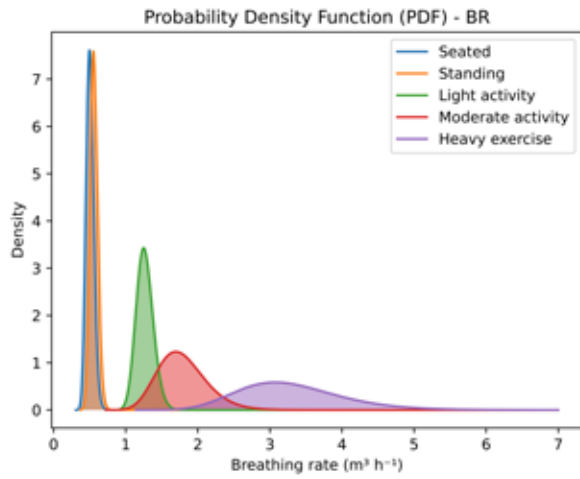


Figure 1 – PDFs for the breathing rate

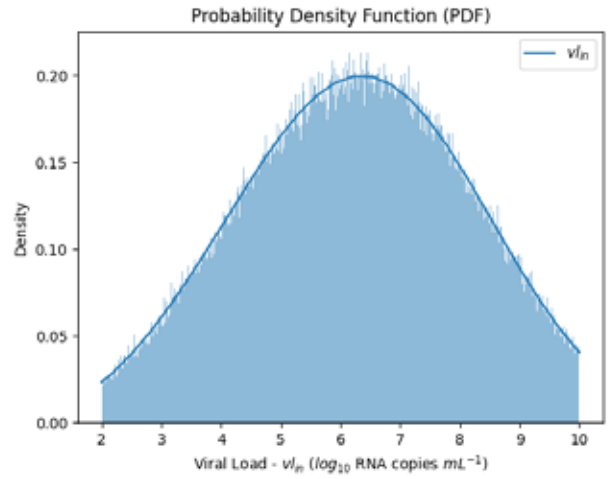


Figure 2 – PDF for the viral load

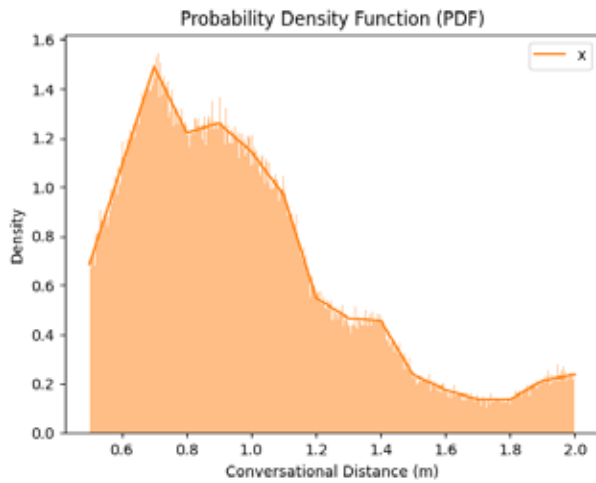
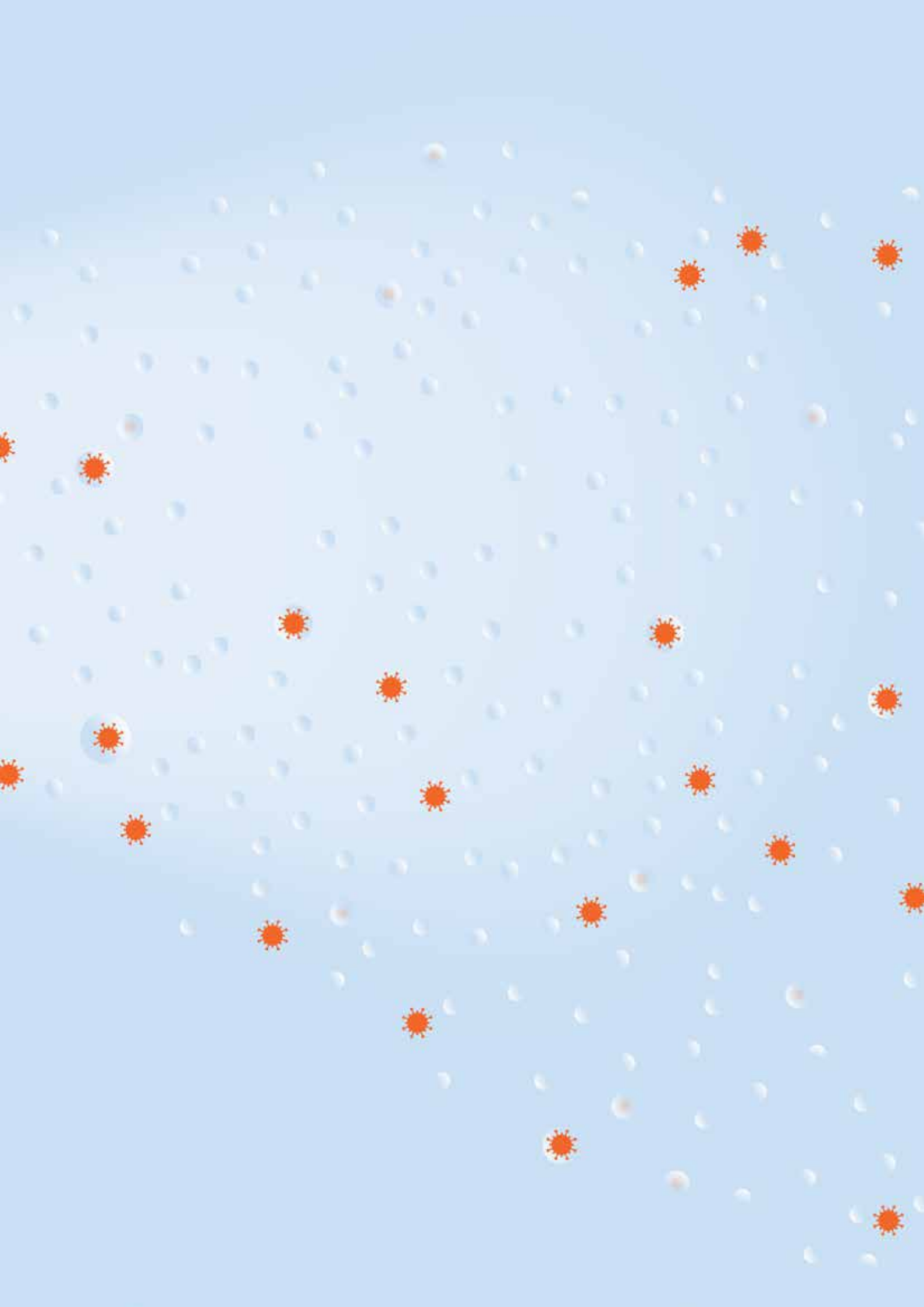


Figure 3 – PDF for the conversational distance





**World Health
Organization**

For more information, please contact:

Techne

World Health Organization

Avenue Appia 20

CH-1211 Geneva 27

Switzerland

Email: techne@who.int



CERN

Esplanade des Particules 1

P.O. Box

1211 Geneva 23

Switzerland

